University of Alberta
Department of Civil &
Environmental Engineering

Structural Engineering Report No. 278

END TEAR-OUT FAILURES OF BOLTED TENSION MEMBERS

by

Qing Cai

and

Robert G. Driver

January 2008

End Tear-out Failures of Bolted Tension Members

by

Qing Cai
and
Robert G. Driver

Structural Engineering Report 278

Department of Civil and Environmental Engineering
University of Alberta
Edmonton, Alberta, Canada

January 2008

ABSTRACT

Relatively few tests for bolt tear-out failure in connections of steel tension members have been conducted, and significantly fewer investigations among them were on sections other than flat plates. Moreover, many of these tests used one or two bolts rather than being typical of actual structural connections for tension members. A reliability analysis of design equations in current standards in North America using test data collected from the literature indicates that these standards give highly conservative predictions and inconsistent reliability indices. A better understanding of bolt tear-out failure is required so that these design equations can be improved.

An experimental study that included a total of 50 full-scale connection tests on wide-flange shapes was conducted to investigate the strength and behaviour of connections that fail by bolt tear-out. The principal variables considered in the tests were bolt gauge, the number of bolt rows, and end distance. Based on the results of these tests and those from the literature, design recommendations are presented that provide accurate predictions of capacity as well as a uniform reliability.

ACKNOWLEDGEMENTS

This research project was funded by the Steel Structures Education Foundation and the Natural Sciences and Engineering Research Council of Canada. Support from Waiward Steel Fabricators Ltd. in the form of a donation of 32 test specimens designed by Waiward engineer Logan Callele is gratefully acknowledged.

The authors thank Mr. Richard Helfrich, a technician in the I.F. Morrison Structural Engineering Laboratory, for his great help in successfully conducting 50 tests in a short period of time. Mr. Andrew Neilson, a graduate student in the department of Civil and Environmental Engineering, also helped with the experimental work, especially the ancillary tests.

TABLE OF CONTENTS

LIST OF TABLES

LIST OF FIGURES

LIST OF SYMBOLS

A_b = nominal cross-sectional area of bolt (mm^2)

A_{gv} = gross shear area (mm^2)

A_n = net area (mm^2)

A_{ne} = effective net area (mm^2)

A_{nt} = net tension area (mm^2)

A_{nv} = net shear area (mm^2)

d_b = bolt diameter (mm)

d_o = bolt hole diameter (mm)

e_1 = end distance (mm)

e_2 = edge distance (mm)

F_{nv} = nominal shear stress capacity (MPa)

F_u = ultimate stress (MPa)

F_y = yield stress (MPa)

g = gauge (transverse spacing between bolt lines) (mm)

L_c = clear end distance

m = number of shear planes

n = number of bolts in a connection

P_r = factored ultimate connection resistance (kN)

p = pitch (longitudinal spacing between bolt rows) (mm)

t = flange or plate thickness (mm)

U = shear lag factor

V_d = coefficient of variation of the discretization factor

V_G = coefficient of variation of the geometry factor

V_M = coefficient of variation of the material factor

V_P = coefficient of variation of the professional factor

V_R = coefficient of variation of resistance

V_r = bolt shear strength

w = web thickness (mm)

α_R = separation variable for resistance

β = reliability index

ρ_d = bias coefficient of the discretization factor

ρ_G = bias coefficient of the geometry factor

ρ_M = bias coefficient of the material factor

ρ_P = bias coefficient of the professional factor

ρ_R = bias coefficient of resistance

Φ_β = modification factor for resistance factor

ϕ = resistance factor

ϕ_b = bolt shear resistance factor

ϕ_{br} = bolt bearing resistance factor

1. INTRODUCTION

1.1 General

Bolt tear-out is a connection failure mode that has not been well understood, nor has it been clearly addressed in current design standards in North America. It can be the governing failure mode for bolted connections that have a relatively small end distance and pitch. Generally, for bolt tear-out failure, shear tearing occurs along the two shear planes at the sides of a bolt, and there is no tension fracture in the block of material that tears out since these two shear planes are only the diameter of the bolt hole apart. However, test observations of single bolt connections have indicated that the final fracture path could be the aforementioned two shear tears or one central splitting crack, depending on the length of the end distance (Aalberg and Larsen, 2001). An investigation is needed to clarify the number of shear planes that contribute to the connection strength in order to propose a valid design method.

In bolted connections, bolt tear-out failures are generally associated with connections that have a relatively small end distance and pitch, while having a comparatively large edge distance and gauge to avoid failure in net section rupture or block shear. Bearing is another failure mode that is considered to constitute failure by the excessive deformation of material behind the bolt, regardless of whether the connection has reserve strength. These two failure modes are closely related and there is not a clear line to distinguish between them. As the end distance increases, the failure mode would gradually be expected to change from bolt tear-out to bearing (Kim and Yura, 1999). Ultimately, in either case the bolts tear out if the applied load is maintained to final collapse.

A comprehensive literature review indicates that only a limited number of connection tests on bolt tear-out failure have been conducted, and the majority of them used flat plates and only one or two bolts. For plates, the number of bolts that can be used in test connections is limited because connections having a larger number of bolts are unlikely to fail in bolt tear-out unless the plates are wide enough to avoid other failure modes, such as block shear or net section rupture. In spite of the fact that gusset plates are commonly used in steel structural connections to transfer loads, the members themselves, which are often rolled shapes, must also be checked for this type of failure. W-Shapes as

structural members acting principally in tension are commonly used in large trusses and in frames as bracing members, and larger groups of bolts are usually required for such members. Figures 1-1 and 1-2 show typical splice connections of wide flange shapes in a web diagonal and top chord, respectively, of a pedway truss at the Royal Alexandra Hospital in Edmonton, Alberta. Due to the insufficiency of test data on shapes available from the literature, additional full-scale connection tests are required in order to investigate the mechanism of bolt tear-out failure.

1.2 Objectives and Scopes

The main objectives of this research project are to investigate the strength and behaviour of connections failing by bolt tear-out, or a combination of modes that includes bolt tear-out, and the effects of connection variables on the behaviour.

Other objectives are as follows:

- Collect from the literature and analyse test data on bolt tear-out failure for different types of sections and connection configurations from previous research projects;

- Conduct a number of full-scale tests on wide-flange shapes to examine closely the strength and behaviour of connections in tension members failing by bolt tear-out or combination failures that involve bolt tear-out (Objectives of the three individual test series conducted as part of this research are outlined in Chapter 3.);

- Evaluate the accuracy and suitability of current design equations in North American design standards for bolt end tear-out failure and, if necessary, propose an alternative design approach that provides accurate predictions and a consistent level of reliability; and

- Present design recommendations based on the laboratory test results that unify the net section rupture, block shear failure, and bolt tear-out failure modes.

1.3 Units

The units used in this report follow the SI system except where common shop practice is to use imperial units, such as in the layout of the bolt holes and the bolt diameters.

1.4 Organization of Chapters

This report contains six chapters. Chapter 2 reviews previously-conducted research projects on bolt tear-out and bearing failure and, using the test data collected from the literature, compares the accuracy of several design equations for predicting connection capacity. Chapter 3 describes the details of the experimental program, including test specimen geometry, the test set-up, instrumentation, and material properties. Chapter 4 discusses test procedures and test results. Discussions of the test results for each group of specimens are also presented. A reliability analysis of the test results is presented in Chapter 5. Finally, conclusions and design recommendations are drawn in Chapter 6. Appendices A and B present, respectively, the details of test results collected from the literature and test-to-predicted ratios calculated using the design equations considered. Load vs. deformation curves and photos of the failed connections for specimens in series C are presented in Appendices C and D, respectively.

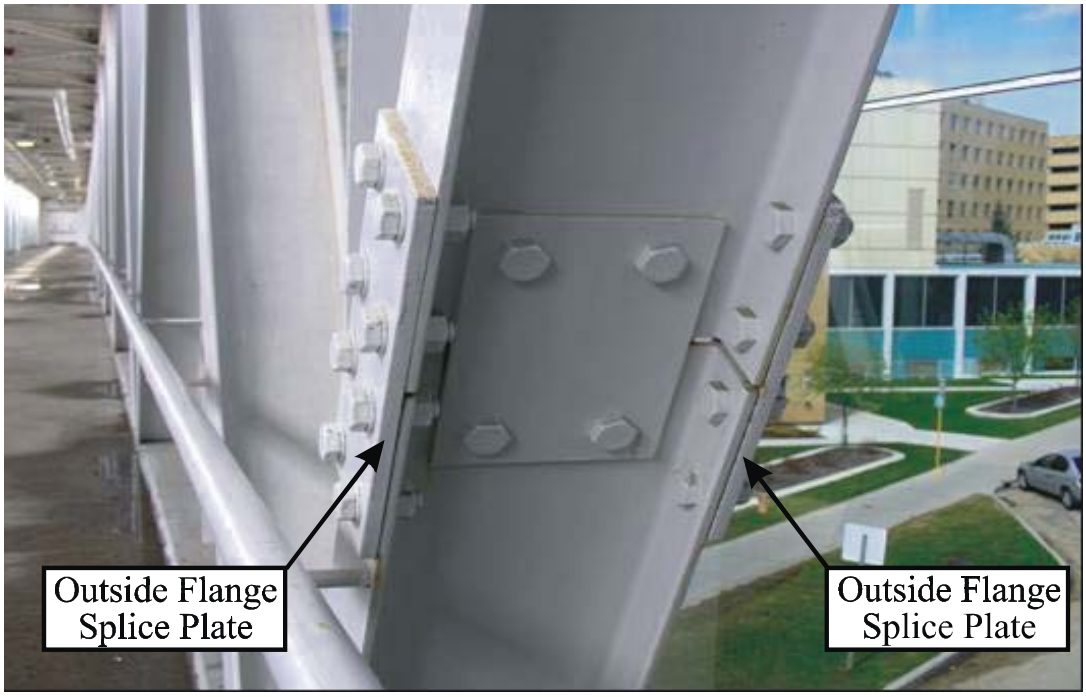

Figure 1-1: Wide-Flange Connection with Outside Flange Splice Plates Only (Photograph courtesy of R. G. Driver)

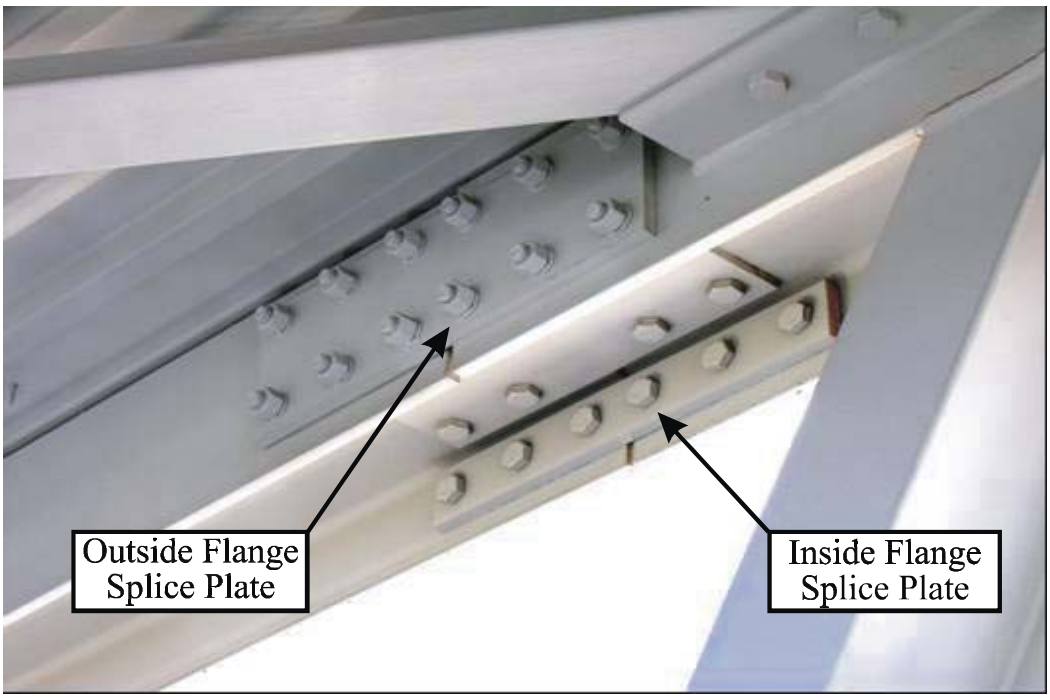

Figure 1-2: Wide-Flange Connection with Inside and Outside Flange Splice Plates (Photograph courtesy of R. G. Driver)

2. LITERATURE REVIEW

2.1 Introduction

This chapter describes recent experimental research projects on bolted connections that were conducted to investigate the failure modes of either bolt tear-out or bearing. As this is an extension of previous research at the University of Alberta on block shear failure (Franchuk *et al*., 2002; Huns *et al*., 2002), also included for completeness are tests of flange-connected Tees that failed in block shear that were not considered in the previous studies. Ultimately, it is desired to unify the procedures for designing for block shear, bolt tear-out, and net section rupture due to their analogous behaviours. Figure 2-1 shows definitions of dimensional parameters used hereafter in this report.

2.2 Bolt Tear-Out Failure in Bolted Connections

2.2.1 Udagawa and Yamada (1998)

In order to investigate the influence of bolt arrangement on the ultimate tensile strength of connections loaded in tension, a total of 219 gusset plates were tested by Udagawa and Yamada (1998), and 47 of them failed in the bolt tear-out failure mode. Three grades of steel were used in the tests, which had nominal tensile strengths of 400 MPa, 590 MPa, or 780 MPa. The nominal thickness of the plates was 12 mm. The detailed information is listed in Appendix A.

The tests covered a wide variety of bolt layouts. For the 47 specimens that failed in bolt tear-out, the number of bolts in the direction parallel to the applied load (*i.e.*, number of bolt lines) was either one or two and the number of bolts perpendicular to the applied load (*i.e.*, number of bolt rows) ranged from two to four. Other variables were end distance, edge distance, and gauge, while plate thickness, bolt diameter, and pitch were taken as fixed parameters.

None of the test specimens met both the minimum end/edge distance and pitch requirements prescribed by North American design standards. Bolts used in the tests were 16 mm in diameter, which are somewhat smaller than commonly-used structural bolts. Even with such small bolts, the 40 mm pitch, which is $2.5d_b$, where d_b is the nominal bolt diameter, still violated the minimum requirement of $2.7d_b$ by 7.4% and the

recommended minimum of $3.0d_b$ by 16.7%. The end distances for the specimens varied from 15.2 mm to 40.6 mm, and the method of cutting the plates was not determined conclusively, as the research was reported in Japanese. The minimum end/edge distance requirements for 16 mm bolts are 28 mm for sheared edges and 22 mm for rolled, sawn, or gas-cut edges. In addition, CSA-S16-01 also requires that the end distance not be less than $1.5d_b$ for members having one or two bolts in a bolt line.

Conclusions were drawn by the authors based on the test results, but they cannot be discussed here since the original paper is written in Japanese.

2.2.2 Kim and Yura (1999)

This experimental study focused on the effects of end distance and bolt spacing (pitch) on bearing strength for one or two bolts in a single line parallel to the applied load. Two different types of steel, one with a high F_u / F_y ratio and the other with a low F_u / F_y ratio, where F_u and F_y are the ultimate and yield strengths, respectively, were used in the tests. The nominal thickness of the plates was 5 mm and the width of the plates was selected to be wide enough to avoid rupture on the net section. The variable for the one-bolt connections was end distance, while for the two-bolt connections both end distance and pitch were varied. A total of 19 steel plates were tested in lap connections, and nine of them met both the minimum end/edge distance and pitch requirements specified in North America design standards. A detailed description of the connections is listed in Appendix A.

The tests showed that the bolt tear-out strength was more affected by the ultimate stress rather than the yield stress of the connected material, and deformation was influenced more by the end distance than by the F_u / F_y ratio when end tear-out failure was ensured.

2.2.3 Aalberg and Larsen (2001; 2002)

Two experimental studies were performed on bolted steel plates to determine bearing strength, wherein one had 16 single-bolt connections (Aalberg and Larsen, 2001) and the other had 24 two-bolt connections (Aalberg and Larsen, 2002). The plate thickness was

5 mm and the connection geometry of the one- and two-bolt connections of Kim and Yura (1999) were used. The width of specimens was chosen to ensure connection failure would be by bolt tear-out, and the variables were end distance and pitch. For the one-bolt connections, the clear end distance was varied from $0.5d_b$ to $2.0d_b$ in $0.5d_b$ increments, while for the two-bolt connections, the clear end distance was either $0.5d_b$ or $1.5d_b$ and the clear pitch was $1.0d_b$, $2.0d_b$, or $3.0d_b$ A total of 19 specimens met both the minimum end/edge distance and pitch requirements specified in North American standards. Three grades of steel with minimum yield strengths of 355 MPa, 700 MPa, and 1100 MPa were used in the tests. The detailed information is listed in Appendix A.

Observations of the final location of fracture were made from the tests. For small end distances, shear fracture took place along the two sides of the bolt hole (a bolt diameter apart), while for larger end distances, a tensile crack started at the free edge of the specimen within the region in front of the bolt and finally the specimen failed by the so-called “splitting action of the bolt”.

2.2.4 Puthli and Fleischer (2001)

A series of 25 tests on relatively thick plates (17.5 mm) was carried out on bolted connections that had two M27 bolts, with corresponding 30 mm bolt holes aligned perpendicular to the applied load (*i.e.*, two bolt lines and one bolt row). The end distance was chosen as 36 mm according to the minimum allowable limit of Eurocode 3 (1992), which is 1.2 times the hole diameter. However, this fixed end distance violates the minimum end distance requirement of CSA-S16-01 which is $1.5d_b$ by 11.1%.

Variables in the tests were edge distance, bolt spacing (gauge), and plate width. As expected, relatively small edge distances combined with a small gauge resulted in net section rupture, while relatively small edge distances with a large gauge or large edge distances with a small gauge resulted in block shear failure. Only relatively large edge distances and gauges resulted in bearing failure. Nine out of the 25 specimens failed in bearing, thus ultimately failed in bolt tear-out. A detailed description of the connections is listed in Appendix A.

Conclusions were made based on the test results. Tests showed that the reduction of bearing resistance for edge distances or/and gauges less than the minimum requirements in Eurocode 3 (1992) may not be necessary. Reduced minimum edge distance and gauge requirements were recommended.

2.2.5 Rex and Easterling (2003)

Rex and Easterling (2003) conducted 46 single bolt bearing tests in order to examine lap plate connection behaviour. For the 20 tests that ultimately failed in bolt tear-out, test variables included end distance (varied from 25 mm to 51 mm), plate thickness (6.5 mm and 9.5 mm), plate width (114 mm and 127 mm), bolt diameter (22 mm and 25 mm), and edge conditions (sheared or sawn). Material properties also varied (F_y varied from 299 MPa to 414 MPa, and F_u varied from 439 MPa to 690 MPa).

A model for approximating the load–deformation behaviour associated with plate bearing was developed in the research project.

2.2.6 Udagawa and Yamada (2004)

In order to investigate the effects of bolt hole arrangement and end distance of bolted connections on ultimate strength and failure mode, a total of 42 tests were conducted on channel sections, and five of them failed by bolt tear-out. Each of these five test specimens had only one bolt line in the web, and the number of bolt rows varied from two to four. Two different sizes of high strength bolt—M16 and M20—were used. The bolt pitch in these five specimens was $2.5d_b$, which slightly violates the minimum requirement of $2.7d_b$ specified in the North American design standards. Although the end distances used in the program varied from $2.5d_b$ to $4.5d_b$, the five specimens that failed in bolt tear-out all had the smallest value of end distance. A detailed description of the connections is listed in Appendix A.

Design equations with a series of semi-empirical strength coefficients for different failure modes were proposed based on the test results. For bolt tear-out failure, the prediction equation was based on the five one-line bolt tests. The bolt tear-out capacity is calculated

from the net shear area and the web tensile strength multiplied by a shear strength coefficient. The shear strength coefficient was a function of the ratio of connection length to the bolt diameter, and its proposed value varied from 0.50 to 0.46 for two bolt rows to four bolt rows.

2.3 Combined Modes and Atypical Failures in Bolted Connections

Typical failure modes for a steel tension member with bolted connections include net section rupture, gross section yielding, block shear, bolt tear-out, and bearing. However, there are connection failures that do not necessarily fit into one of the above mentioned categories.

For a wide-flange shape that is connected through both the web and flanges, failure involves both of these elements, and the web and flanges do not necessarily fail in the same mode. For example, the web bolts could tear-out and the flanges could exhibit block shear failure, as shown in Figure 2-2(a). Alternatively, the web and flanges could all fail in multi-block shear, as shown in Figure 2-2(b). These and other potential combined failure modes are demonstrated in more detail in Kato (2003b).

A previously undocumented failure mode observed in Tees connected only by their flanges was termed “alternate block shear” (ABS) failure by Epstein and Stamberg (2002). This atypical failure path is similar to traditional block shear of the flanges except that the shear plane develops in the stem instead of the flanges.

2.3.1 Kato (2003b)

Kato (2003b) reported the results of 15 tests that were conducted by Udagawa (1998) on high-strength bolted joints of H-to-H shapes. These wide-flange shapes were connected by both the web and flanges. The number of bolt lines in the web was either three or four, while the number of bolt rows was one or two. There was only one bolt line in each flange, and the number of bolt rows was either two or three. Five of the specimens, which all had only one row of bolts in the web, failed in a combination of bolt tear-out in the web and block shear in the flanges, while another seven specimens, which had either one or two bolt rows in the web, failed in multi-block shear in the web and each flange. The

remaining three specimens failed by net section rupture. The detailed information is listed in Appendix A.

Due to the difficulty of obtaining the original Japanese paper by Udagawa, nominal values of the cross-sectional properties and material properties were preliminarily used to analyze the test results, but the results were excluded from the final data pool since it would not give reliable results if assumed values were used to do the reliability analysis.

Kato (2003a) had developed an analysis method to predict the tensile strength and rupture modes for flat plates in his previous work. Kato (2003b) applied the method to shapes by transforming shapes into equivalent flat plates. Equations based on this method, with parameters obtained from the test results, were derived.

2.3.2 Epstein and Stamberg (2002)

A failure mode observed in Tees connected by bolts only through their flanges by Epstein and Stamberg (2002) was termed the alternate block shear failure path, as depicted in Figure 2-3. This failure is similar to traditional block shear except that it has only one shear plane in the Tee stem instead of two shear planes in the flanges adjacent to the lines of bolts. The tension fracture involved the entire flange and resulted in rupture of a single block of material. Variables in the test program were load eccentricity with respect to the centroid, which was influenced by the stem length of the Tees, flange and stem thicknesses, bolt gauge, and number of bolt rows. As a result of changing the variables, the mode of failure transitioned from net section rupture to the alternate block shear path. Fourteen out of 50 specimens failed in ABS, while the others failed in net section rupture. The detailed information is listed in Appendix A.

Test results indicated that as the eccentricity increased or/and the connection length decreased, the efficiency of the connection decreased.

2.4 Design Standards and Capacity Equation

There is no design equation in the current design standards in North America given explicitly for bolt tear-out failure, although the CISC Handbook of Steel Construction (CISC 2006) provides a design example using the block shear equations for bolt tear-out

failure. This approach is clearly based on the assumption that bolt tear-out failure is a type of block shear failure, but without the tension component. Due to the desire to unify these two modes along with the net section rupture mode, equations for both block shear failure and net section rupture are presented below.

2.4.1 CSA-S16-01 Block Shear and Net Section Rupture Equations

The CSA-S16-01 (CSA, 2001) design equations for block shear are based on the assumption that the available strength is the sum of the strengths along the tension plane and the shear plane(s). The block shear capacity in tension members is taken as the lesser of:

$$P_r = \phi A_{nt} F_u + 0.60 \phi A_{gv} F_y \qquad [2\text{-}1]$$

$$P_r = \phi A_{nt} F_u + 0.60 \phi A_{nv} F_u \qquad [2\text{-}2]$$

where:

P_r is the factored ultimate connection resistance;

ϕ is the resistance factor with a value of 0.9;

A_{nt} is the net tension area;

A_{gv} is the gross shear area;

A_{nv} is the net shear area.;

F_y is the material yield strength; and

F_u is the material ultimate strength.

Equation [2-1] applies when the net tension area reaches the ultimate tensile strength and the gross shear area reaches the yield shear strength. This phenomenon has been observed and proved by many researchers (*e.g.*, Franchuk *et al*., 2003). However, Equation [2-2], representing the development of the ultimate capacities of both the net tension and net shear areas, is not supported by test observations. On the contrary, experimental evidence (*e.g.*, Huns *et al.*, 2002) showed that tension fracture occurs before shear fracture and the ductility of materials in tension is inadequate to allow the shear ultimate stress to be reached. A load drop accompanied tension fracture and thereafter only the shear planes

carried the load. A slight increase in load was then observed as the shear planes continued to develop, but it never exceeds the peak load at tension fracture. This indicated that the shear stress has not reached ultimate shear stress at the peak. By the time the shear stress eventually reaches its ultimate value, the tension plane has already fractured and the peak load has passed.

Although design equations for bolt tear-out are not explicitly expressed in CSA-S16-01, the block shear equations can implicitly be used for this purpose. This means that the failure path consists of a pair of shear planes at the sides of each bolt as long as the end distance and pitch meet the minimum end/edge distance and pitch requirements. Since there is no tension plane in this case, Equations [2-1] and [2-2] become (the lesser of):

$$P_r = 0.60\phi A_{gv} F_y \qquad [2\text{-}3]$$

$$P_r = 0.60\phi A_{nv} F_u \qquad [2\text{-}4]$$

Currently, CSA-S16-01 provides a design equation for net section rupture as follows:

$$P_r = 0.85\phi A_{ne} F_u \qquad [2\text{-}5]$$

where:

A_{ne} is the effective net area reduced for shear lag.

When fasteners transmit loads to every cross-sectional element efficiently (*i.e.*, without significant shear lag effects), then $A_{ne} = A_n$, where A_n is net area. Otherwise, a shear lag factor from 0.6 to 0.9 is applied to A_n in order to obtain A_{ne}.

2.4.2 AISC 2005 Block Shear and Net Section Rupture Equations

The AISC LRFD Specification (AISC 2005) design equation for block shear failure is, in effect, identical to CSA-S16-01. It also assumes that the ultimate capacity of the tension plane can be reached on the net area and takes the concomitant shear plane capacity as $0.6F_y A_{gv}$, not to exceed $0.6F_u A_{nv}$. It can be expressed for tension members as follows:

$$P_r = \phi\,[A_{nt} F_u + 0.6A_{nv} F_u] \le \phi\,[A_{nt} F_u + 0.6A_{gv} F_y] \qquad [2\text{-}6]$$

and the AISC 2005 design equation for tensile rupture in the net section is as follows:

$$P_r = \phi A_{ne} F_u \qquad [2\text{-}7]$$

where:

ϕ is the resistance factor and is taken as 0.75 (LRFD) for both block shear and tensile rupture; and

$$A_{ne} = A_n U \qquad [2\text{-}8]$$

where:

U is the shear lag factor.

2.4.3 Unified Block Shear Equation

Based on a large database of experimental results from the literature, Kulak and Grondin (2001) observed that equations existing at that time were highly inconsistent in predicting the capacities of connections failing in block shear. To address this deficiency, Driver *et al.* (2006) proposed a single unified block shear equation that has been shown to provide excellent results for a variety of member and connection types failing in block shear, as well as consistent reliabilities. It represents the observation from tests that rupture on the net tension area occurs after yielding has taken place on the gross shear plane, but prior to shear rupture. Based on the test results of 42 gusset plate specimens, Hardash and Bjorhovde (1985) concluded that the ultimate shear stress on the gross shear area was appropriate for short connections, while the tendency is to approach the shear yield stress for long connections. Furthermore, they also concluded that the shear stress distribution is not uniform; it depends on the particular connection geometry and material. The authors recommended taking this into account by considering interpolation between the yield and ultimate shear stress. The effective shear stress in the unified equation is simply taken as the average of the shear yield and shear ultimate stresses to reflect this fact. For tension members with symmetrical blocks, it takes the following form:

$$P_r = \phi A_{nt} F_u + \phi A_{gv} \left(\frac{F_y + F_u}{2\sqrt{3}} \right) \quad [2\text{-}9]$$

where:

P_r is the factored ultimate connection resistance; and

ϕ is the resistance factor, proposed to be taken as 0.75 for block shear.

The unified block shear equation can be used for bolt tear-out failure by simply dropping the tension component, since no tension fracture is involved. The unified equation then becomes:

$$P_r = \phi A_{gv} \left(\frac{F_y + F_u}{2\sqrt{3}} \right) \quad [2\text{-}10]$$

The unified block shear equation can also be used for net section rupture by using the tension component only. The unified equation is consistent in form with both CSA-S16-01 (noting that 0.85ϕ in CSA-S16-01 is approximately equal to the proposed resistance factor for the unified equation of 0.75) and AISC 2005 (where the resistance factor is also 0.75):

$$P_r = \phi A_{nt} F_u \quad [2\text{-}11]$$

A shear lag factor must be applied if the connection configuration is such that shear lag is significant.

In conclusion, it is postulated that the unified block shear equation can be adopted for a truly unified equation that could be used for block shear, net section rupture, and bolt tear-out failures. Sufficient evidence for the use of the unified equation for block shear failure and net section rupture already exists and in this research project it is evaluated for use also with the bolt tear-out failure mode.

2.4.4 CSA-S16-01 Bolt Shear and Bearing Equations

In order to predict the strengths of the connections in this research that involve bolt shear and bolt bearing failure, the relevant existing design equations are utilized. As such, the

design equations in the Canadian standard are introduced in this section, and those in the American standard in the next section.

In Canadian standard S16-01 (CSA. 2001), the shear strength of a group of bolts, V_r, is calculated using the following equation:

$$V_r = 0.60\phi_b mnA_b F_u \qquad [2\text{-}12]$$

where:

ϕ_b is the resistance factor and is taken as 0.80;

m is the number of shear planes;

n is the total number of bolts in the connection; and

A_b is the nominal cross-sectional area of the bolt.

When the bolt threads are intercepted by a shear plane, the combined shear resistance of the bolts in a joint is taken as $0.70V_r$. Therefore, the shear strength of a single bolt in double-shear, with its threads in the shear planes, can be obtained as follows:

$$V_r = 2 \times 0.42\phi_b F_u A_b \qquad [2\text{-}13]$$

In CSA-S16-01, the bearing strength, B_r, for bolted connections is given as:

$$B_r = 3\phi_{br} t d_b n F_u \qquad [2\text{-}14]$$

where:

ϕ_{br} is the bearing resistance factor and is taken as 0.67; and

t is the thickness of the connected material.

In order to use Equation [2-14], the minimum end/edge distance and pitch requirements stated in CSA-S16-01 must be met. It may not seem reasonable for the bearing capacity of end bolts to be insensitive to the end distance, as implied by Equation [2-14]. However, the bolt tear-out strength equations usually govern for connections with small end distances.

2.4.5 AISC 2005 Bolt Shear and Bearing Equations

In the AISC Specification (AISC. 2005), the shear strength of a bolt, V_r, is calculated using the following equation:

$$V_r = \phi_b F_{nv} A_b \qquad [2\text{-}15]$$

where:

ϕ_b is taken as 0. 75; and

F_{nv} is the nominal shear stress capacity.

When threads are not excluded from the shear plane, F_{nv} is taken as $0.40F_u$. Therefore, the shear strength of a single bolt in double-shear, with its threads in the shear planes, can be obtained as follows:

$$V_r = 2 \times 0.4\phi_b F_u A_b \qquad [2\text{-}16]$$

Comparing Equations [2-13] and [2-16], it can be seen that the two design standards give very similar predictions of bolt shear capacity.

In AISC 2005, the bearing strengths at bolt holes have different coefficients depending on whether or not the deformation at the bolt hole at the service load is a design consideration. For the case where the deformation is not a design consideration, the bearing strength at a bolt hole can be calculated using the following equation:

$$B_r = 1.5\phi L_c t F_u \le 3.0\phi d_b t F_u \qquad [2\text{-}17]$$

where:

ϕ is taken as 0. 75; and

L_c is the clear end distance.

2.5 Summary

A number of laboratory tests have been conducted on plates that failed by bolt tear-out. Conversely, only a very small number were done on shapes and the available data is minimal for evaluating design equations for bolt tear-out in typical tension member connections. Furthermore, most connection configurations tested do not meet the minimum end distance and bolt spacing requirements specified in North American design standards. Appendix A lists published test results that include 135 tests on plates (Table A-1) and five tests on channels (Table A-1) failing by bolt tear-out (often characterised as bearing failures). Another 12 tests on wide-flange shapes (Table A-2) involving combined failure modes and 14 tests on Tees (Table A-3) failing along the alternate block shear path are also listed in Appendix A. In order to understand the behaviour of bolt tear-out failure better and provide test data for realistic bolt configurations (rather than one or two bolts connections), more research on shapes for this failure mode is required.

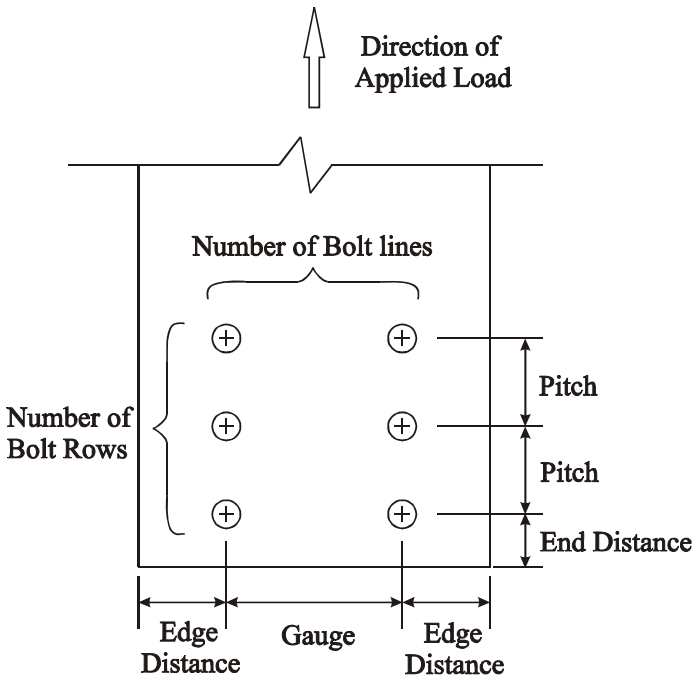

Figure 2-1: Definitions of Dimensional Parameters

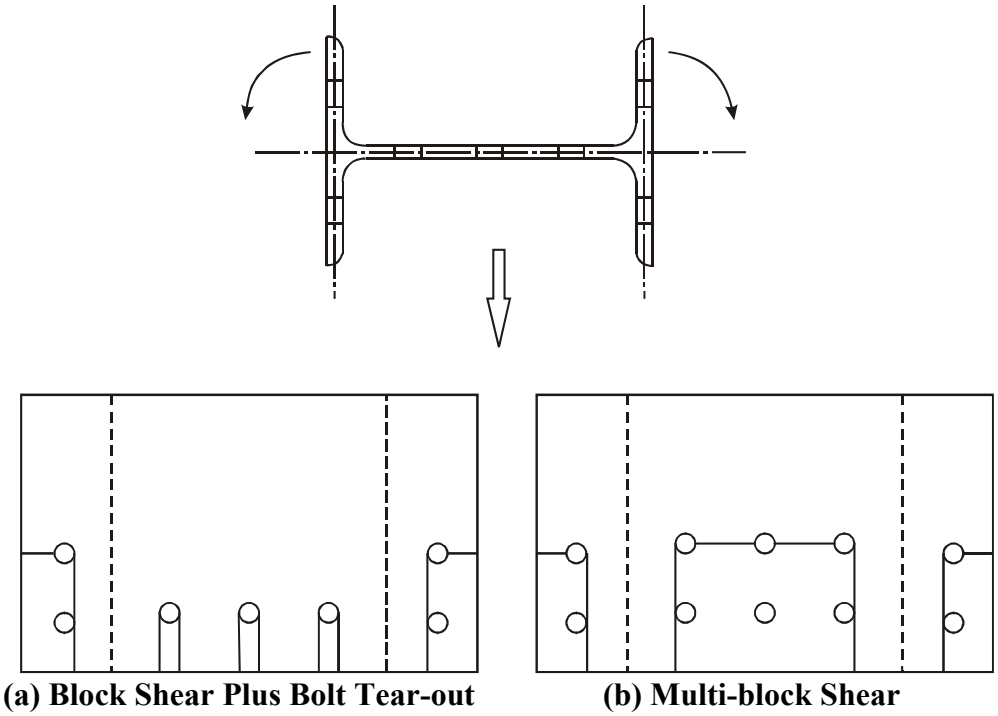

(a) Block Shear Plus Bolt Tear-out **(b) Multi-block Shear**

Figure 2-2: Combined Failures in Wide-Flange Shape

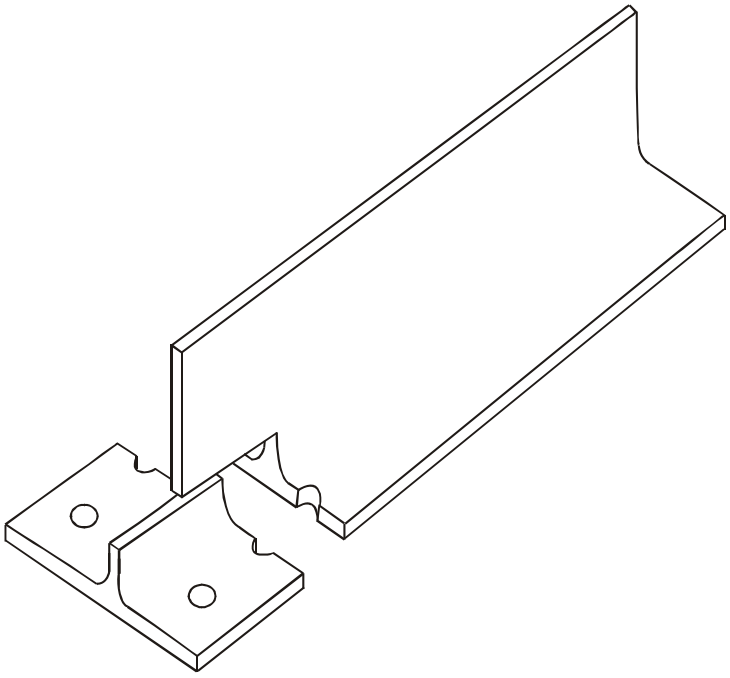

Figure 2-3: Alternate Block Shear (ABS) Path in Tees

3. EXPERIMENTAL PROGRAM

3.1 Introduction

In order to investigate the strength and behaviour of end tear-out failure in bolted connections, a number of physical tests were carried out as a part of this research project. Test specimens were designed to examine the effects of a number of variables, which were limited to meet the requirements in design standards in North America, on connection strength. The main purpose of this experimental program is to assess the ability of the current block shear equations in design standards in North America and the unified equation to predict the capacity of connections that fail either by bolt tear-out or by a combination mode that includes bolt tear-out. Additionally, it also expands the pool of available experimental data.

The experimental program consisted of a total of 50 tests on wide-flange specimens and was carried out in three separate series. Series A had 12 specimens, which were connected through the web only and were expected to fail by bolt tear-out, while series B had six specimens connected by both the web and flanges, which were expected to fail in a combination of bolt tear-out in the web and block shear in the flanges. Most specimens in series A are duplicates that allow a check on repeatability. Series C consisted of 32 web-connected wide-flange specimens donated by Waiward Steel Fabricators Ltd. and designed by Waiward engineer Logan Callele to assess the economics of their design practice for these types of connections. Specifically, this series investigated the behaviour of bolt groups with different end distances and material thicknesses in order to clarify how connections that fail by bolt tear-out in only the end bolts, resulting in a sequential failure, should be designed. This chapter describes the test objectives, specimens, test set-up, instrumentation, and ancillary tests.

3.2 Test Objectives

Each of the three test series had separate, but complementary, objectives. The main objectives of the series A tests are to evaluate the accuracy and suitability of current block shear equations in North American design standards and the unified equation for pure bolt tear-out failure and to make a recommendation for incorporation into design standards. The main objectives of the series B tests are to examine the behaviour of

bolted connections that fail in a combination of two distinct modes and to verify the strength additive criteria for bolt tear-out failure in the web and block shear failure in the flanges of W-shapes. The main objectives of the series C tests are to clarify how the end distance affects the behaviour of a bolt group that may involve more than one failure mode and to provide design guidelines that reflect the sequence of failure at the individual fasteners.

3.3 Description of Test Specimens

3.3.1 Specimen Designations

A description of specimen designations is listed in Table 3-1. The first upper case letter of a specimen designation—A, B, or C—denotes the test series, and the second upper case letter represents the variable being studied: “G” for gauge, “E” for end distance, or “R” for the number of bolt rows in the web. The lower case letter—a, b, or c—represents the triplicate specimens in series C.

3.3.2 Connection Geometry and Parametric Variables

In bolted connections, bolt tear-out failure occurs when the available strength of all shear planes is less than any one of the other strength combinations of shear planes and tension plane. The strength of the shear planes is determined by the number of bolt lines and rows, end distance, and pitch for a certain type of connection. Gauge has little effect on the ultimate capacity of the connection if the bolt tear-out failure mode governs the connection capacity. However, gauge plays an important role in changing failure modes; a relatively small gauge may change the failure mode to block shear instead of bolt tear-out.

Specimens in series A and B were designed to ensure that web bolt tear-out failure would occur. A few factors were considered in selecting the sections. First, the sections should be practical; thus, they should be realistic for use in structures as tension members. Second, a relatively deep section is required to ensure that the gauge distance can be large enough so that bolt tear-out in the web is the governing failure mode instead of block shear. Third, very thick webs and flanges could not be used without shifting the limit state to shear failure of the structural bolts. Three types of wide-flange rolled shape—

$W310\times60$, $W310\times39$ and $W250\times49$—were used in series A and B, and the nominal and as-built sectional properties are listed in Table 3-2. As shown in the table, specimens of different sections in series A and B had different web and flange thicknesses ranging from 5.8 mm to 7.5 mm and 9.7 mm to 13.1 mm, respectively. In each series, groups of identical shapes were tested, each with only one variable parameter: either gauge, the number of bolt rows, or end distance.

The bolts in series A and B had diameters of 19.1 mm (3/4") and 22.2 mm (7/8"), respectively, and this resulted in different pitches in these two series since both CSA-S16-01 and AISC 2005 specify that the bolt pitch should not be less than $2.7d_b$ Pitches as fixed parameters in series A and B were 54 mm (2-1/8") and 60 mm (2-3/8") correspondingly. Pitches near the minimum permissible value were required to ensure the desired failure mode. The minimum end distances specified in CSA-S16-01 and AISC 2005 are 25 mm for 3/4" bolts and 28 mm for 7/8" bolts for gas-cut edges. The end distance used in the tests was 28.6 mm (1-1/8") for both series, except for the specimens where end distance was taken as a variable and the increased end distance was 44.5 mm (1-3/4"). Additionally, CSA-S16-01 also specifies that the end distance should be not less than $1.5d_b$ for connections that have either one or two bolts in a bolt line. However, AISC 2005 does not have this requirement. It was decided to use an end distance in Series B of 28.6 mm, which slightly violates this requirement in CSA-S16-01 by 4.7 mm (but meet the AISC 2005 end distance requirements) to ensure that bolt tear-out failure in the web would be the governing mode. All bolt holes were drilled and of standard size, namely 20.6 mm (13/16") for 3/4" bolts and 23.8 mm (15/16") for 7/8" bolts.

Two different cross sections of rolled wide-flange shape—$W250\times58$ and $W310\times39$—were used in test series C. Specimens in series C had a relatively large fixed pitch, as compared to those in series A and B, of 152 mm (6"). For each of the two wide-flange shapes, the only variable was the end distance, and the various values are denoted as E1 to E6. E1 to E5 varied from 25.4 mm (1") to 50.8 (2") with 6.4 mm (1/4") increments, and E6 had an end distance of 69.9 mm (2-3/4"). All specimens in Series C were tested in triplicate except for the two that had the largest end distance (E6), which were considered

control specimens where the failure was expected to occur in the bolts themselves for thicker web sections and in bearing behind the bolts for thinner web sections.

The nominal dimensions of the specimens in series A, B, and C are demonstrated in Figures 3-1 to 3-3, respectively, and as-built web and flange connection dimensions are listed in Tables 3-3a and 3-3b, respectively.

3.4 Test Set-Up

An overall view of the test set-up and a schematic diagram of the test assembly configuration for series A are shown in Figure 3-4, while for series B they are shown in Figure 3-5. The test arrangement of series C is identical to that of series A. All specimens were 1220 mm (48") long. The test set-up was designed to simulate a typical bolted connection in a tension bracing member or truss member.

Figure 3-4 shows a series A test specimen assembly consisting of the wide-flange shape test specimen and four clevis plates. Two 25.4 mm (1") thick clevis plates at each end were connected to the testing machine through a pin connection to transfer the applied load. The overall lengths of clevis plates are 508 mm (20") and 610 mm (24") at the test end and the non-test end, respectively. The widths of the clevis plates are 229 mm (9") for specimens A1 to A4 and A7 to A10, and 191 mm (7-1/2") for specimens A5, A6, A11, and A12. All the clevis plates remained elastic during the tests.

Figure 3-5 shows a series B test specimen assembly, which consists of the wide-flange shape test specimen, a wide-flange shape splice complement (the same section as test specimen), two web splice plates, two outside flange splice plates, four inside flange splice plates, and four clevis plates.

The dimensions of the web splice plates are 333 mm ×191 mm ×12.7 mm (13-1/8"×7-1/2"×1/2") for B5 and B6, 333 mm ×229 mm ×12.7 mm (13-1/8"×9"×1/2") for B1, and 394 mm ×229 mm ×12.7 mm (15-1/2"×9"×1/2") for B2 to B4. The dimensions of the outside flange splice plates are 394 mm ×203 mm ×19 mm (15-1/2"×8"×3/4") for B1, B2, B5, and B6, and 394 mm ×165 mm ×19 mm (15-1/2"×6-1/2"×3/4") for B3 and B4. The dimensions of inside flange splice plates are

400 mm ×90 mm ×12.7 mm (15-3/4"×3-1/2"×1/2") for B2 to B5. The dimensions of clevis plates are 1118 mm ×229 mm ×32 mm (44"×9"×1-1/4") for B1 to B4, and 1118 mm ×191 mm ×32 mm (44"×7-1/2"×1-1/4") for B5 and B6. Both clevis plate widths enlarged to 254 mm (10") at the pin end to avoid pin connection failure.

The test set-up for series C is similar to that of series A. The clevis plates used in series C have a thickness of 32 mm (1-1/4"). The lengths of clevis plates are 711 mm (28") at the test end and 787 mm (31") at the non-test end. The widths of clevis plates are 191 mm (7-1/2") for specimens C1 to C16, and 229 mm (9") for specimens C17 to C32. All the clevis plates remained elastic during the tests.

Bolts in series A and B had standard thread lengths that excluded the threads from the shear planes, and were tightened to the snug-tight condition as stated in CSA-S16-01. The bolt shanks in series C were fully threaded in order to provide a well-defined upper bound capacity of the connections (bolt shear failure). In all tests, clevis plates were first installed and connected to the testing machine, followed by the test specimen and splice complement for a series B specimen. For series A and C specimens, a specimen was fastened loosely to the clevis plates at both ends using 3/4" A490 bolts or 3/4" A325 bolts, respectively. For series B specimens, a specimen and its splice complement were fastened loosely to clevis plates at both ends using 3/4" A490 bolts, and the specimen and splice complement were then connected together by web and flange splice plates using 7/8" A490 bolts. All bolts were installed in the finger tight condition at this stage.

After the specimen and its attachments were centred and seated in the MTS 6000 testing machine, all bolts were tightened to a snug-tight condition with an open-ended wrench.

3.5 Instrumentation

The load applied to the test specimens was monitored using the internal load cell of the testing machine. Measurements of the relative displacement between the specimen and the splice plate were taken by LVDTs, which were mounted at different locations to obtain an average reading. For specimens in series A and C, two identical LVDTs were

mounted on each side of a specimen; while for specimens in series B, an additional two identical LVDTs were mounted on the outside of each flange.

As shown in Figure 3-6, LVDT holders in series A were welded at the edges of the clevis plates at the same level as the end of the specimen, and the references were on the specimen web at the centreline of the last bolt row. The arrangement for series C was similar except that the references were on the flanges instead of the web. Figure 3-7 shows that LVDT holders in series B were welded at the edges of the splice plates at the location of the centreline of the last bolt row (note that the elevation is therefore the same for the web and the flanges only for specimen B4, which had two rows of bolts in the web), and the references were at the end of the specimen. At each of the flange reference points, an L-shaped bracket tack welded to the flange tip was used in order to clear the splice plate as the connection deformed. Photographs of the positions of the LVDTs in series A, B and C are shown in Figure 3-8. LVDTs captured connection slip, bolt bearing distortions, and deformations in the test region.

3.6 Ancillary Tests

The specimens came to the lab in two shipments. Specimens of same cross-section and shipment are from the same heat of steel. The first shipment included specimens A1 to A6 and the series C specimens, and the remaining specimens (A7 to A12, and B1 to B6) came in the second shipment.

Tension coupons were fabricated from both the web and flanges of each section to obtain the actual material properties. For each section from the same heat, three sheet-type coupons (ASTM, 2007) were taken from the web and an additional three sheet-type coupons were taken from the flanges if connection failure also involved the flanges (series B). The coupons were oriented parallel to the axis of the tension members in all cases. A 50 mm gauge extensometer was mounted on each coupon to obtain the strain readings, and stress was calculated using the measured initial area of the coupon. Tension coupons were tested as per the specifications outlined in ASTM standard A370 (ASTM, 2007). A summary of ancillary test results is provided in Table 3-4.

In the series C tests, fully threaded 3/4" A325 bolts were used in the double-shear condition. It was anticipated that bolt shear failure would occur in some series C tests, especially for the specimens with the thicker webs. In order to predict bolt shear capacities using equations from the design standards, six standard tension coupons were fabricated from bolts of the same lot and tested as per the specifications outlined in ASTM standard A370 (ASTM, 2007) to obtain the actual ultimate tensile strength. These six tension coupons gave very similar stress–strain curves, with the average ultimate tensile strength of 912 MPa. Two supplementary double-shear individual bolt tests were also conducted to obtain the bolt double-shear strength directly, with an average value of 223 kN.

Table 3-1: Specimen Designations

Specimen	Cross Section	Bolt configuration		Specimen	Cross Section	Bolt configuration	
		Web	Flange			Web	Flange
A1G1	W310×60	W2×2	–	C8E3b	W250×58	W2×3	–
A2G1	W310×60	W2×2	–	C9E3c	W250×58	W2×3	–
A3R1	W310×39	W2×2	–	C10E4a	W250×58	W2×3	–
A4R2	W310×39	W2×3	–	C11E4b	W250×58	W2×3	–
A5E1	W250×49	W2×2	–	C12E4c	W250×58	W2×3	–
A6E2	W250×49	W2×2	–	C13E5a	W250×58	W2×3	–
A7G1	W310×60	W2×2	–	C14E5b	W250×58	W2×3	–
A8G2	W310×60	W2×2	–	C15E5c	W250×58	W2×3	–
A9R1	W310×39	W2×2	–	C16E6	W250×58	W2×3	–
A10R2	W310×39	W2×3	–	C17E1a	W310×39	W2×3	–
A11E1	W250×49	W2×2	–	C18E1b	W310×39	W2×3	–
A12E2	W250×49	W2×2	–	C19E1c	W310×39	W2×3	–
B1G1	W310×60	W2×1	F1×2	C20E2a	W310×39	W2×3	–
B2G2	W310×60	W2×1	F1×2	C21E2b	W310×39	W2×3	–
B3R1	W310×39	W2×1	F1×2	C22E2c	W310×39	W2×3	–
B4R2	W310×39	W2×2	F1×2	C23E3a	W310×39	W2×3	–
B5E1	W250×49	W2×1	F1×2	C24E3b	W310×39	W2×3	–
B6E2	W250×49	W2×1	F1×2	C25E3c	W310×39	W2×3	–
C1E1a	W250×58	W2×3	–	C26E4a	W310×39	W2×3	–
C2E1b	W250×58	W2×3	–	C27E4b	W310×39	W2×3	–
C3E1c	W250×58	W2×3	–	C28E4c	W310×39	W2×3	–
C4E2a	W250×58	W2×3	–	C29E5a	W310×39	W2×3	–
C5E2b	W250×58	W2×3	–	C30E5b	W310×39	W2×3	–
C6E2c	W250×58	W2×3	–	C31E5c	W310×39	W2×3	–
C7E3a	W250×58	W2×3	–	C32E6	W310×39	W2×3	–

Table 3-2: Sectional Properties for Series A, B, and C

Section	Specimen	Section Depth (mm)		Flange Width (mm)		Web Thickness (mm)		Flange Thickness (mm)	
		Nominal	Measured	Nominal	Measured	Nominal	Measured	Nominal	Measured
W310X60	A1G1	303	305.4	203	202.7	7.5	7.48	13.1	13.09
	A2G1	303	305.4	203	202.7	7.5	7.52	13.1	13.20
	A7G1	303	304.0	203	202.6	7.5	7.43	13.1	13.11
	A8G2	303	304.5	203	202.7	7.5	7.44	13.1	13.12
	B1G1	303	304.7	203	202.5	7.5	7.52	13.1	13.16
	B2G2	303	304.5	203	202.6	7.5	7.45	13.1	13.34
W310X39	A3R1	310	310.0	165	165.1	5.8	6.30	9.7	9.45
	A4R2	310	309.7	165	164.5	5.8	6.22	9.7	9.39
	A9R1	310	311.6	165	163.0	5.8	6.54	9.7	9.29
	A10R2	310	311.5	165	163.0	5.8	6.55	9.7	9.21
	B3R1	310	311.5	165	162.8	5.8	6.45	9.7	9.20
	B4R2	310	311.5	165	162.7	5.8	6.63	9.7	9.21
W250X49	A5E1	247	248.5	202	203.2	7.4	7.55	11.0	10.38
	A6E2	247	248.0	202	203.0	7.4	7.51	11.0	10.37
	A11E1	247	249.9	202	203.6	7.4	7.30	11.0	10.77
	A12E2	247	249.5	202	203.5	7.4	7.34	11.0	10.69
	B5E1	247	249.6	202	203.3	7.4	7.29	11.0	10.66
	B6E2	247	249.5	202	203.3	7.4	7.34	11.0	10.64
W250X58	C1E1a	252	254.8	203	203.2	8.0	9.09	13.5	12.79
	C2E1b	252	254.3	203	203.3	8.0	9.16	13.5	12.64
	C3E1c	252	254.3	203	203.2	8.0	9.15	13.5	12.64
	C4E2a	252	254.1	203	203.6	8.0	9.10	13.5	12.53
	C5E2b	252	254.4	203	203.5	8.0	9.20	13.5	12.59
	C6E2c	252	254.1	203	203.7	8.0	9.08	13.5	12.44
	C7E3a	252	254.0	203	203.3	8.0	9.06	13.5	12.46

Table 3-2: Sectional Properties for Series A, B, and C (Cont'd)

Section	Specimen	Section Depth (mm)		Flange Width (mm)		Web Thickness (mm)		Flange Thickness (mm)	
		Nominal	Measured	Nominal	Measured	Nominal	Measured	Nominal	Measured
W250X58	C8E3b	252	254.0	203	203.3	8.0	9.08	13.5	12.52
	C9E3c	252	254.3	203	203.4	8.0	9.14	13.5	12.47
	C10E4a	252	254.3	203	203.2	8.0	9.08	13.5	12.38
	C11E4b	252	254.9	203	203.5	8.0	9.16	13.5	12.69
	C12E4c	252	254.6	203	–*	8.0	9.13	13.5	12.65
	C13E5a	252	254.5	203	203.3	8.0	9.11	13.5	12.70
	C14E5b	252	254.2	203	203.8	8.0	9.13	13.5	12.61
	C15E5c	252	254.4	203	203.5	8.0	9.09	13.5	12.63
	C16E6	252	254.4	203	203.8	8.0	9.12	13.5	12.57
W310X39	C17E1a	310	312.0	165	164.7	5.8	5.90	9.7	9.26
	C18E1b	310	311.8	165	164.6	5.8	5.86	9.7	9.21
	C19E1c	310	311.8	165	164.5	5.8	5.90	9.7	9.28
	C20E2a	310	311.9	165	164.6	5.8	5.91	9.7	9.20
	C21E2b	310	312.0	165	164.6	5.8	5.89	9.7	9.13
	C22E2c	310	312.1	165	164.5	5.8	5.90	9.7	9.19
	C23E3a	310	311.9	165	164.9	5.8	6.03	9.7	9.13
	C24E3b	310	312.2	165	165.0	5.8	5.97	9.7	9.20
	C25E3c	310	311.6	165	164.6	5.8	5.90	9.7	9.14
	C26E4a	310	312.3	165	164.9	5.8	6.04	9.7	9.19
	C27E4b	310	312.1	165	164.9	5.8	5.99	9.7	9.15
	C28E4c	310	312.1	165	164.7	5.8	5.94	9.7	9.15
	C29E5a	310	312.1	165	164.7	5.8	5.87	9.7	9.19
	C30E5b	310	312.1	165	164.7	5.8	5.90	9.7	9.09
	C31E5c	310	312.1	165	164.6	5.8	5.92	9.7	9.11
	C32E6	310	312.0	165	164.6	5.8	5.99	9.7	9.20

* Flange width not measured (note that flange widths are not required for series C strength calculations)

Table 3-3a: As-Built Web Connection Dimensions for Series A, B and C

Specimen	Gauge			End-Distance		Pitch				Hole Dia.
	g_{W1} (mm)	g_{W2} (mm)	g_{W3} (mm)	e_{1WL} (mm)	e_{1WR} (mm)	p_{WL1} (mm)	p_{WL2} (mm)	p_{WR1} (mm)	p_{WR2} (mm)	d_0* (mm)
A1G1	140.6	140.5	–	28.07	28.52	54.23	–	54.38	–	20.62
A2G1	139.8	139.9	–	29.14	29.40	54.31	–	53.88	–	20.57
A3R1	178.8	178.8	–	27.99	28.30	53.79	–	53.81	–	20.40
A4R2	178.6	178.6	178.6	28.24	28.37	54.14	54.03	54.30	53.86	20.56
A5E1	140.0	140.1	–	31.44	30.58	54.12	–	54.12	–	20.50
A6E2	140.0	140.0	–	47.82	47.64	54.12	–	54.16	–	20.53
A7G1	139.5	139.9	–	28.45	28.65	54.04	–	53.57	–	20.75
A8G2	177.7	177.8	–	27.15	26.96	54.10	–	54.11	–	20.75
A9R1	178.2	178.2	–	27.57	27.56	53.58	–	53.52	–	20.66
A10R2	178.1	178.2	178.0	27.32	26.82	54.59	53.88	54.47	54.24	20.79
A11E1	140.2	140.1	–	28.24	28.30	54.00	–	57.47	–	20.58
A12E2	139.9	139.9	–	44.05	44.00	54.51	–	57.19	–	20.73
B1G1	139.8	–	–	27.95	28.03	–	–	–	–	23.81
B2G2	177.7	–	–	27.61	27.84	–	–	–	–	23.85
B3R1	178.4	–	–	29.10	28.85	–	–	–	–	23.70
B4R2	178.3	178.3	–	27.35	27.76	60.51	–	60.32	–	23.67
B5E1	139.5	–	–	28.59	28.28	–	–	–	–	23.69
B6E2	139.6	–	–	44.51	44.23	–	–	–	–	23.61
C1E1a	138.9	139.7	138.5	25.33	25.33	152.6	152.4	152.3	152.3	20.41
C2E1b	139.2	139.3	139.2	25.51	25.45	152.5	152.3	152.4	152.4	20.45
C3E1c	139.0	139.1	139.0	25.47	25.54	152.6	152.5	152.6	152.5	20.58
C4E2a	139.0	139.2	138.9	31.80	31.76	152.5	152.3	152.6	152.7	20.59
C5E2b	138.8	138.7	138.8	32.12	31.93	152.9	152.0	152.8	151.7	20.59
C6E2c	138.8	138.9	138.9	32.02	31.79	152.3	152.1	152.1	152.4	20.44
C7E3a	139.5	139.6	139.4	38.20	38.11	152.5	152.3	152.3	152.4	20.41
C8E3b	138.9	138.9	138.9	38.14	38.15	152.7	152.4	152.6	152.5	20.61
C9E3c	140.2	140.1	139.7	38.22	38.37	152.5	152.3	152.5	152.4	20.69
C10E4a	139.9	139.9	139.9	44.76	44.62	152.1	152.3	152.3	152.1	20.54
C11E4b	138.8	138.9	139.0	44.39	44.37	152.5	152.0	152.5	152.1	20.39
C12E4c	139.1	139.1	139.1	44.57	44.50	152.4	152.3	152.6	152.3	20.59
C13E5a	139.7	139.7	139.7	50.82	50.92	152.4	152.3	152.5	152.4	20.53
C14E5b	138.9	138.8	138.8	50.92	50.83	152.4	152.3	152.4	152.5	20.51
C15E5c	139.1	139.1	139.2	50.99	51.03	152.6	152.5	152.5	152.4	20.61
C16E6	139.5	139.7	139.7	69.94	70.07	152.7	152.3	152.7	152.2	20.60
C17E1a	177.3	177.3	177.4	25.62	25.39	152.3	152.4	152.3	152.6	20.51
C18E1b	177.4	177.4	177.5	25.50	25.58	152.3	152.5	152.7	152.5	20.65
C19E1c	177.8	178.8	178.7	25.55	25.55	152.3	152.2	152.6	151.9	20.57

Table 3-3a: As-Built Web Connection Dimensions for Series A, B and C (Cont'd)

Specimen	Gauge			End-Distance		Pitch				Hole Dia.
	g_{W1} (mm)	g_{W2} (mm)	g_{W3} (mm)	e_{1WL} (mm)	e_{1WR} (mm)	p_{WL1} (mm)	p_{WL2} (mm)	p_{WR1} (mm)	p_{WR2} (mm)	d_0* (mm)
C20E2a	177.2	177.1	177.2	31.87	31.87	152.3	152.4	152.4	152.3	20.60
C21E2b	177.6	177.6	177.6	31.89	31.92	152.5	152.4	152.8	152.2	20.59
C22E2c	177.6	177.8	177.7	31.93	31.95	152.6	152.4	152.9	152.1	20.62
C23E3a	177.5	177.5	177.5	38.15	38.16	152.5	152.2	152.4	152.2	20.61
C24E3b	177.3	177.2	177.2	37.96	37.88	152.4	152.2	152.1	152.6	20.42
C25E3c	177.2	177.2	177.2	38.05	38.06	152.8	151.7	152.5	152.0	20.41
C26E4a	177.5	177.6	177.5	44.52	44.79	152.3	152.7	152.5	152.3	20.66
C27E4b	177.5	177.4	177.5	44.81	44.83	152.3	152.5	152.2	152.5	20.62
C28E4c	177.3	177.3	177.3	44.57	44.63	152.3	152.6	152.2	152.6	20.53
C29E5a	177.4	177.5	177.6	50.91	50.91	152.0	152.5	152.5	152.6	20.48
C30E5b	177.7	177.7	177.6	50.89	50.84	152.9	152.1	152.7	152.2	20.57
C31E5c	177.6	177.8	177.8	50.90	50.63	152.5	152.1	152.4	152.3	20.52
C32E6	177.3	177.3	177.3	70.17	70.24	152.7	152.5	152.8	152.3	20.60

* Mean diameter for all bolt holes in the connection

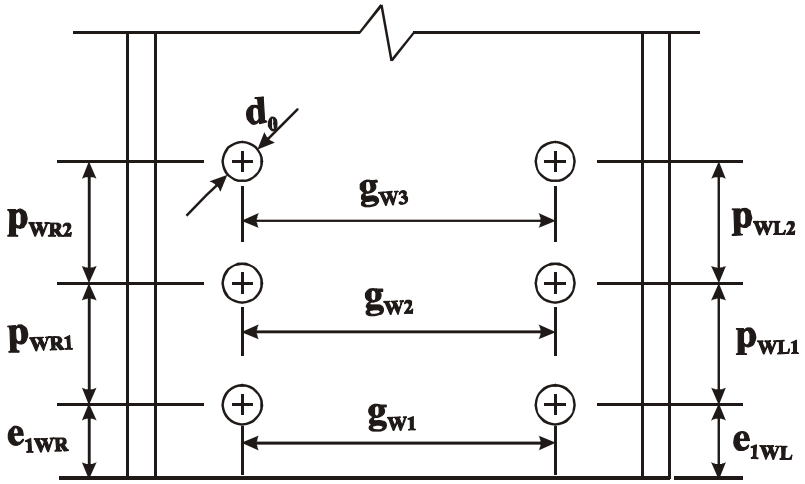

Table 3-3b: As-Built Flange Connection Dimensions for Series B

Specimen	Left Flange							Right Flange						
	Gauge		End-Distance	Pitch		Edge-Distance		Gauge		End-Distance	Pitch		Edge-Distance	
	g_{FL1} (mm)	g_{FL2} (mm)	e_{1FL} (mm)	p_{FL1} (mm)	p_{FL2} (mm)	e_{2FL1} (mm)	e_{2FL2} (mm)	g_{FR1} (mm)	g_{FR2} (mm)	e_{1FR} (mm)	p_{FR1} (mm)	p_{FR2} (mm)	e_{2FR1} (mm)	e_{2FR2} (mm)
B1G1	127.1	126.9	27.83	59.81	60.20	34.51	40.38	126.6	126.7	26.61	59.98	59.96	35.20	39.98
B2G2	126.6	126.8	27.64	59.69	59.90	34.57	40.39	127.0	126.8	26.82	59.98	60.19	35.61	39.81
B3R1	101.3	101.3	28.87	60.01	59.94	30.66	30.70	101.4	101.1	27.43	60.14	59.76	30.54	30.31
B4R2	101.3	101.3	27.99	60.34	60.26	31.18	30.01	101.7	101.0	27.16	60.02	60.25	29.80	30.60
B5E1	126.4	126.6	28.68	59.63	59.95	38.89	36.75	126.7	126.7	27.60	60.36	60.10	36.58	39.71
B6E2	126.8	126.7	44.33	60.22	60.05	38.66	36.80	126.8	126.7	43.50	60.21	60.44	39.95	36.21

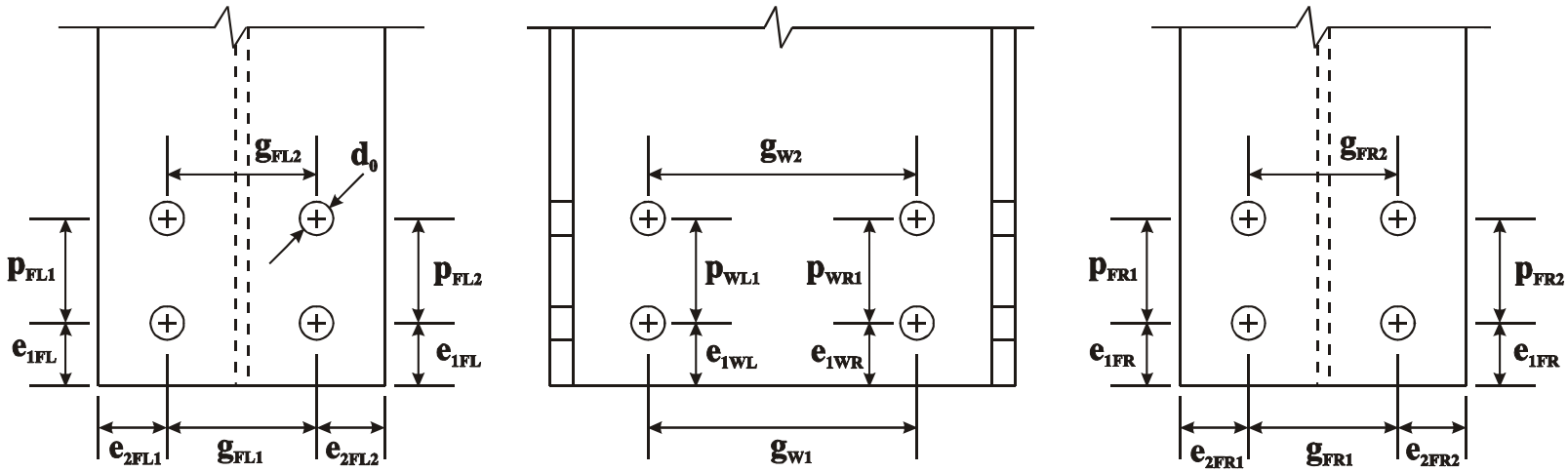

Table 3-4: Ancillary Test Results

Coupon Mark			Elastic Modulus (MPa)	Static Yield 1 (MPa)	Static Yield 2 (MPa)	Static Yield 3 (MPa)	Mean Static Yield (MPa)	Static Ultimate (MPa)	Rupture Strain (%)	Reduction of Area (%)
W310X60	A1/A2 Web	Ma1	204 400	447	440	–	444	521	31.3	55.9
		Ma2	202 000	434	433	427	431	515	29.7	55.6
		Ma3	199 200	445	442	441	443	522	29.6	53.8
		Mean	201 900	–	–	–	439	519	30.2	55.1
	A7/A8/B1/B2 Web	Ma16	193 600	420	421	417	419	501	30.3	57.5
		Ma17	191 300	403	402	404	403	485	32.6	60.6
		Ma18	203 500	411	412	410	411	497	30.5	59.9
		Mean	196 100	–	–	–	411	494	31.1	59.2
	B1/B2 Flange	Ma19	207 700	352	351	353	352	470	38.8	64.5
		Ma20*	–	–	–	–	–	470	–	63.3
		Ma21	195 800	350	352	352	351	469	37.5	65.5
		Mean	201 800	–	–	–	352	470	38.2	64.4
	B1/B2 Web & Flange Mean		198 900	–	–	–	382	482	34.7	62.1
W250X49	A5/A6 Web	Ma7	212 700	348	355	349	351	488	31.8	57.4
		Ma8	202 900	338	341	344	341	487	29.3	55.1
		Ma9**	–	340	334	339	338	488	26.7	53.1
		Mean	207 800	–	–	–	343	487	29.3	55.2
	A11/A12/B5/B6 Web	Ma28	200 000	373	376	374	374	498	34.2	58.9
		Ma29	205 600	380	381	380	380	499	28.7	58.6
		Ma30	198 200	376	373	373	374	503	31.0	61.8
		Mean	201 300	–	–	–	376	500	31.3	59.8
	B5/B6 Flange	Ma31	207 000	346	344	–	345	490	34.8	62.2
		Ma32	217 400	345	348	345	346	494	38.0	61.8
		Ma33	209 500	344	345	344	345	493	36.3	63.0
		Mean	211 300	–	–	–	345	492	36.4	62.3
	B5/B6 Web & Flange Mean		206 300	–	–	–	361	496	33.9	61.1

Table 3-4: Ancillary Test Results (Cont'd)

Coupon Mark			Elastic Modulus (MPa)	Static Yield 1 (MPa)	Static Yield 2 (MPa)	Static Yield 3 (MPa)	Mean Static Yield (MPa)	Static Ultimate (MPa)	Rupture Strain (%)	Reduction of Area (%)
W310X39	A3/A4 Web	Ma4	203 900	378	381	376	378	475	34.7	62.5
		Ma5	205 400	384	379	–	381	472	30.1	55.8
		Ma6	211 100	380	375	–	378	471	31.6	58.0
		Mean	206 800	–	–	–	379	472	32.13	58.8
	A9/A10/B3/B4 Web	Ma22	207 700	377	377	376	377	486	–	62.5
		Ma23	201 000	352	354	349	352	469	37.1	63.2
		Ma24	204 900	377	378	378	378	480	36.2	63.2
		Mean	204 500	–	–	–	369	478	36.7	63.0
	C17-C32 Web	Ma13	209 000	372	375	376	374	465	36.0	62.0
		Ma14**	–	369	369	369	369	460	31.2	63.1
		Ma15	205 100	373	374	373	373	456	33.4	59.0
		Mean	207 100	–	–	–	372	457	35.5	61.4
	B3/B4 Flange	Ma25	201 700	344	345	343	344	467	38.5	67.7
		Ma26	204 200	344	344	343	343	474	37.9	66.1
		Ma27	207 400	338	330	–	334	469	38.5	66.2
		Mean	204 400	–	–	–	340	470	38.3	66.7
	B3/B4 Web & Flange Mean		204 500	–	–	–	355	474	36.9	64.9
W250X58	C1-C16 Web	Ma10	201 300	397	400	394	397	511	32.3	62.1
		Ma11	206 800	401	393	400	398	512	31.9	59.7
		Ma12	205 200	395	396	395	395	511	33.8	61.7
		Mean	204 400	–	–	–	397	511	32.7	61.2

* Coupon Ma20 was found to be bent slightly prior to testing

** Accurate measurements were not obtained in the elastic region for coupons Ma9 and Ma14

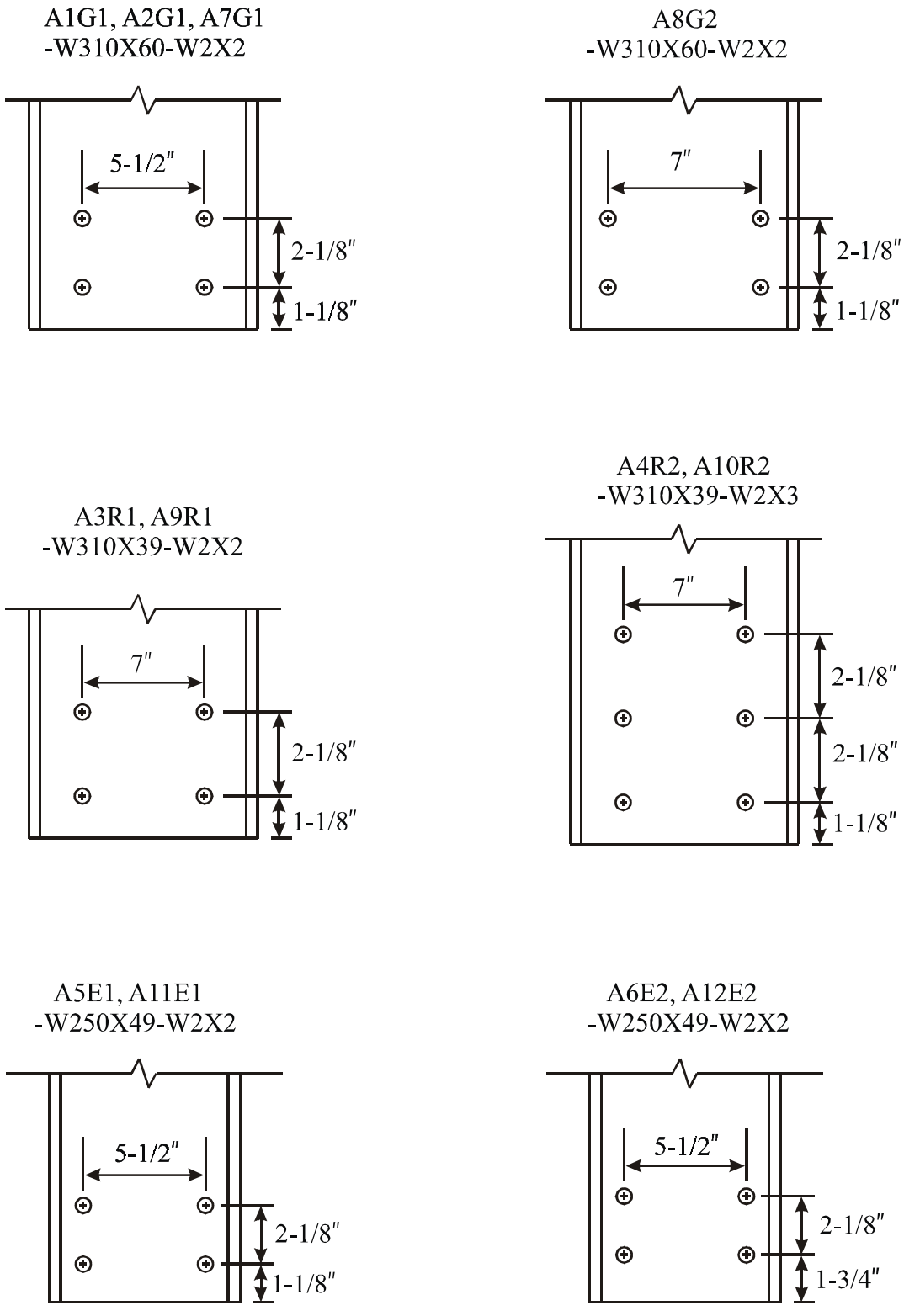

Figure 3-1: Nominal Dimensions of Specimens in Series A

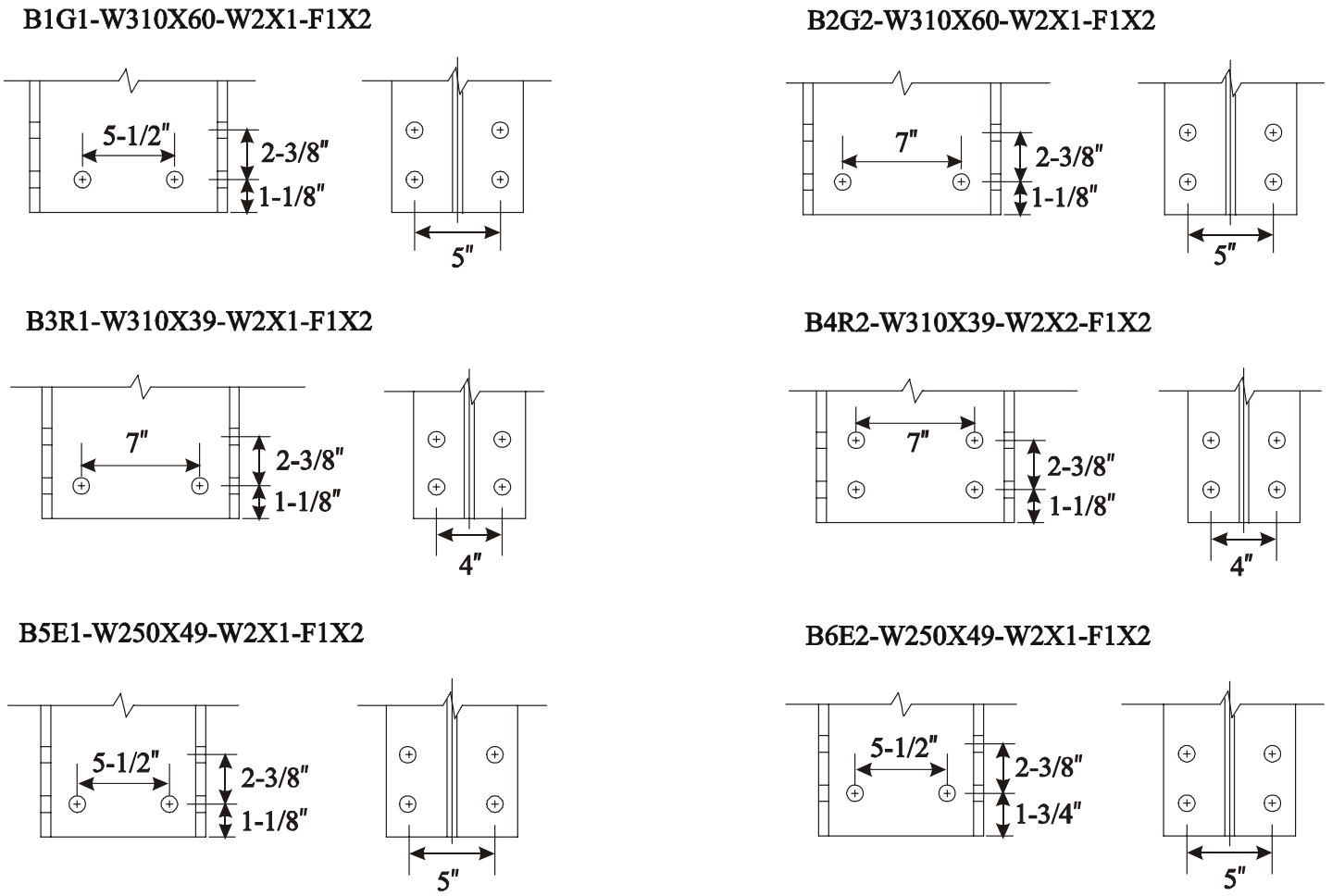

Figure 3-2: Nominal Dimensions of Specimens in Series B

C1~C16
-W250X58-W2X3

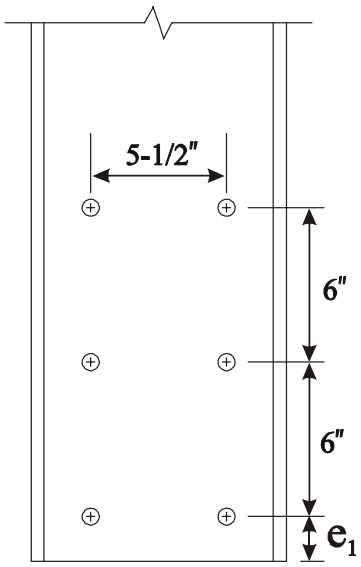

C17~C32
-W310X39-W2X3

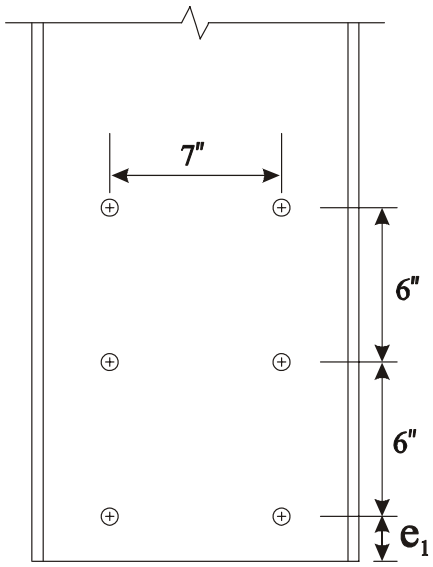

Specimen	End Distance (e_1)	
	(in.)	(mm)
C1E1a	1	25.4
C2E1b	1	25.4
C3E1c	1	25.4
C4E2a	1-1/4	31.8
C5E2b	1-1/4	31.8
C6E2c	1-1/4	31.8
C7E3a	1-1/2	38.1
C8E3b	1-1/2	38.1
C9E3c	1-1/2	38.1
C10E4a	1-3/4	44.5
C11E4b	1-3/4	44.5
C12E4c	1-3/4	44.5
C13E5a	2	50.8
C14E5b	2	50.8
C15E5c	2	50.8
C16E6	2-3/4	69.9

Specimen	End Distance (e_1)	
	(in.)	(mm)
C17E1a	1	25.4
C18E1b	1	25.4
C19E1c	1	25.4
C20E2a	1-1/4	31.8
C21E2b	1-1/4	31.8
C22E2c	1-1/4	31.8
C23E3a	1-1/2	38.1
C24E3b	1-1/2	38.1
C25E3c	1-1/2	38.1
C26E4a	1-3/4	44.5
C27E4b	1-3/4	44.5
C28E4c	1-3/4	44.5
C29E5a	2	50.8
C30E5b	2	50.8
C31E5c	2	50.8
C32E6	1-3/4	69.9

Figure 3-3: Nominal Dimensions of Specimens in Series C

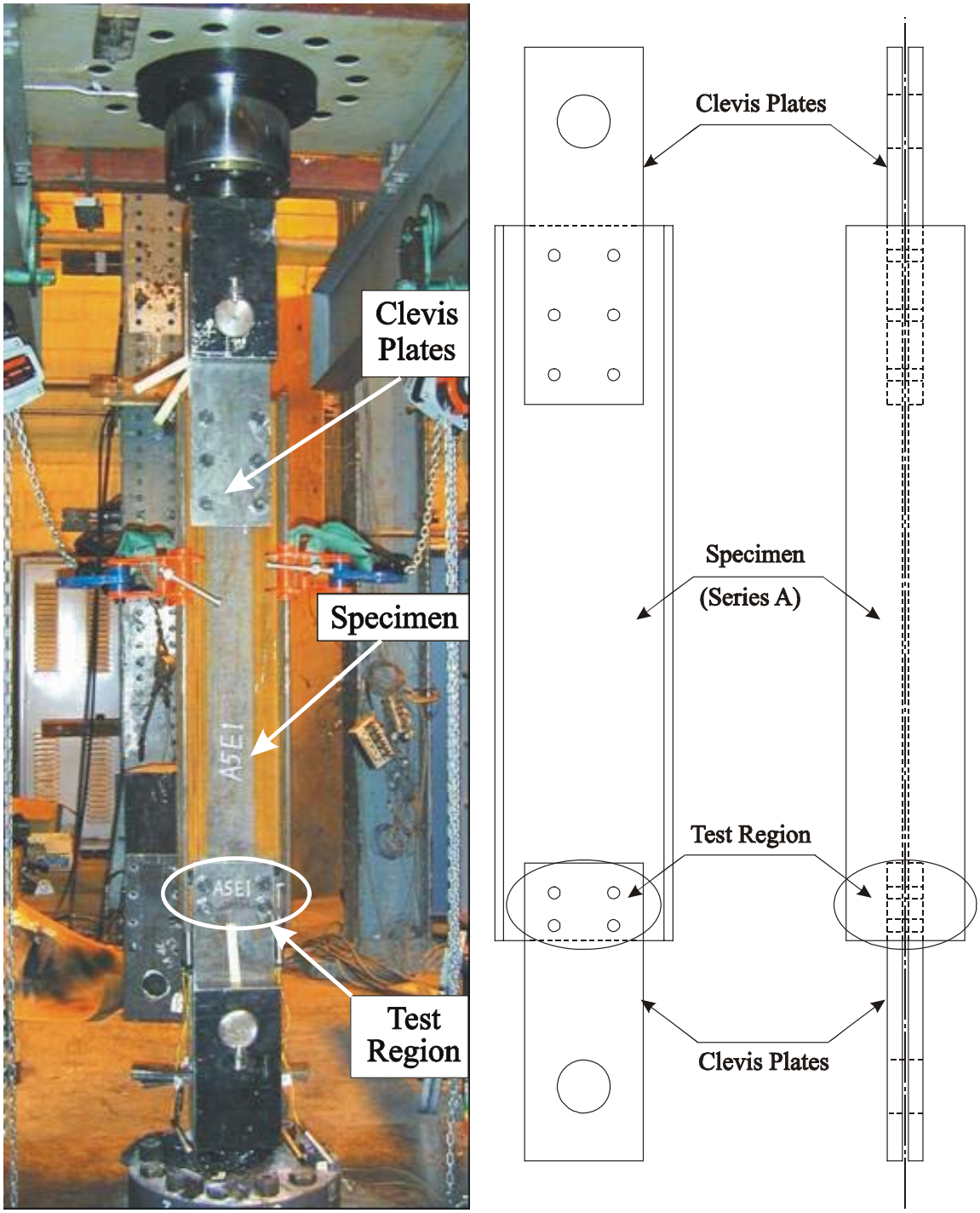

Figure 3-4: Test Set-Up for Series A (Series C similar)

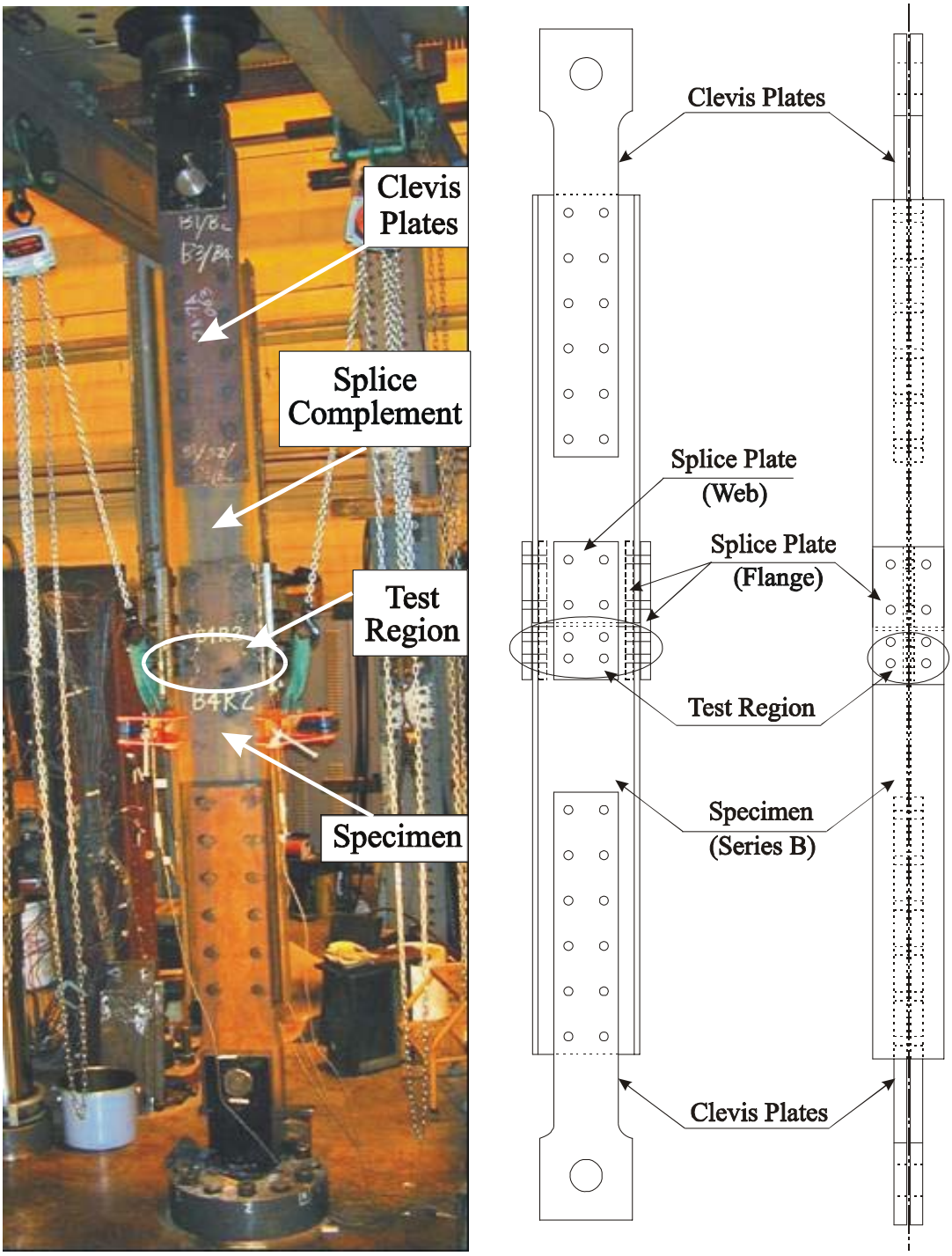

(a) (b)

Figure 3-5: Test Set-Up for Series B

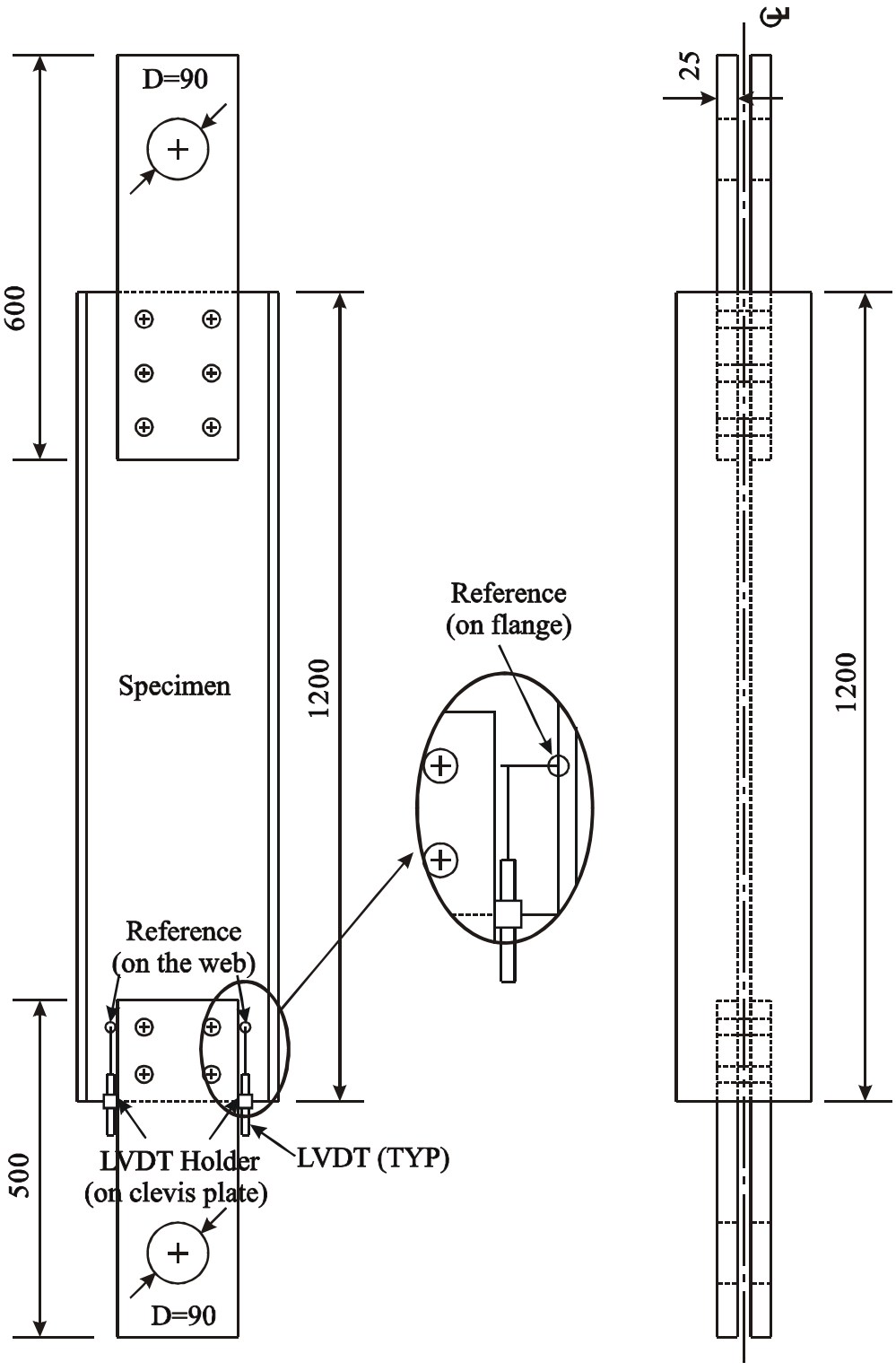

Figure 3-6: Instrumentation (LVDTs) for Series A Specimens (Series C — see inset)

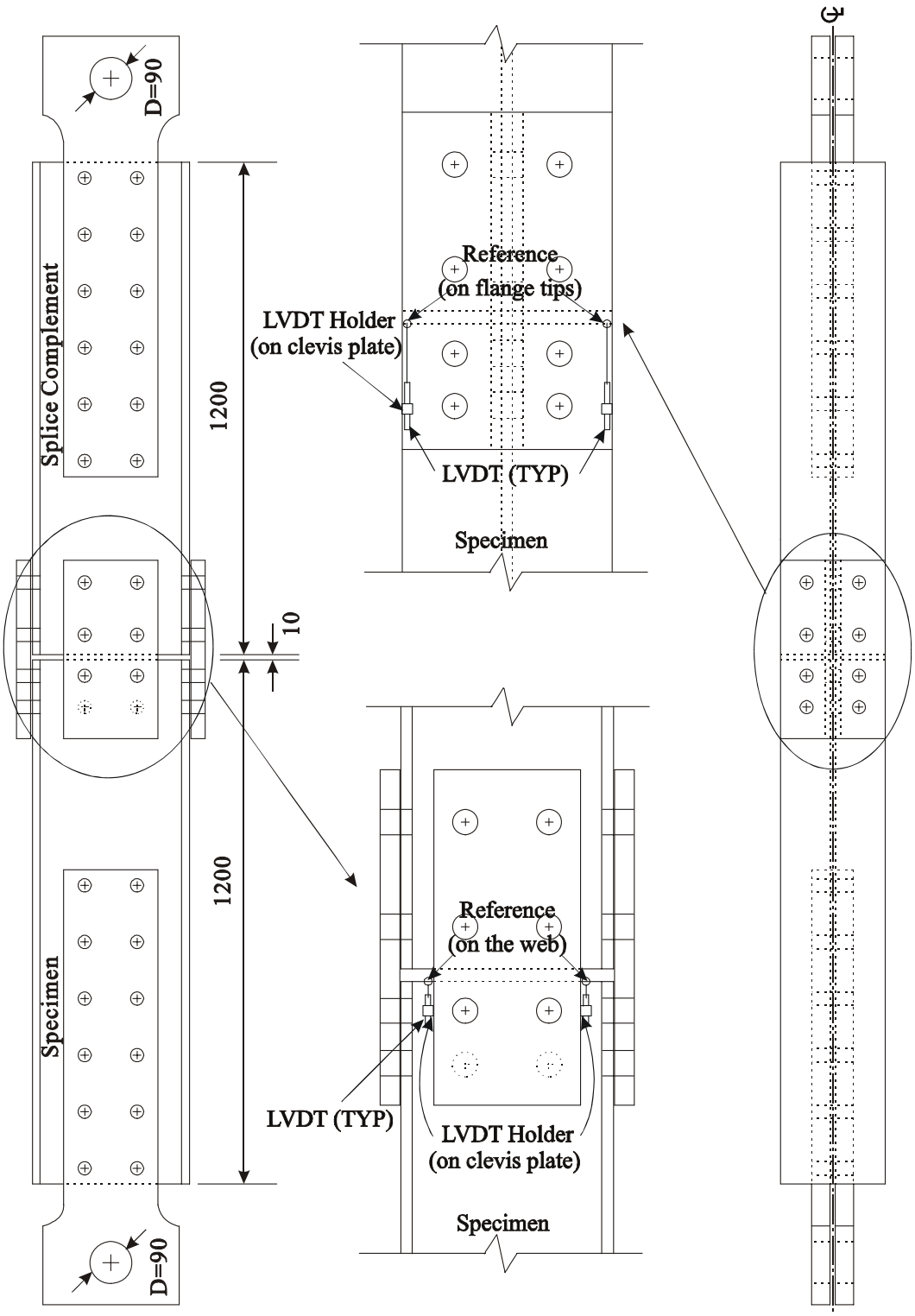

Figure 3-7: Instrumentation (LVDTs) for Series B Specimens (web LVDTs used on B1 only)

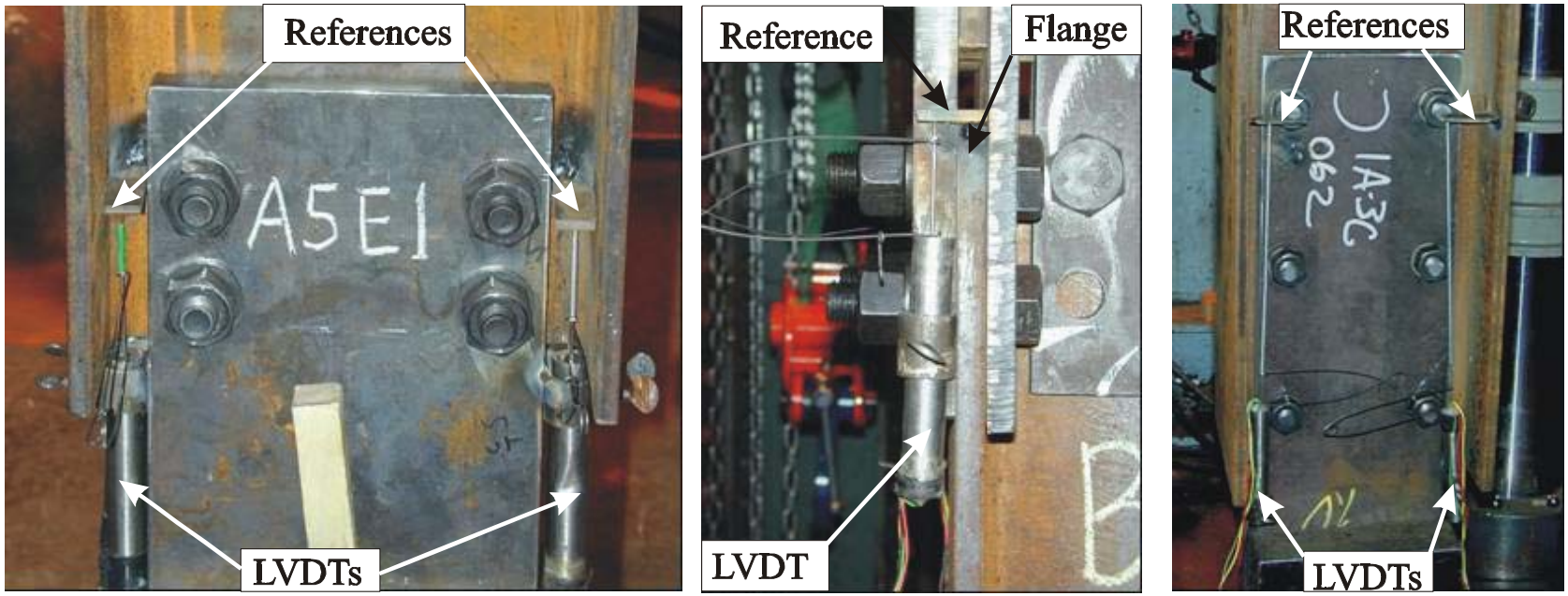

(a) Series A **(b) Series B** **(c) Series C**

Figure 3-8: Photos of Instrumentation (LVDTs) for (a) Series A; (b) Series B; and (c) Series C

4. Test Procedures and Results

4.1 Test Procedures

Fifty full-scale bolted connections were tested in tension in a 4000 kN (tension) capacity universal testing machine (MTS 6000). The load was applied quasi-statically under stroke control at 0.76 mm/min. Electronic readings of load and displacement were taken at regular intervals.

One of three typical unloading points was chosen at the terminus of each test in this experimental program: “right after the peak load”, “drop of 5% of the peak load”, and “all the way to failure”. Unloading point “drop of 5% of the peak load” was chosen to ensure that the ultimate strength of the connection had been captured, whereas “right after the peak load” was selected in order to observe the load carrying mechanism at the peak load. Unloading points “right after the peak load” and “drop of 5% of the peak load” were typically used in the series A tests.

“Right after the peak load” usually means about a 5 kN to 10 kN load drop in the series A tests and also in the series B and C tests if it was possible. However, in the series B and C tests, the load did not always drop gradually since the failures involved shear rupture, tension rupture, and bolt failure. This sometimes resulted in a sudden load drop which could be several tens to several hundreds of kilonewtons after the peak load. All series B tests were unloaded “right after the peak load”, except B3 which was loaded “all the way to failure” to examine the typical final failure paths.

“All the way to failure” in the series C tests means that a specimen was loaded until its residual strength was about 300 kN after several “breaking” sounds being heard. Unfortunately, these sounds could not be identified individually since they could be shear rupture, tension rupture, or bolt shear failure and the presence of the clevis plates made it impossible to reveal the specific sequence of failure. Specimens in series C were either tested “all the way to failure” or unloaded “right after the peak load”.

4.2 Test Descriptions and Results

A summary of the test results is listed in Tables 4-1a and 4-1b, and a description of each test is presented in the following sections.

4.2.1 Specimens A1G1, A2G1, A7G1, and A8G2

These four specimens had the same cross section—$W310\times60$—and the only variable was the bolt gauge, which was 140 mm (5-1/2") for A1G1, A2G1, and A7G1 and 178 mm (7") for A8G2 (Figure 3-1). Load vs. deformation curves for these four specimens are shown in Figures 4-1, 4-2, 4-3, and 4-4.

This was the only group that had triplicate specimens, and specimen A8G2 was the only one in series A that did not have a duplicate. The triplicate specimen ultimate loads (Table 4-1a) were similar, with the specimens having the higher material strength (A1G1 and A2G1) giving higher capacities (Test-to-predicted ratios vary by 3% for all methods, as shown in Table 4-2. Refer to Section 4.3.2). However, the maximum connection deformation for A2G1 was much smaller than those of A1G1 or A7G1 because specimen A2G1 was unloaded right after the peak load with only a 5 kN drop, while specimens A1G1 and A7G1 were unloaded after a drop of 5% of the peak load. The initial portions of the A7G1 and A8G2 curves, which exhibit a relatively flat region (Figures 4-3 and 4-4), show that the specimens had not been properly seated with the bolts in bearing before the test started. The connection deformation of A8G2 was similar to that of A2G1, both of which were unloaded right after the peak, if the initial part of the A8G2 curve that represents the slip of the connection is disregarded.

4.2.2 Specimens A3R1, A9R1 and A4R2, A10R2

The specimens in this group had the same cross section—$W310\times39$—and the only variable was the number of bolt rows, and thus A3R1 and A9R1 had two rows of bolts and A4R2 and A10R2 had three rows of bolts (Figure 3-1). Load vs. deformation curves for these four specimens are shown in Figures 4-5, 4-6, 4-7, and 4-8.

Specimens A3R1 and A4R2 were each unloaded after a 5 kN drop beyond the peak load, while specimens A9R1 and A10R2 were unloaded after a drop of 5% of the peak load.

During the A4R2 test, it was found that the core of one LVDT had been stuck for the first part of the test, and it was properly reset and worked normally thereafter (see Figure 4-7). A comparison of connection deformations revealed that for each set of two connections that were unloaded at the same unloading point, but having a different number of bolt rows in the web (A3R1 and A4R2; A9R1 and A10R2), the difference in connection deformation is almost indistinguishable due to their relatively thin webs.

The capacities of specimens A3R1 and A9R1 were nearly identical (with only 1.3 kN difference), as expected due to the similar material properties. The capacities of specimens A4R2 and A10R2 should also be close since these two specimens are nominally identical. However, specimen A10R2 had a relatively low peak load which is believed caused by premature failure. At the peak loads, well defined yield lines could be clearly observed in specimen A4R2 but only a few yield lines were present in A10R2. This led to the conclusion that specimen A10R2 failed prematurely, although the specific defect that accelerated the failure was not identified. Despite the apparent premature failure, this test result is included in all subsequent assessments of the design equations discussed in Chapter 2.

4.2.3 Specimens A5E1, A11E1 and A6E2, A12E2

These four specimens had the same cross section—$W250\times49$—and the only variable was the end distance, which was 28.6 mm (1-1/8") for A5E1 and A11E1 and 44.5 mm (1-3/4") for A6E2 and A12E2 (Figure 3-1). Load vs. deformation curves for these four specimens are shown in Figures 4-9, 4-10, 4-11, and 4-12.

Specimens A5E1 and A6E2 were unloaded after a drop of 5 kN beyond the peak load, while specimens A11E1 and A12E2 were unloaded after a drop of 5% of the peak load. Like the specimens in the previous group, a similar conclusion can be made about connection deformations; thus, connection deformations are essentially the same for specimens with different end distances if they were unloaded at the same unloading point.

Figure 4-11 shows that specimen A6E2 had a sudden load drop after reaching the peak. It was observed that the load dropped from 776 kN to 737 kN, accompanied by a breaking

sound. The specimen was unloaded at this point. Hairline cracks were observed at the tack weld toe of the LVDT reference tab on the specimen, and one LVDT failed because of the fracture. The web had not deformed much (and seemed as though it had reserve capacity) because of the relatively large end distance, and the slope of the load vs. deformation curve had remained positive prior to the sudden load drop. Therefore, it was decided to reload the specimen, but the specimen did not reach the previous peak before the load started to drop again and the fractures propagated. As such, only the first load excursion is presented in Figure 4-11 and the capacity and the deformation at the peak load are considered to be lower bound values due to the influence of the tack weld. Nevertheless, because of the similar capacity of nominally identical specimen A12E2, the peak load for specimen A6E2 is believed to be close to the true connection capacity. After this test, it was decided that tack welding should be further away from any possible failure path, especially the critical net section, to avoid any reduction of connection capacity.

The capacities of specimens A5E1 and A11E1 were almost identical, with only 1% difference, and the capacities of specimens A6E2 and A12E2 were also close, with about 2% difference. The difference in capacity between E2 specimens and E1 specimens was the contribution of the increment of end distance.

4.2.4 Specimens B1G1 and B2G2

Specimens B1G1 and B2G2 had the same cross section—$W310\times60$—and these two specimens were identical except for the web bolt gauge which was 140 mm (5-1/2") for B1G1 and 178 mm (7") for B2G2 (Figure 3-2). Load vs. deformation curves are shown in Figures 4-13 and 4-14.

The B1G1 test was set up and tested as shown in Figure 3-5, but without the four inside flange splice plates. At a load of about 1970 kN, the load started to drop, and at about 1950 kN, the four flange bolts in the first row failed suddenly. The failure was brittle because these bolts were loaded in a combination of single shear and tension. After this test, four 12.7 mm (1/2") thick steel strips were added inside the flanges, as shown in Figure 3-5, to put these flange bolts in double shear and eliminate eccentric loading, since

bolt failure was not an intended limit state for the series B tests. In any case, the slope of the load vs. deformation curve (Figure 4-13) at the peak indicates that the capacity of the connection had been reached.

Eight LVDTs, including four on the web and four on the flanges (see Figure 3-7), were installed on specimen B1G1. It can be seen in Figure 4-13 that deformations of the flanges are less than those of the web. The location of the flange LVDT reference point is at the tip of a flange, and the location of the web LVDT reference point is near the junction of the web and the flange (as shown in Figure 3-7). This causes the movement of the reference point on the flange to be less than that of the reference point on the web as the specimen moves as a unit during loading (see the photographs of the deformed series B specimens in Figure 4-26, discussed in Section 4.3.3). Also, the flanges are thicker than the web and therefore less susceptible to bearing deformations. Due to the difficulty of installing web LVDTs for specimens that have a relatively large bolt gauge in the web, only the four flange LVDTs were mounted for the rest of the series B tests.

A comparison of the ultimate capacities of specimens B1G1 and B2G2 shows that the capacities are within 3% of one another. This is expected because the nominal failure paths and the material properties are identical.

4.2.5 Specimens B3R1 and B4R2

Specimens B3R1 and B4R2 had the same cross section—$W310\times39$—and these two specimens were identical except for the number of bolt rows in the web: B3R1 had one row of bolts and B4R2 had two rows of bolts (Figure 3-2). Load vs. deformation curves are shown in Figures 4-15 and 4-16. Unlike the load vs. deformation curves of series A that showed web deformations, the flange deformations at the four corners of a section in series B were relatively different, especially for specimens that had not been well seated before the tests.

B3R1 was the only specimen in series B that was loaded until complete failure (*i.e.*, until after the tension faces had ruptured in the flanges and blocks of material had sheared out from the flanges) to verify the final failure paths. These failure paths clearly showed that

the web bolts had torn out and the flanges had failed in block shear as designed. Specimen B4R2 was the only specimen in series B that had the same connection length in the web and flanges. This specimen was unloaded right after the peak, and after the test it was observed that necking and tension fracture had begun in the tension planes of the blocks in the flanges, while shear fracture of these blocks had not yet appeared due to insufficient deformation at the peak load to allow it to take place.

The capacity of specimen B4R2 was higher than B3R1 by about 340 kN as a result of the extra bolt row in the web.

4.2.6 Specimens B5E1 and B6E2

Specimens B5E1 and B6E2 had the same cross section—$W250\times49$—and these two specimens were identical except for the end distance: B5E1 and B6E2 had end distances of 28.6 mm (1-1/8") and 44.5 mm (1-3/4"), respectively (Figure 3-2). Load vs. deformation curves are shown in Figures 4-17 and 4-18.

The deformation for B6E2 was less than that for B5E1 if both initial flat parts of the curves, which are the evidence of connection slip, are ignored.

The capacity of specimen B6E2 was higher than B5E1 by about 327 kN (20%) due to the 16 mm (5/8") of extra end distance in both the web and flanges.

4.2.7 Specimens C1E1 to C16E6

Specimens C1E1 to C16E6 had the same cross section—$W250\times58$—and the only variable in this group was the end distance. There were six different end distances, denoted as E1 to E6, and there were three identical specimens for end distance E1 to E5, symbolized by “a”, “b” and “c”. The results of the series C tests are listed in Table 4-1b. Load vs. deformation curves are shown in Appendix C (Figures C-1 to C-16), and Appendix D (Figures D-1 to D-6) shows photographs of the series C failed connections.

The nominal value of gauge was 140 mm (5-1/2") and the nominal value of web thickness is 8 mm for specimens C1E1 to C16E6. From Equation [2-17], it can be concluded that in order for a bolt to develop its full bearing capacity, the clear distance,

L_c, in the direction of the applied force between the edge of a hole and the edge of the adjacent hole or the edge of the material must be not less than $2d_b$. For an individual bolt, the load applied to the bolt in the form of bearing must not exceed the bolt shear capacity; otherwise the bolt itself would fail. For the case of fully threaded 3/4" A325 bolts, a maximum material thickness of 7.7 mm is required in order that $2d_b$ clear end distance allows a bolt to develop its full bearing capacity before shear failure occurs. The failures of the tests in this group generally involved both bolt failure and failure in the specimens themselves.

Figure 4-19 (a) shows that when the specimen was loaded all the way to failure, the elongation of the end bolt holes is much greater than the inner bolt holes because of bolt shear failure of the four inner bolts and the large shear deformations in the web adjacent to the end bolts (with shear tears being exhibited at the end of the test). Figure 4-19 (b) shows that when the specimen was unloaded right after the peak, the elongation of the end bolt holes is slightly greater than the inner bolt holes. Since the clevis plates remained elastic, the relative hole distortions during the test were determined solely by the web and bolt deformations.

For the specimens that were loaded to complete failure, at least four bolts failed (Figure 4-20a). None of the specimens exhibited typical block shear or pure bolt tear-out failure modes—although some of the end row bolts with small end distances did tear out—and the damage that can be observed at the interior bolts is best characterised as bearing damage (Figures D-1 to D-6). The three specimens wherein none of the bolts failed (C2E1, C11E4, and C14E5) were unloaded right after the peak load, while another two specimens (C6E2 and C8E3) that were also unloaded right after the peak load had either one or two bolts fail. Once a bolt started to fail, the load began to drop and although other subsequent local peaks may have occurred, they never exceeded the original peak in value. This indicates that every bolt carried a portion of the peak load but the peak load was not necessarily distributed equally among the six bolts.

4.2.8 Specimens C17E1 to C32E6

The connection configurations of specimens C17E1 to C32E6 were identical to those in the previous series C group (C1E1 to C16E6), except for the cross-section, which was $W310 \times 39$, and the nominal value of bolt gauge, which was 178 mm (7"). The load vs. deformation curves are shown in Appendix C (Figures C-17 to C-32), and photographs of the series C failed connections are shown in Appendix D (Figures D-7 to D-12).

The main difference between specimens C1 to C16 and specimens C17 to C32 was the web thickness; the nominal web thickness for specimens C17E1 to C32E6 was 5.8 mm. The thinner web caused failure in this group to be influenced more by the specimens than by bolt failure, as compared to specimens C1E1 to C16E6 with the thicker web. For the specimens that were unloaded right after the peak, no bolts failed (Figure 4-20b). A typical final failure path for a specimen in this group was bolt tear-out at the end of the connection and a tearing mode resembling block shear failure of the area enclosed by the four inner bolts (Figure 4-21a). Another failure path in this group was bolt tear-out failure (with large bearing deformations at the interior bolts), especially when the two bolts near the tension plane failed before tension rupture across the gauge distance took place (Figure 4-21b).

4.3 Discussions of Test Results

4.3.1 Shear Tears versus Tensile Splitting Cracks

Two kinds of fractures were observed in the bolt tear-out failures of the series A tests: shear tears on one or both shear planes adjacent to the hole, as shown in Figure 4-22 (a), or a single tensile splitting crack initiating at the free edge near the hole centreline, as shown in Figure 4-22 (b). Tensile splitting cracks were a result of the development of transverse tensile stress as the material behind the bolt shank deformed into an arch shape. Necking can be clearly observed before the splitting cracks finally developed.

In the series A tests, most specimens exhibited either shear tears or splitting cracks after they were unloaded, although it is believed that splitting cracks did not occur until the peak load had been reached. Even if shear tearing had not occurred, there was typically considerable shear deformation on the two shear planes. In the series B tests, no splitting

cracks were observed in any of the specimens, although shear tears, as shown in Figure 4-23, may or may not have occurred. It was observed that the type of fracture that may appear at failure seemed to be influenced by the confinement of the fracture location. In the series A tests, the web received less confinement from the flanges since the specimens were only loaded through the web and the flanges had a tendency to bend outward. On the other hand, in the series B tests, the web got more confinement from the flanges since the specimens were also loaded through the flanges, which tended to keep straight because of the relatively large applied load and the presence of the flange splice plates.

From the test results, it is evident that two shear planes adjacent to each bolt participate in resisting the peak load in bolt tear-out failure despite the subsequent occurrence of tensile splitting in some specimens. In addition, the great ductility of the material behind an end bolt hole, even with a small end distance (as shown in Figure 4-24), is sufficient to allow the shear stress in the two shear planes to be developed well beyond the yield stress but not necessarily up to the ultimate stress. Further evidence of this assertion is presented subsequently in the discussion of test-to-predicted capacity ratios.

4.3.2 Series A Tests (A1 to A12)

These 12 specimens were web-connected only, and the observed failure mode was bolt tear-out failure in the web. Photographs of the series A failed connections are shown in Figure 4-25. The three variables designed to investigate bolt tear-out failure were gauge, number of bolt rows, and end distance.

Specimens A1G1, A2G1, A7G1 and A8G2 are identical except for the bolt gauge. As discussed before, it can be concluded that gauge had no effect on the connection capacity since all these specimens failed in the bolt end tear-out failure mode and their failure paths were identical.

Specimens A3R1, A9R1 and A4R2, A10R2 are identical except for the number of bolt rows. One more bolt row, which gave a 54 mm (2-1/8") or 65% longer connection, resulted in a 33% higher connection strength.

Specimens A5E1, A11E1 and A6E2, A12E2 are identical except for the end distance. Increasing the end distance by 15.9 mm (5/8"), or 19% of the connection length, resulted in an increase in the connection strength of 13%.

Predicted capacities for each test in series A considering measured material and geometric properties (and no resistance factor), with the assumption that two shear planes at each bolt carried the peak load, were calculated using the CSA-S16-01/AISC 2005 block shear equations (Equations [2-3] and [2-4]) and the unified equation (Equation [2-10]). Predicted capacities and the resulting test-to-predicted ratios are shown in Table 4-2. The mean test-to-predicted ratio for CSA-S16-01/AISC 2005 is 1.46, while for the unified equation it is 1.08. The coefficient of variation (COV) for CSA-S16-01/AISC 2005 is 0.10, while for unified equation it is 0.09. A mean test-to-predicted ratio much closer to 1.0, combined with a slightly lower coefficient of variation, indicates that the unified equation better represents the behaviour of these connections than does the set of equations used currently in the North American design standards.

4.3.3 Series B Tests (B1 to B6)

These six specimens were connected by both the web and flanges, and the observed failure mode was bolt tear-out in the web combined with block shear in flanges. Photographs of the series B failed connections are shown in Figure 4-26. The three main variables designed to investigate combined failures were web bolt gauge, number of bolt rows in the web, and end distance.

It can be concluded that gauge has no effect on the connection capacity if the bolt tear-out failure mode can be ensured. The connection deformations at the peak loads for B1G1 and B2G2, B3R1 and B4R2, B5E1 and B6E2 are similar since their flange bolt configurations were the same for each variable and the peak was reached when necking started to occur in the tension plane of the flange blocks.

An additional bolt row in the web, which means 60.3 mm (2-3/8") more connection length in the web (and the same connection length in the web and flanges), resulted in an

increase in connection strength of 27%. An increase in the end distance of 15.9 mm (5/8") in both the web and flanges resulted in an increase in connection strength of 20%.

Predicted capacities for each test in series B considering measured material and geometric properties (and no resistance factor), with the assumption that the strength of the web and that of the flanges at the peak load are directly additive, were calculated using the CSA-S16-01/AISC 2005 block shear equations (Equations [2-1] to [2-4]) and the unified equation (Equations [2-9] and [2-10]). Predicted capacities and the test-to-predicted ratios are shown in Table 4-2. The mean test-to-predicted ratio for CSA-S16-01/AISC 2005 is 1.24, while the unified equation gives a test-to-predicted ratio of 1.00. The coefficient of variation (COV) for CSA-S16-01/AISC 2005 is 0.03; while for the unified equation it is 0.02. These results indicate that the unified equation gives a much better representation of the actual connection behaviour. All predictions in series B by the unified equation are within 3% of the test capacity.

4.3.4 Series C Tests (C1 to C32)

4.3.4.1 Series C Tests with Thicker Webs (C1 to C16)

These 16 tests were conducted on specimens with thicker webs, resulting in connection failures that involved bolt shear failure. The four inner bolts, which were away from the edge of a specimen, tended to fail before the two end bolts because the end distance was significantly less than the bolt pitch and the material near the edge tends to be more flexible. This phenomenon indicates that these inner bolts carried more load at the peak compared to the bolts near the free end. In fact, it could be further concluded that when the inner bolts developed their full shear strength, the end bolts may only have been able to develop their bolt shear capacities partially, depending on their clear end distances. The upper bound of the connection capacity of specimens C1 to C16 is the strength of six bolts failing in double shear.

Dealing with the predicted capacities of such connections, the six “traditional” failure modes shown in Figure 4-27 are considered first. This group is based on the presumption that the ductility of the connection is great enough to develop the full capacity at each individual bolt or that it would fail in a global connection failure mode. Moreover, these

cases assume that if the connection fails at each individual bolt, the failure modes are the same at all six locations. The traditional failure modes considered here are gross section yielding, net section rupture, block shear, 6-bolt tear-out, 6-bolt bearing, or 6-bolt shear.

Besides the traditional modes described above, it is common for connections to fail differently at the end bolts as compared to the inner bolts. Therefore, five potential combination failure modes, shown in Figure 4-28, were introduced to consider that the four inner bolts (IB) and the two end bolts (EB) may fail differently due to the large pitch and relatively small end distance. Combinations 1 through 3 (shown in Figure 4-28a) imply that, like for the traditional modes, the connection is sufficiently ductile to develop the full capacity at each of the six bolts.

Another two types of failure—both of which are included in each of Combinations 4 and 5 (shown in Figure 4-28b)—are considered that are based on the assumption that the connection does not have sufficient ductility for the four inner bolts to develop their full capacity by the time the end bolts tear out (or fail in bearing). As a result, the connection capacity would be either six times the end bolt capacity (just prior to failure of the shaded region in Figure 4-28b, assuming the load is shared among the six bolts equally) or the capacity of the inner four-bolt region acting alone (subsequent to failure of the end bolts, assuming the remaining four inner bolts share the load equally until they fail as a group), whichever is greater. (Note that the representations shown as Combinations 4 and 5 in Figure 4-28 are symbolic since they do not indicate all the ways the inner four bolts can fail, such as bolt shear or bolt bearing. Nevertheless, all such possibilities were considered in the assessment of these “non-ductile” combinations.) Combinations 4 and 5 do not provide consistent predictions of the test capacities for specimens C1 to C16; the test-to-predicted ratios vary from 0.91 to 1.37. For the nine specimens where these combinations would govern the connection capacity, the mean test-to-predicted ratio is 1.22. Moreover, neither of the modes represented by these combinations is consistent with the connection behaviour observed in the tests. For all these reasons, it is believed that the non-ductile behaviour represented by Combinations 4 and 5 is not realistic. This implies that the connections had sufficient ductility to develop the full capacity at each

individual bolt or develop a global connection failure mode—the six traditional modes or Combinations 1 through 3.

The governing predicted capacity for the series C specimens with the thicker web is the sum of four fully developed inner bolt shear capacities and the strength of either the end material or two additional bolts failing in shear. The strength of the end material is the lesser of the bolt tear-out strength (using the unified equation) and the bearing capacity at the two end bolts. Predicted capacities, using measured material and geometric properties (and no resistance factor), and test-to-predicted ratios for specimens with thicker webs in series C are shown in Table 4-3, along with the governing failure modes. Good results are achieved, regardless of the design standard used for the bolt shear and bearing calculations. CSA-S16-01 gives a mean test-to-predicted ratio of 0.97 combined with a coefficient of variation of 0.04, while AISC 2005 gives a mean test-to-predicted ratio of 1.02, also with a coefficient of variation of 0.04. The lack of a reduced bearing capacity for small end distances in S16-01 (see Eq. [4-5]) does not seem detrimental since the unified equation serves a similar purpose at these locations. In fact, for the six specimens where the bearing equation in AISC 2005 governs for the end bolts (*i.e.*, specimens C1 to C6), the mean test-to-predicted ratio is 1.05. Eliminating the bearing equation check at the end bolts changes the governing mode at this location to bolt tear-out in all six cases (Combination 2) and results in an improved mean test-to-predicted ratio of 1.00 (with the same coefficient of variation—0.03) using the unified equation. It should be noted that the bolt shear stress in CSA-S16-01 is taken as 60% of bolt ultimate tensile stress ($0.60F_u$), and this resulted in the mean test-to-predicted ratio is 0.97. However, if the von Mises criterion is used (*e.g.*, shear stress is taken as $F_u/\sqrt{3}$ instead of $0.60F_u$), it gives a mean test-to-predicted ratio of 1.02, which is identical to AISC 2005. The coefficient of variation remains the same (0.04) in all cases.

4.3.4.2 Series C Tests with Thinner Webs (C17 to C32)

These 16 tests were conducted on specimens with thinner webs, resulting in failure that was more involved in the specimens than in the bolts. As shown in Figures D-7 to D-12, for specimens that were unloaded right after the peak load, no end ruptures occurred,

which indicates that the end material in front of the first row of bolts contributes to the connection capacity. Bearing damage adjacent to the four inner bolt holes is also clearly evident in these photographs.

After the peak load, the failure of the connection is believed to be a series of sequential failures, which means that the material in front of each bolt (a portion of the shear plane) or the material between the two bolts in the last row (the tension plane) were not able to reach their individual peaks simultaneously. This is evident by the fact that the tested connection strength is far less than the sum of the individual component strengths along the failure path displayed after unloading for the specimens loaded well beyond the peak.

As for specimens C1 to C16, Combinations 4 and 5 do not provide consistent predictions of the test capacities for specimens C17 to C32; in this case, the test-to-predicted ratios vary from 1.20 to 1.65 and all 16 specimens would be governed by these combinations. Moreover, neither of the modes represented by these combinations is consistent with the connection behaviour observed in the tests. Again, it is believed that the non-ductile behaviour represented by Combinations 4 and 5 is not realistic and that the connections had sufficient ductility to develop the full capacity at each individual bolt or develop a global connection failure mode—the six traditional modes or Combinations 1 through 3.

The governing predicted capacity for the series C specimens with the thinner web is the sum of the bearing capacity at the four inner bolts and the strength of the end material taken as the lesser of the bolt tear-out strength (using the unified equation) and the bearing capacity at the two end bolts. Predicted capacities, using measured material and geometric properties (and no resistance factor), and test-to-predicted ratios for specimens with thinner webs in series C are shown in Table 4-3, along with the governing failure modes. The mean test-to-predicted ratios using CSA-S16-01 and AISC 2005 for the bearing equations are 1.22 and 1.23, respectively, and the associated coefficients of variation are 0.05 and 0.06, respectively.

The main conclusion that can be drawn from the test-to-predicted ratios is that the AISC 2005 and CSA-S16-01 bearing equations seem very conservative. Control

specimen C32, which failed purely in bearing, had a test-to-predicted ratio of 1.32, which implies that the bearing equations underestimate the actual bearing capacity by 32% if deformation is not a design consideration. If this is the case, these bearing equations could be improved by changing $1.5L_ctF_u$ to $2.0L_ctF_u$, and $3.0d_btF_u$ to $4.0d_btF_u$. This would increase the bearing capacity by 33% and give a mean test-to-predicted ratio of 0.98, with a coefficient of variation of 0.04 for both CSA-S16-01 and AISC 2005. The test-to-predicted ratio much closer to 1.0, combined with a lower coefficient of variation, implies that the revised equations give better representations of the actual bearing behaviour. For the six specimens where the reduced bearing equation in AISC 2005 governs for the end bolts (*i.e.*, specimens C17 to C22), the mean test-to-predicted ratio is 1.29, with a coefficient of variation of 0.05. Eliminating the bearing equation check at the end bolts changes the governing mode at this location to bolt tear-out in all six cases (Combination 3) and, combined with the modified bearing equations proposed above for the inner bolts, results in a greatly improved mean test-to-predicted ratio of 1.00, with a coefficient of variation of 0.03, using the unified equation for bolt tear-out. However, more research on bearing strength is required to verify the proposed increased capacities. Nevertheless, using the unified equation for bolt end tear-out in combination with existing bearing equations does provide conservative predictions of connection capacity.

4.4 Summary

A total of 50 tests were conducted on wide-flange shapes, including 12 series A specimens connected by their webs only, six series B specimens connected by both the web and flanges, and 32 series C specimens connected by their webs only. Specimens in series A failed by bolt tear-out failure, while specimens in series B failed in a combination of bolt tear-out in the web and flange block shear failure. Specimens with thicker webs in series C failed in a combination of shear failure of the four inner bolts and either tear-out, bolt bearing, or bolt shear of the two end bolts, depending on the end distance. Specimens with thinner webs in series C failed in a combination of bearing at the four inner bolts and tear-out or bearing failure at the two end bolts.

Based on results from series A, regardless of whether a tensile crack appeared at the free edge by the time the specimen was unloaded, the unified equation taken on two shear

planes adjacent to the bolt provides a good estimate of capacity for the bolt tear-out mode. For specimens with combined failure modes like the ones that developed in the specimens of series B, the connection has sufficient ductility for the strength to be taken as the sum of the individual strengths of the web and flanges.

Specimens in the series C tests exhibited sequential failure rather than simultaneous failure of the individual components. Based on the test results and test observations, it can be concluded that the connections had adequate ductility to allow each individual bolt location to achieve its full capacity. For specimens C1 to C16, the bolts did not share the load equally at failure due the difference in local stiffness resulting from a fairly large pitch of 152.4 mm (6") and relatively small end distances that varied from 25.4 mm (1") to 70 mm (2-3/4"). The overall ductility of the connection permitted the four inner bolts to develop their full shear capacity, while the capacity of the material at the end bolts was maintained. For specimens C17 to C32, the failure was more involved with the specimens, although there were several tests that involved bolt failure as well. The exact sequence of failure remains unidentified, although the final failure paths showed elements of block shear failure, bearing failure, and bolt tear-out failure. The tests indicated that the bearing equations in CSA-S16-01 and AISC 2005 where deformations are not a design consideration are highly conservative. Another conclusion from the series C tests is that non-ductile failure modes where the connection capacity is taken as the greater of the capacity of an end bolt times the number of bolts and the capacity of the bolts that remain connected after the end bolts tear out was found not to represent the connection behaviour and these modes need not be checked in design.

The test results show that the unified equation is more suitable for bolt tear-out failure than any of the block shear design equations in current North American design standards. It not only provides test-to-predicted ratio much closer to 1.0, but also gives a lower coefficient of variation for both the series A and series B tests.

Table 4-1a: Series A and B Test Results Summary

Specimen	Ultimate Strength (kN)	Deformation at Peak Load (mm)	Deformation at Unloading Point (mm)	Unloading Point
A1G1	690.7	8.4	14.4	drop of 5% of the peak load
A2G1	723.8	9.1	9.3	right after the peak load
A3R1	634.1	10.1	10.9	right after the peak load
A4R2	912.7	10.9	11.4	right after the peak load
A5E1	697.7	8.6	8.8	right after the peak load
A6E2	775.8*	5.9*	6.3	after a sudden load drop
A7G1	665.1	13.3	15.1	drop of 5% of the peak load
A8G2	622.1	11.6	12.0	right after the peak load
A9R1	632.8	13.6	15.7	drop of 5% of the peak load
A10R2	766.1	12.8	14.0	drop of 5% of the peak load
A11E1	691.2	12.7	14.0	drop of 5% of the peak load
A12E2	792.6	13.0	15.3	drop of 5% of the peak load
B1G1	1968.3	6.4**	7.2**	after a sudden load drop
B2G2	1912.9	6.1**	6.2**	right after the peak load
B3R1	1268.4	4.3**	6.5**	all the way to failure
B4R2	1607.9	4.4**	4.4**	right after the peak load
B5E1	1662.5	6.4**	6.5**	right after the peak load
B6E2	1989.2	6.0**	6.0**	right after the peak load

* Lower bound values

** Measured at flanges

Table 4-1b: Series C Test Results Summary

Specimen	Ultimate Strength (kN)	Deformation at the Peak (mm)	Unloading Point	Bolts Failure at Unloading Point
C1E1a	1082.1	4.8	all the way to failure	four bolts failed
C2E1b	1111.8	5.1	right after the peak load	no bolt failed
C3E1c	1112.8	5.3	all the way to failure	four bolts failed
C4E2a	1244.6	5.6	all the way to failure	four bolts failed
C5E2b	1190.4	6.5	all the way to failure	four bolts failed
C6E2c	1152.3	5.3	right after the peak load	one bolt failed
C7E3a	1211.7	6.0	all the way to failure	four bolts failed
C8E3b	1155.4	5.3	right after the peak load	two bolts failed
C9E3c	1215.3	5.9	all the way to failure	four bolts failed
C10E4a	1215.0	5.2	all the way to failure	five bolts failed
C11E4b	1249.1	5.8	right after the peak load	no bolt failed
C12E4c	1182.8	5.4	all the way to failure	four bolts failed
C13E5a	1293.1	5.2	all the way to failure	five bolts failed
C14E5b	1187.8	5.8	right after the peak load	one bolt failed
C15E5c	1279.8	5.4	all the way to failure	five bolts failed
C16E6	1323.3	4.8	all the way to failure	all bolts failed
C17E1a	967.4	13.5	right after the peak load	no bolt failed
C18E1b	984.6	13.4	all the way to failure	two bolts failed
C19E1c	1013.6	15.8	all the way to failure	no bolt failed
C20E2a	1014.9	15.5	all the way to failure	three bolts failed
C21E2b	961.6	14.6	right after the peak load	no bolt failed
C22E2c	976.2	14.5	all the way to failure	no bolt failed
C23E3a	1033.2	15.6	all the way to failure	no bolt failed
C24E3b	1072.1	16.9	right after the peak load	no bolt failed
C25E3c	1015.3	14.8	all the way to failure	four bolts failed
C26E4a	1023.9	16.7	all the way to failure	no bolt failed
C27E4b	1031.0	15.8	right after the peak load	no bolt failed
C28E4c	1018.6	15.4	all the way to failure	no bolt failed
C29E5a	1043.8	15.5	all the way to failure	three bolts failed
C30E5b	1037.2	15.1	right after the peak load	no bolt failed
C31E5c	1043.8	16.5	all the way to failure	two bolts failed
C32E6	1243.3	20.2	all the way to failure	no bolt failed

Table 4-2: Summary of Test-to-Predicted Ratios of Series A and Series B

Specimen	Capacity				Test-to-Predicted Ratio		
	Test Capacity (kN)	CSA S16-01 (kN)	AISC 2005 (kN)	Unified Equation (kN)	CSA S16-01	AISC 2005	Unified Equation
A1G1	690.7	481.2	481.2	601.4	1.44	1.44	1.01
A2G1	723.8	492.9	492.9	616.1	1.47	1.47	1.04
A7G1	665.1	451.1	451.1	563.9	1.47	1.47	1.04
A8G2	622.1	441.2	441.2	551.5	1.41	1.41	0.99
A3R1	634.1	366.5	366.5	458.1	1.73	1.73	1.25
A4R2	912.7	599.3	599.3	749.1	1.52	1.52	1.09
A9R1	632.8	376.2	376.2	470.3	1.68	1.68	1.22
A10R2	766.1	628.9	628.9	786.1	1.22	1.22	0.88
A5E1	697.7	479.7	479.7	599.6	1.45	1.45	1.13
A6E2	775.8	623.9	623.9	733.2	1.24	1.24	1.06
A11E1	691.2	448.1	448.1	560.2	1.54	1.54	1.14
A12E2	792.6	592.2	592.2	729.8	1.34	1.34	1.09
Mean	–	–	–	–	1.46	1.46	1.08
COV					0.10	0.10	0.09
B1G1	1968.3	1541.5	1541.5	1943.0	1.28	1.28	1.01
B2G2	1912.9	1557.3	1557.3	1964.0	1.23	1.23	0.97
B3R1	1268.5	996.3	996.3	1265.2	1.27	1.27	1.00
B4R2	1607.9	1263.7	1263.7	1648.3	1.27	1.27	0.98
B5E1	1662.5	1355.6	1355.6	1666.0	1.23	1.23	1.00
B6E2	1989.2	1696.4	1696.4	1946.4	1.17	1.17	1.02
Mean	–	–	–	–	1.24	1.24	1.00
COV					0.03	0.03	0.02

Table 4-3: Summary of Test-to-Predicted Ratios of Series C

Specimen	Test Capacity (kN)	CSA-S16-01/Unified Equation		AISC 2005/Unified Equation		Test-to-Predicted Ratio	
		Predicted Capacity* (kN)	Predicted Failure Mode	Predicted Capacity* (kN)	Predicted Failure Mode	CSA-S16-01/ Unified Equation	AISC 2005/ Unified Equation
C1E1a	1082.1	1114.7	Combination 2	1042.5	Combination 1	0.97	1.04
C2E1b	1111.8	1118.0	Combination 2	1046.0	Combination 1	0.99	1.06
C3E1c	1112.8	1118.2	Combination 2	1045.3	Combination 1	1.00	1.06
C4E2a	1244.6	1176.7	Combination 2	1131.6	Combination 1	1.06	1.10
C5E2b	1190.4	1182.4	Combination 2	1138.4	Combination 1	1.01	1.05
C6E2c	1152.3	1177.1	Combination 2	1133.7	Combination 1	0.98	1.02
C7E3a	1211.7	1235.9	Combination 2	1194.3	Combination 2	0.98	1.01
C8E3b	1155.4	1236.4	Combination 2	1194.8	Combination 2	0.93	0.97
C9E3c	1215.3	1240.5	Combination 2	1198.9	Combination 2	0.98	1.01
C10E4a	1215.0	1298.9	Combination 2	1247.7	6-Bolt Shear	0.94	0.97
C11E4b	1249.1	1299.8	Combination 2	1247.7	6-Bolt Shear	0.96	1.00
C12E4c	1182.8	1299.9	Combination 2	1247.7	6-Bolt Shear	0.91	0.95
C13E5a	1293.1	1310.1	6-Bolt Shear	1247.7	6-Bolt Shear	0.99	1.04
C14E5b	1187.8	1310.1	6-Bolt Shear	1247.7	6-Bolt Shear	0.91	0.95
C15E5c	1279.8	1310.1	6-Bolt Shear	1247.7	6-Bolt Shear	0.98	1.03
C16E6	1323.3	1310.1	6-Bolt Shear	1247.7	6-Bolt Shear	1.01	1.06
Mean	–			–	–	0.97	1.02
COV						0.04	0.04

* AISC 2005 and CSA-S16-01 are used for the bearing and bolt shear equations and the unified equation is used for bolt tear-out failure.

Table 4-3: Summary of Test-to-Predicted Ratios of Series C (Cont'd)

Specimen	Test Capacity (kN)	CSA-S16-01/Unified Equation		AISC 2005/Unified Equation		Test-to-Predicted Ratio	
		Predicted Capacity* (kN)	Predicted Failure Mode	Predicted Capacity* (kN)	Predicted Failure Mode	CSA-S16-01/ Unified Equation	AISC 2005/ Unified Equation
C17E1a	967.4	760.8	Combination 3	740.1	6-Bearing	1.27	1.31
C18E1b	984.6	755.0	Combination 3	734.0	6-Bearing	1.30	1.34
C19E1c	1013.6	760.7	Combination 3	739.9	6-Bearing	1.33	1.37
C20E2a	1014.9	798.0	Combination 3	792.5	6-Bearing	1.27	1.28
C21E2b	961.6	795.2	Combination 3	789.8	6-Bearing	1.21	1.22
C22E2c	976.2	796.7	Combination 3	791.3	6-Bearing	1.23	1.23
C23E3a	1033.2	850.9	Combination 3	850.9	Combination 3	1.21	1.21
C24E3b	1072.1	840.7	Combination 3	840.7	Combination 3	1.28	1.28
C25E3c	1015.3	830.7	Combination 3	830.7	Combination 3	1.22	1.22
C26E4a	1023.9	889.7	Combination 3	889.7	Combination 3	1.15	1.15
C27E4b	1031.0	882.6	Combination 3	882.6	Combination 3	1.17	1.17
C28E4c	1018.6	873.7	Combination 3	873.7	Combination 3	1.17	1.17
C29E5a	1043.8	899.7	Combination 3	899.7	Combination 3	1.16	1.16
C30E5b	1037.2	902.9	Combination 3	902.9	Combination 3	1.15	1.15
C31E5c	1043.8	905.5	Combination 3	905.5	Combination 3	1.15	1.15
C32E6	1243.3	938.7	6-Bearing	938.7	6-Bearing	1.32	1.32
Mean	–	–	–	–	–	1.22	1.23
COV						0.05	0.06

* AISC 2005 and CSA-S16-01 are used for the bearing and bolt shear equations and the unified equation is used for bolt tear-out failure.

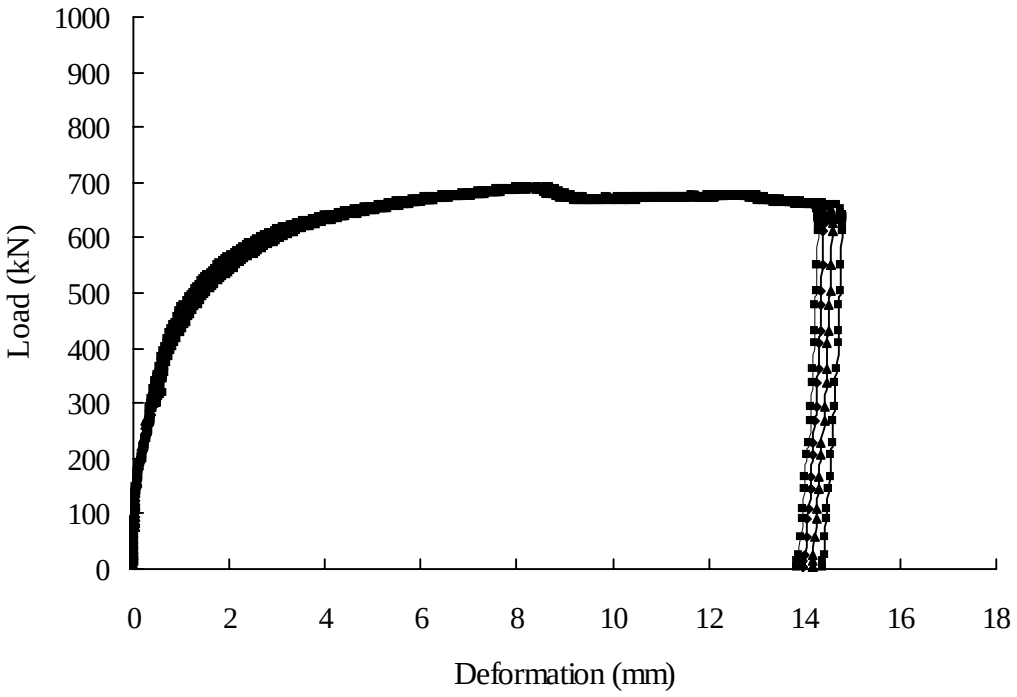

Figure 4-1: Load vs. Deformation Curve for A1G1

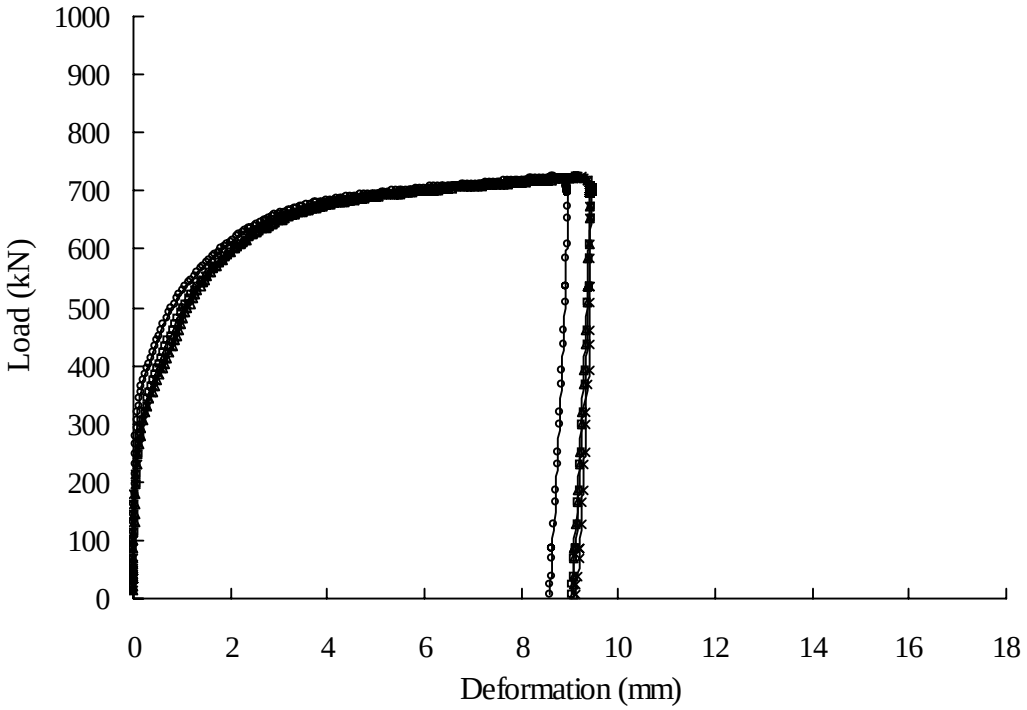

Figure 4-2: Load vs. Deformation Curve for A2G1

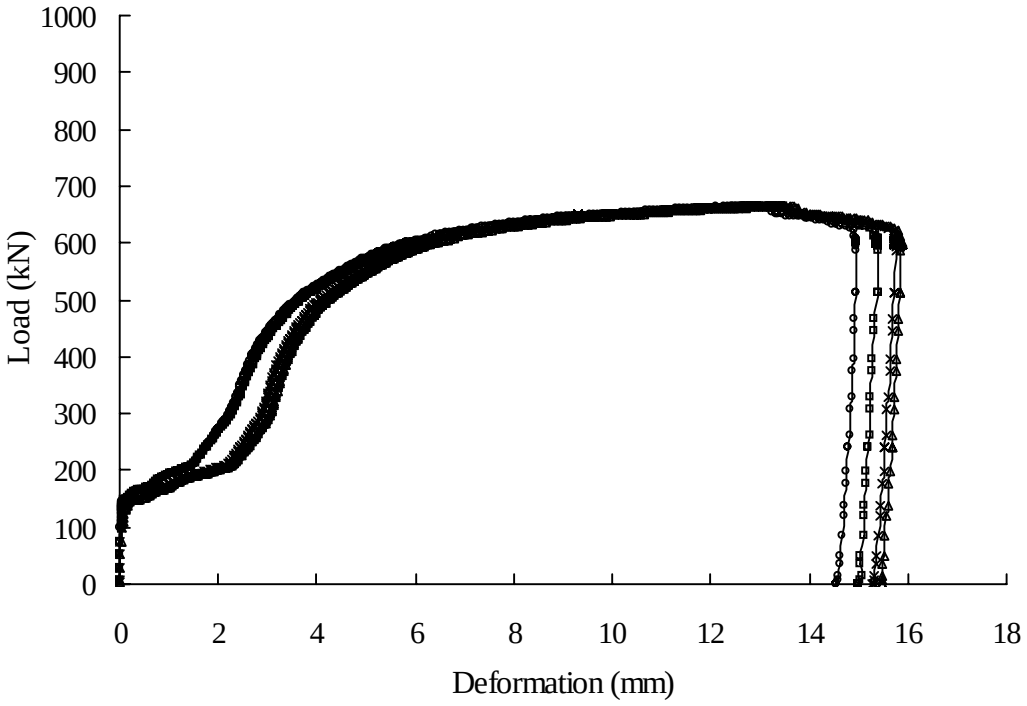

Figure 4-3: Load vs. Deformation Curve for A7G1

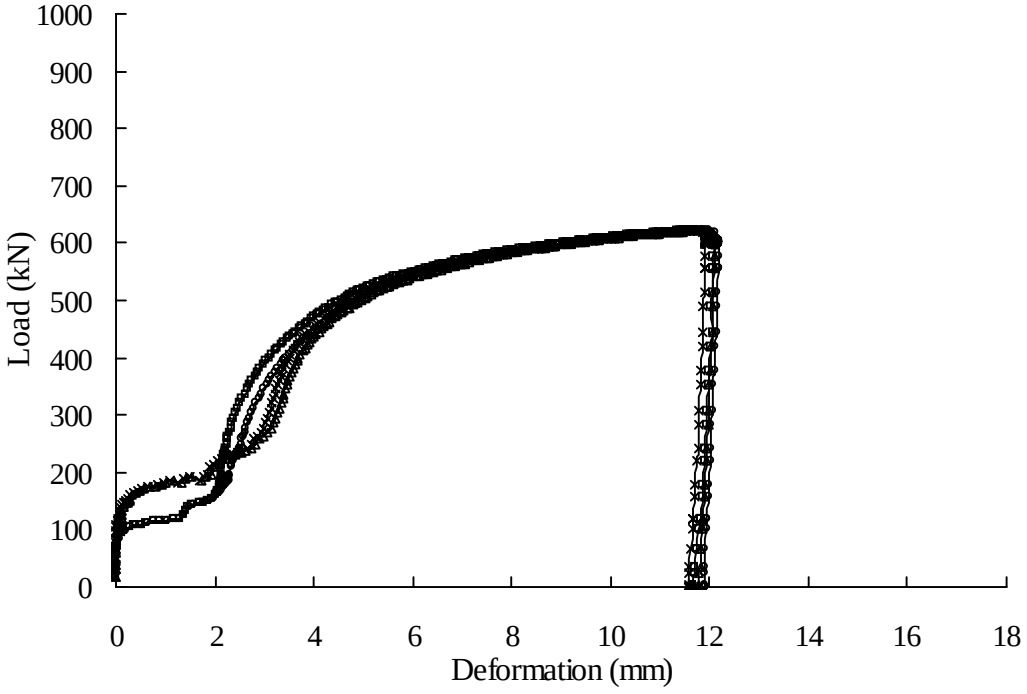

Figure 4-4: Load vs. Deformation Curve for A8G2

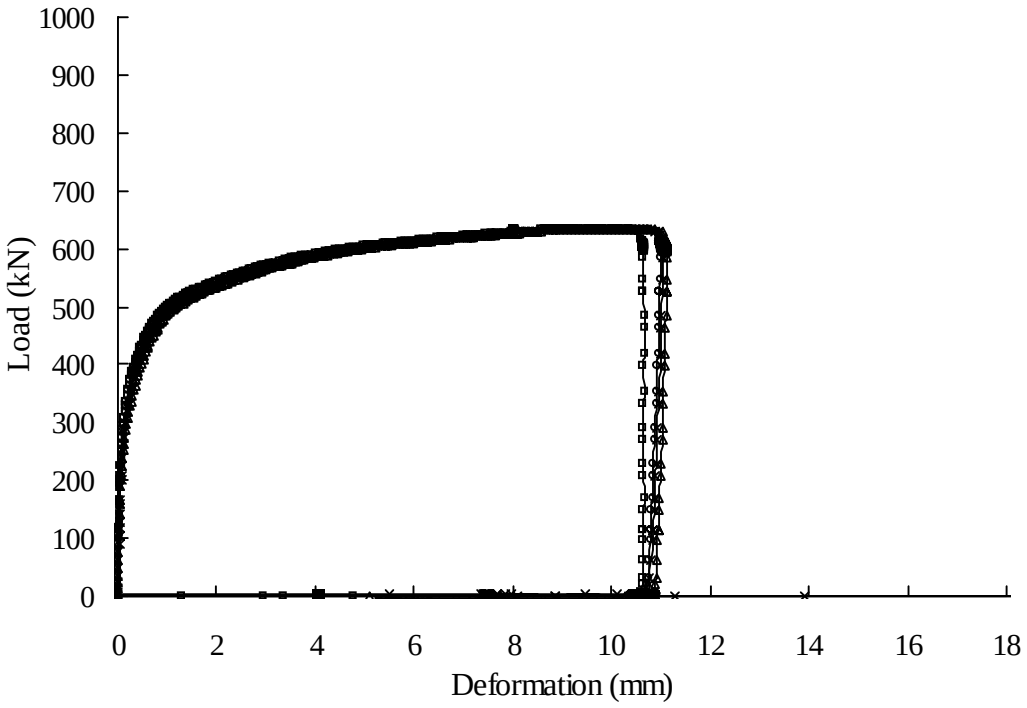

Figure 4-5: Load vs. Deformation Curve for A3R1

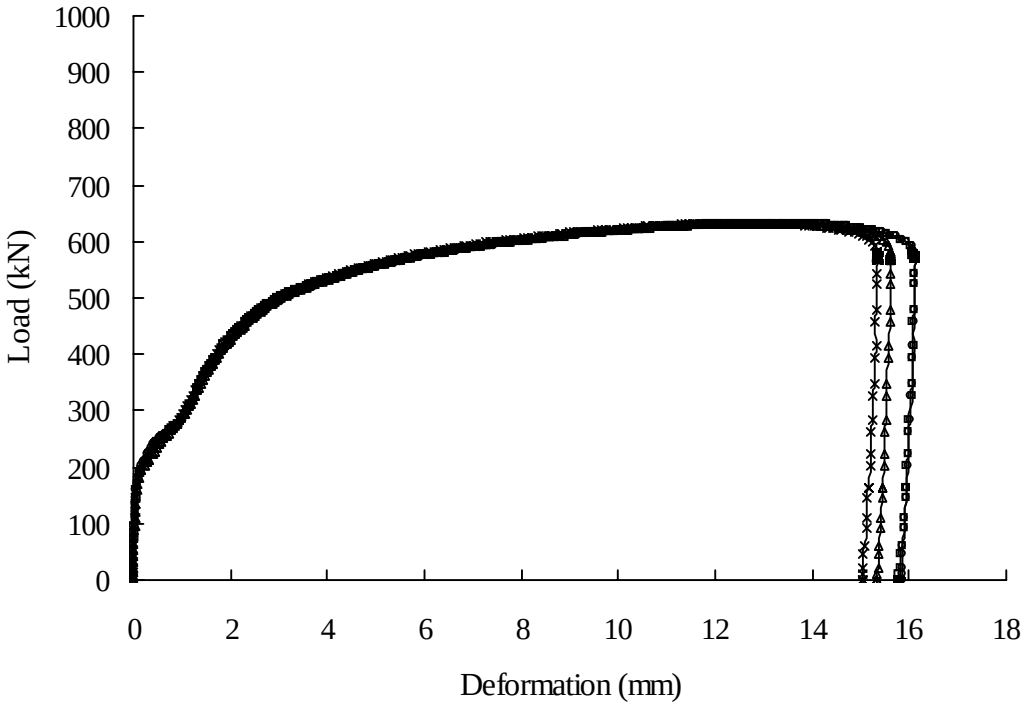

Figure 4-6: Load vs. Deformation Curve for A9R1

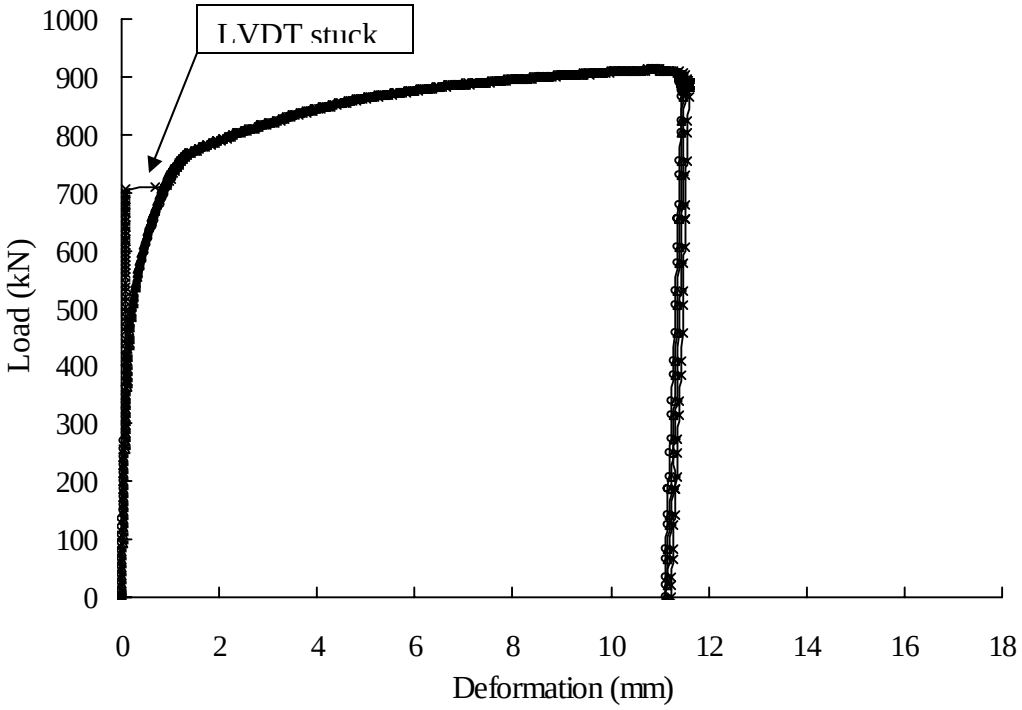

Figure 4-7: Load vs. Deformation Curve for A4R2

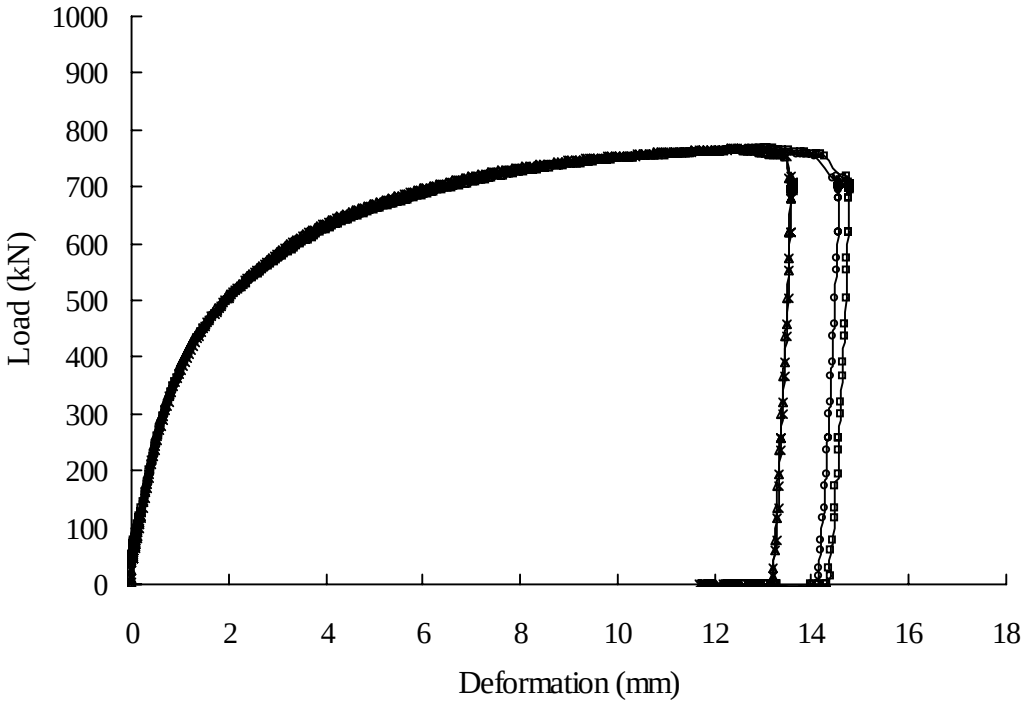

Figure 4-8: Load vs. Deformation Curve for A10R2

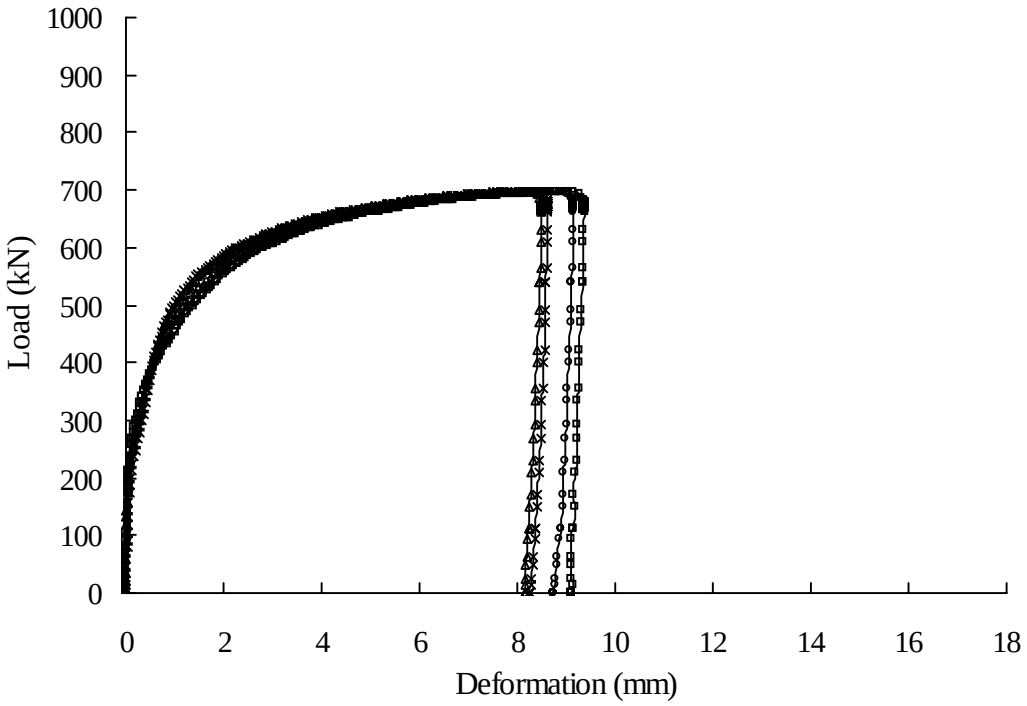

Figure 4-9: Load vs. Deformation Curve for A5E1

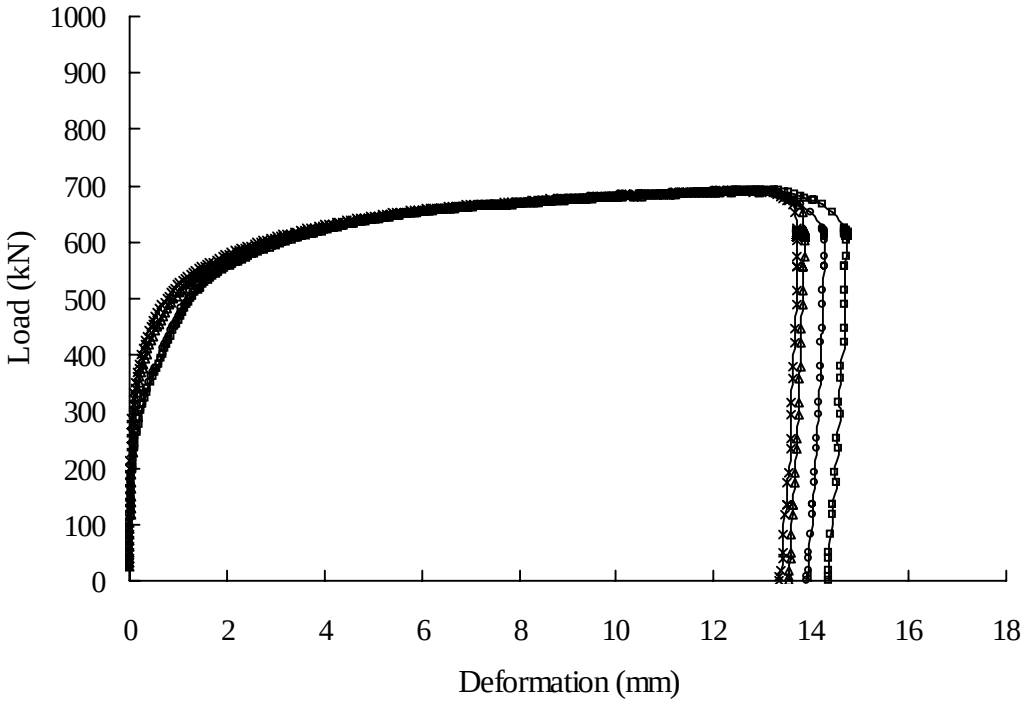

Figure 4-10: Load vs. Deformation Curve for A11E1

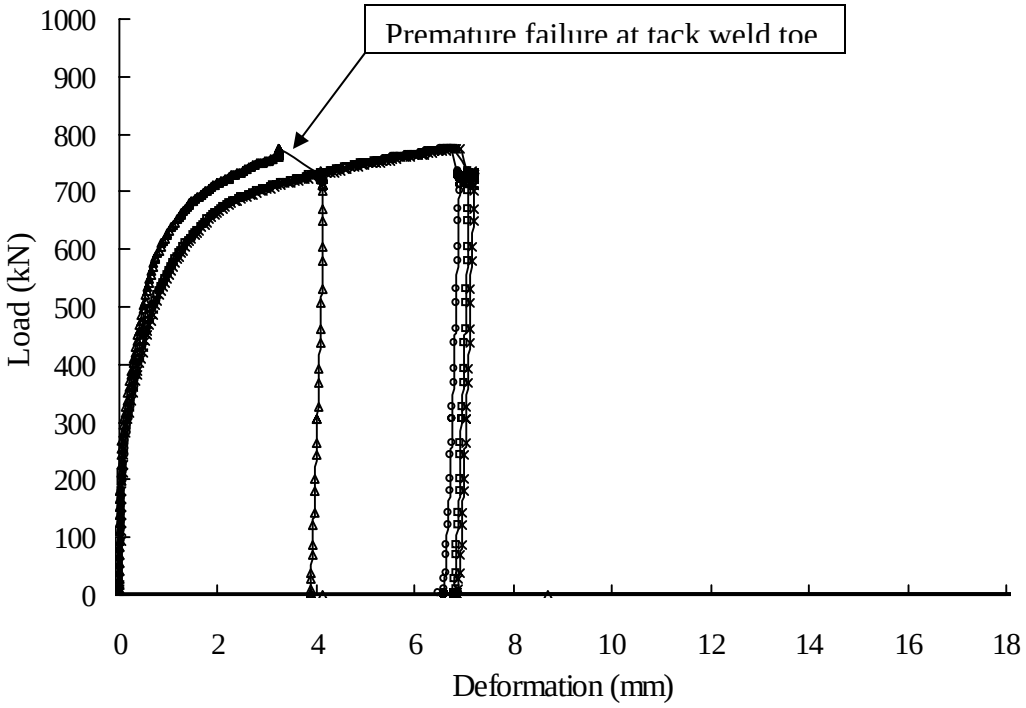

Figure 4-11: Load vs. Deformation Curve for A6E2

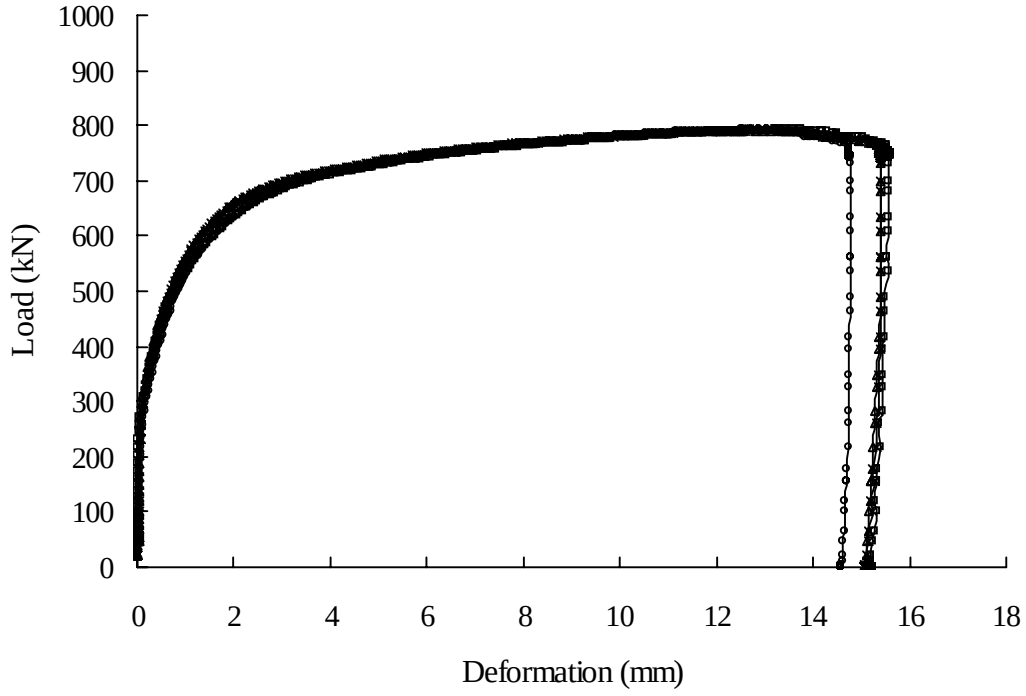

Figure 4-12: Load vs. Deformation Curve for A12E2

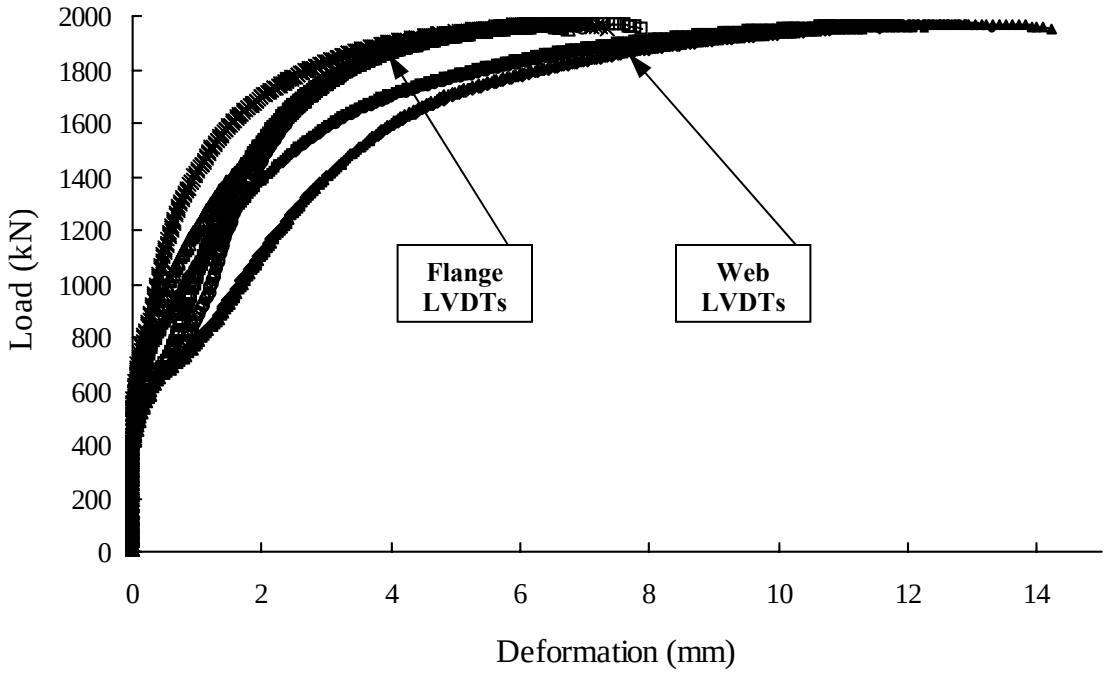

Figure 4-13: Load vs. Deformation Curve for B1G1

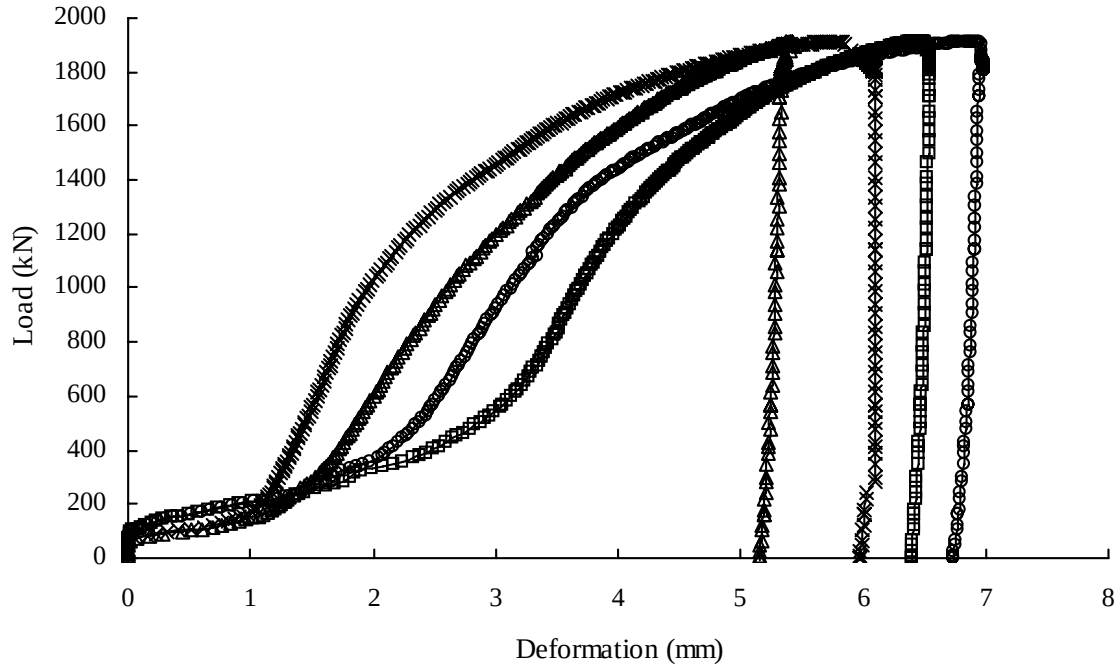

Figure 4-14: Load vs. Deformation Curve for B2G2

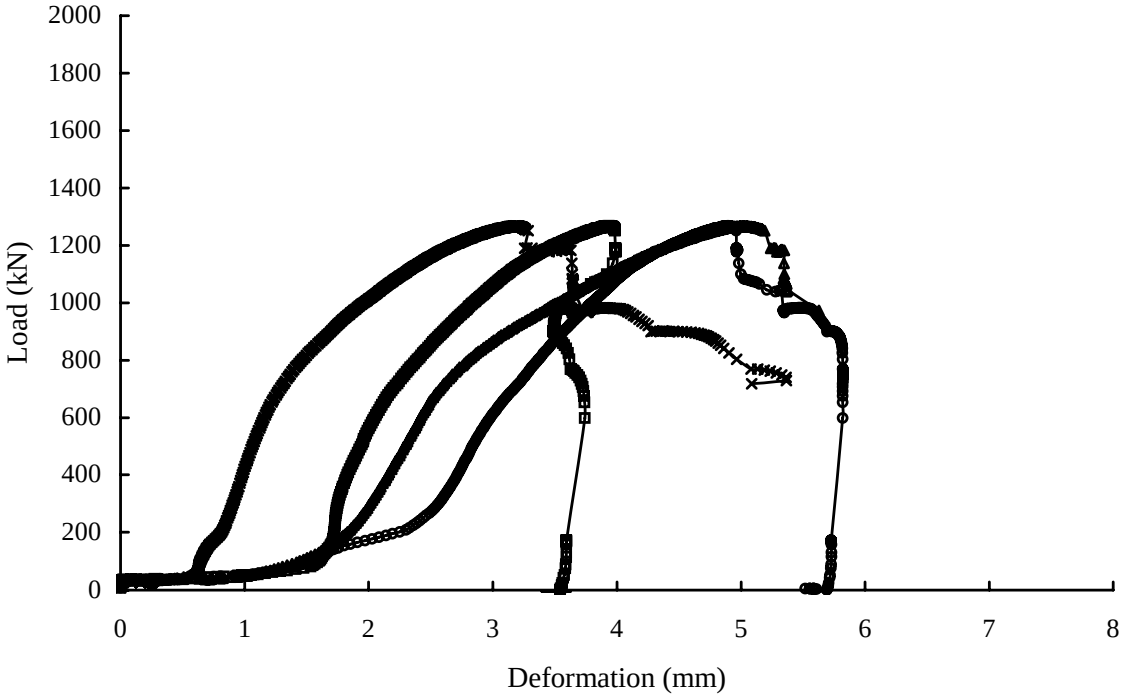

Figure 4-15: Load vs. Deformation Curve for B3R1

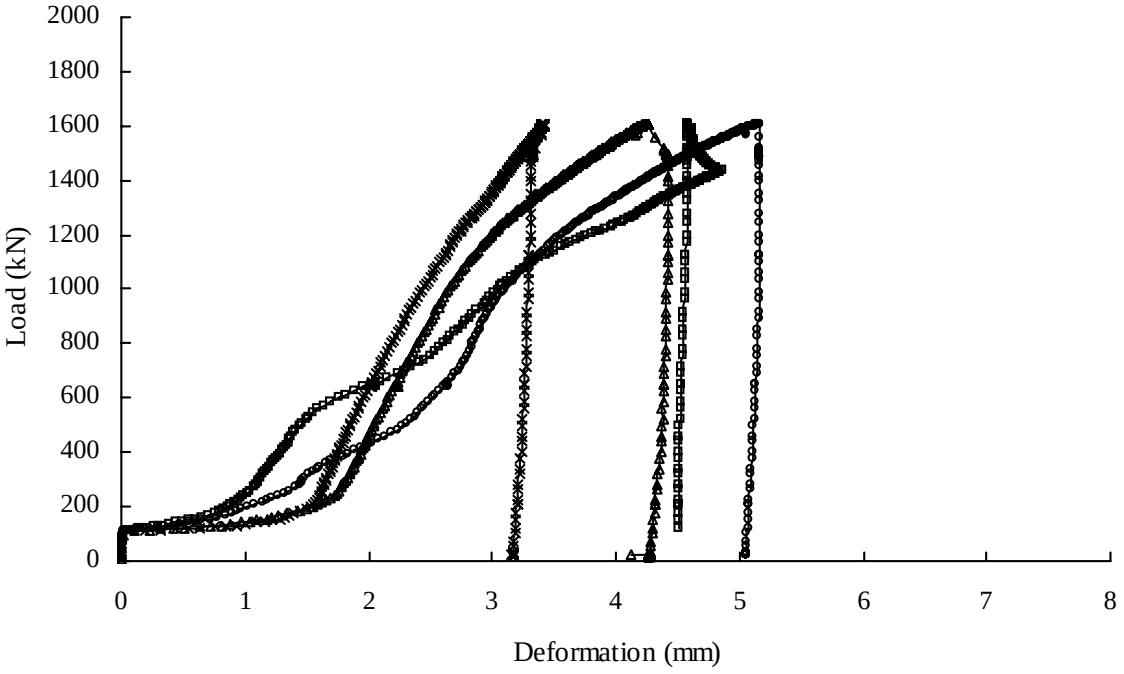

Figure 4-16: Load vs. Deformation Curve for B4R2

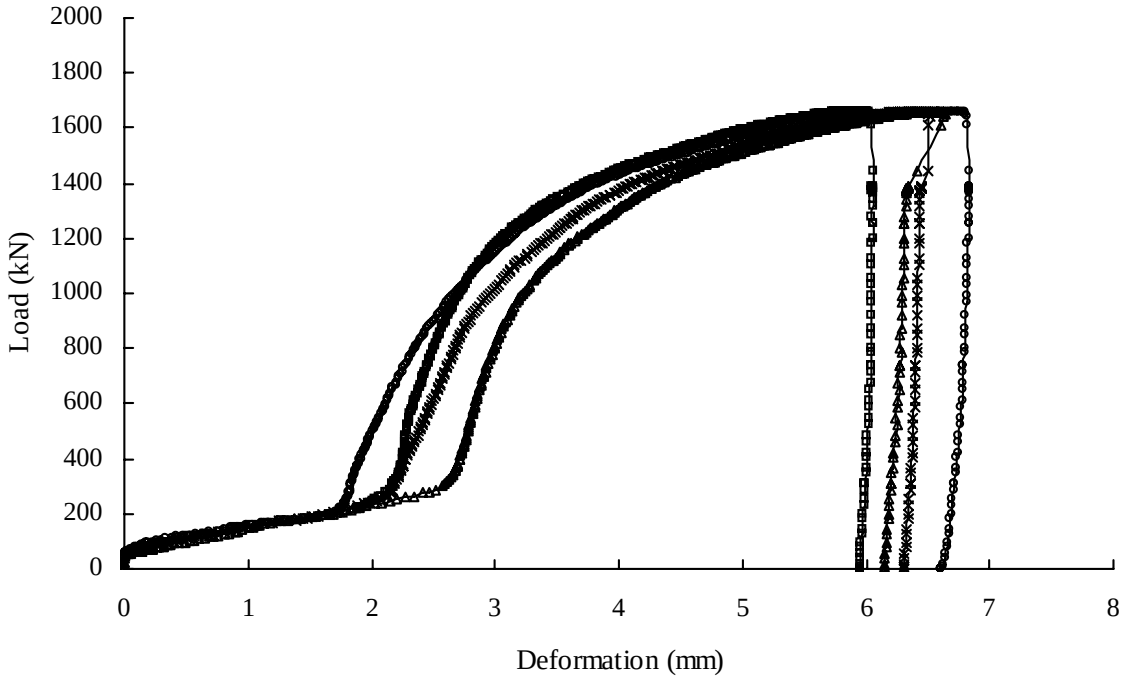

Figure 4-17: Load vs. Deformation Curve for B5E1

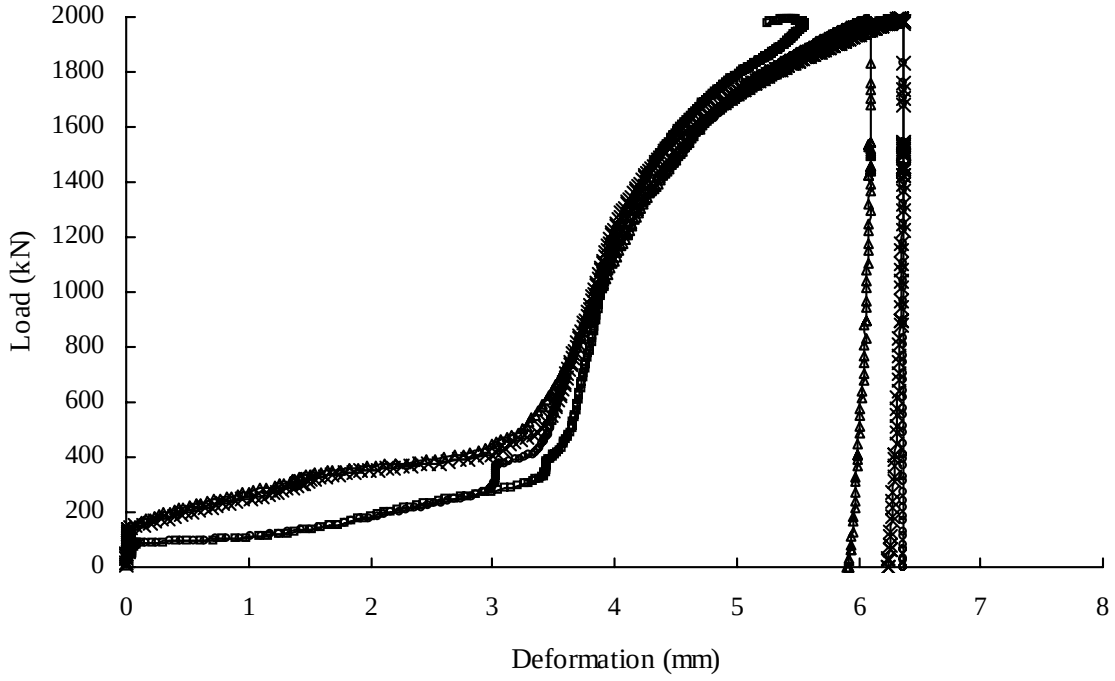

Figure 4-18: Load vs. Deformation Curve for B6E2

(a) Specimen Loaded All the Way to Failure **(b) Specimen Unloaded Right After the Peak**

Figure 4-19: Typical Specimen Failures in Series C (thicker web)

(a) Bolts in Thicker Web Specimens **(b) Bolts in Thinner Web Specimens**

Figure 4-20: Typical Bolt Failures in Series C

(a) With Tension Plane Rupture **(b) Without Tension Plane Rupture**

Figure 4-21: Typical Specimen Failures in Series C (thinner web)

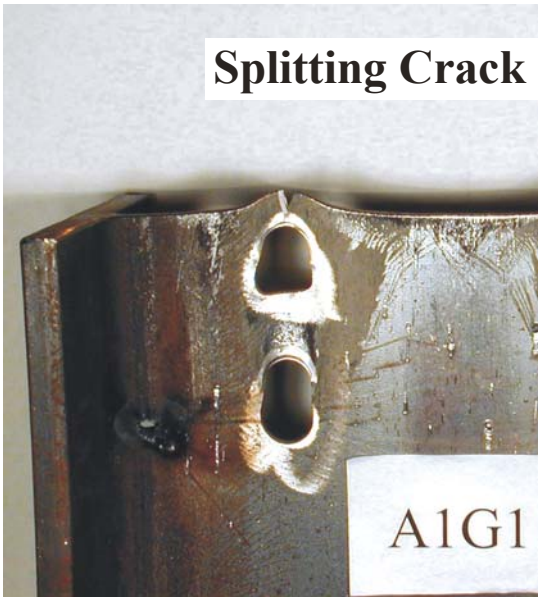

(a) Shear Tear **(b) Tensile Splitting Crack**

Figure 4-22: Typical Shear Tear and Tensile Splitting Crack in Series A

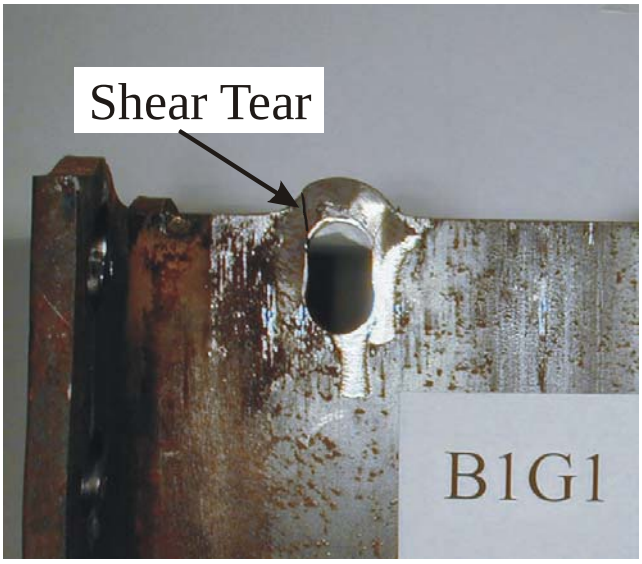

Figure 4-23: Typical Shear Tears in Series B

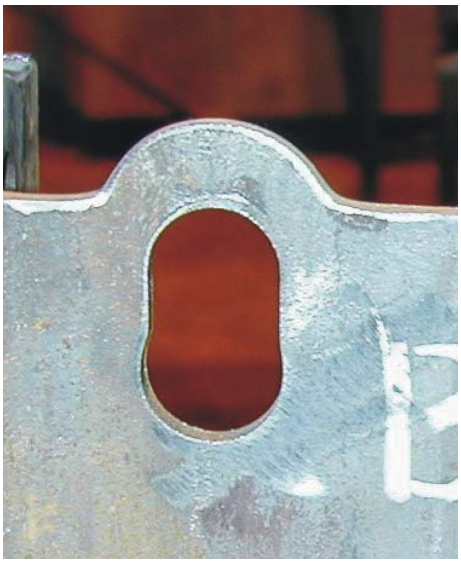

Figure 4-24: Ductility at a Hole (Specimen B5, unloaded at the peak)

Figure 4-25: Series A Failed Connections

Figure 4-25: Series A Failed Connections (Cont'd)

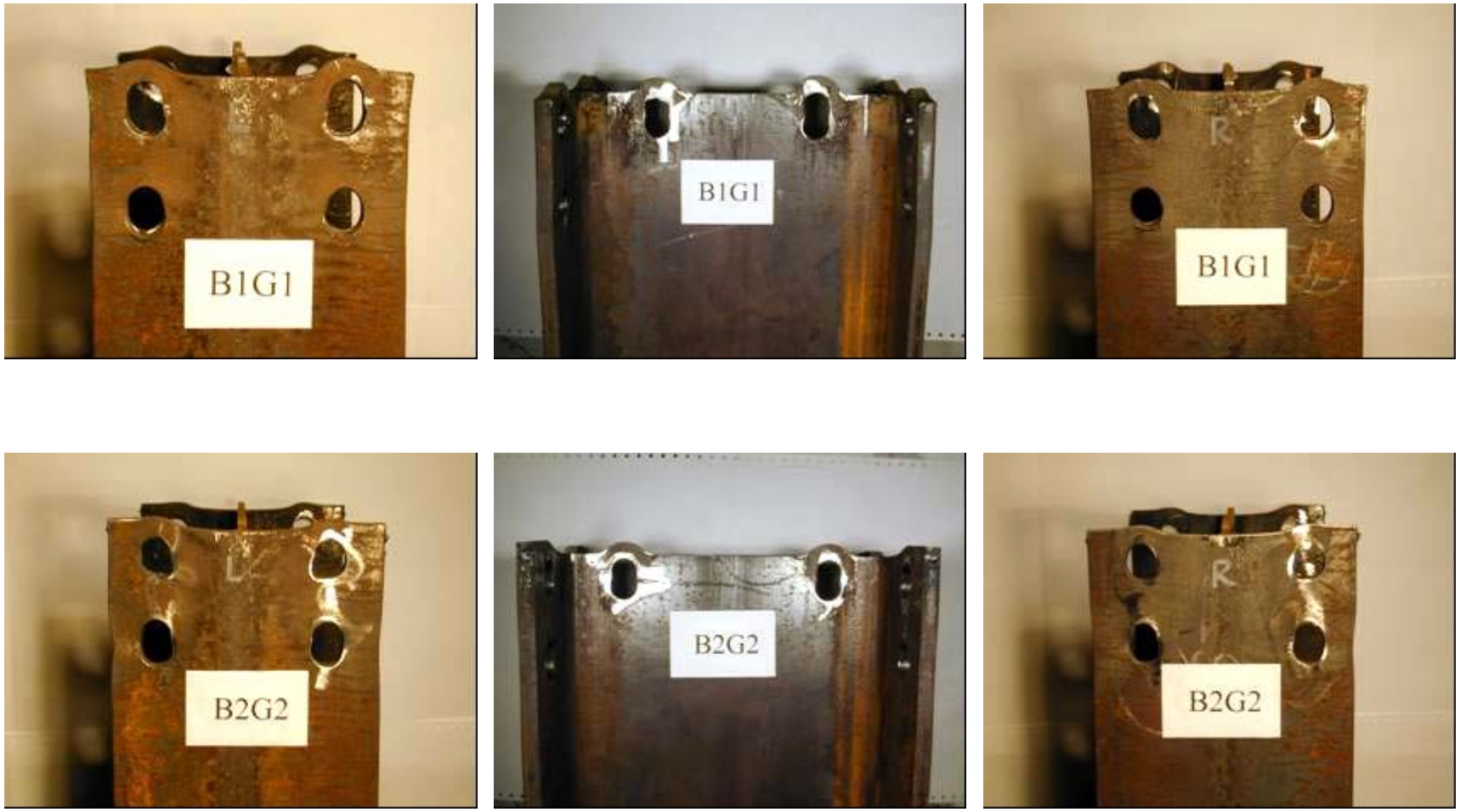

Figure 4-26: Series B Failed Connections

Figure 4-26: Series B Failed Connections (Cont'd)

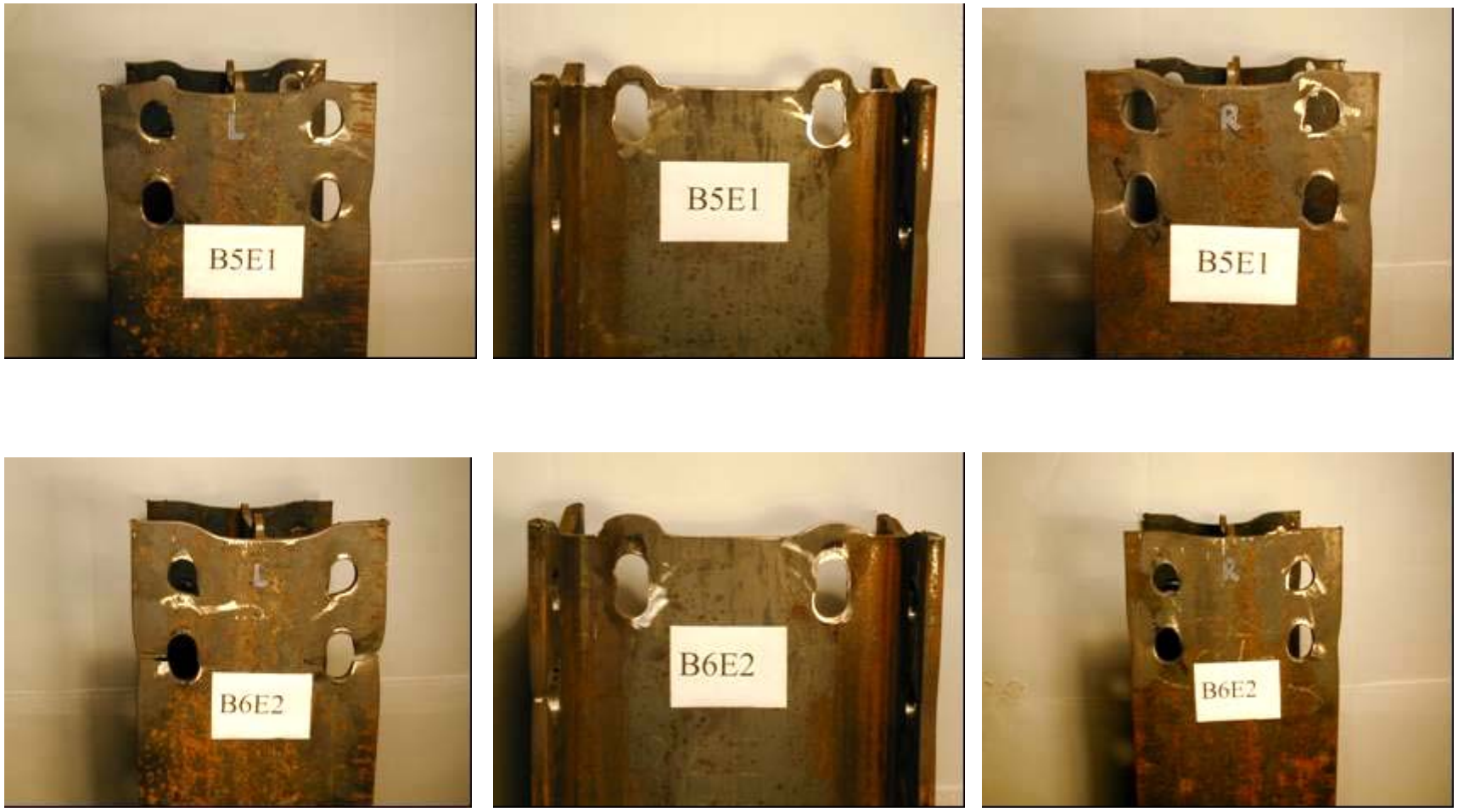

Figure 4-26: Series B Failed Connections (Cont'd)

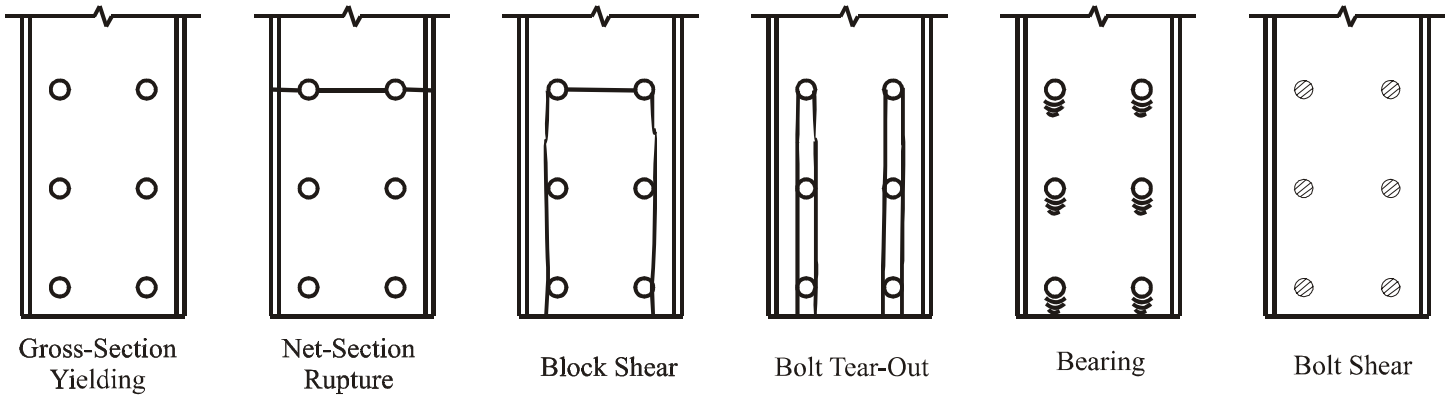

Figure 4-27: Series C Traditional Failure Modes

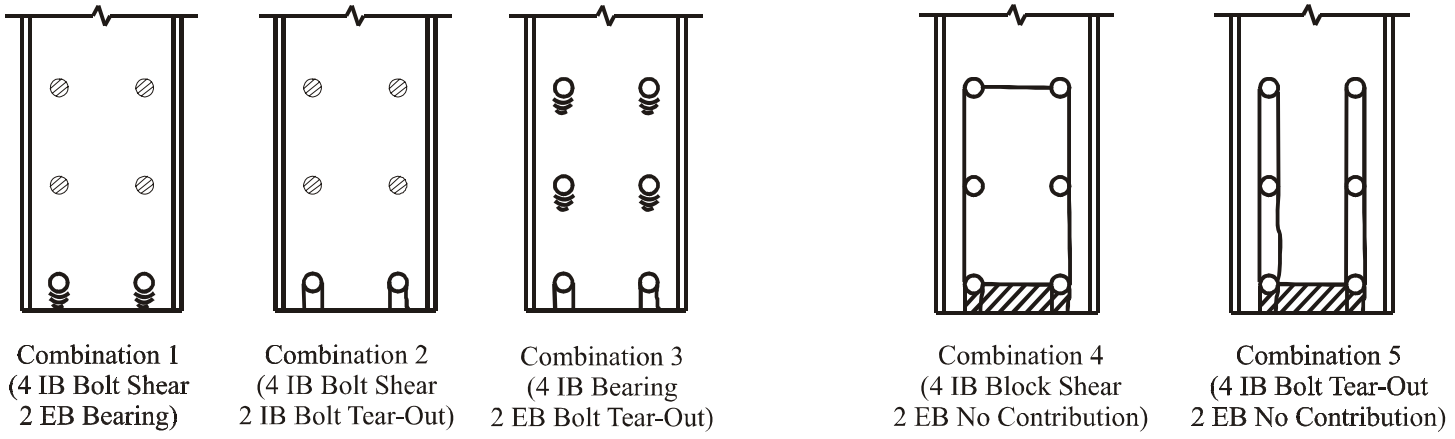

(a) Ductile Behaviour **(b) Non-Ductile Behaviour**

Figure 4-28: Series C Combination Failure Modes

5. RELIABILITY ANALYSES

5.1 Introduction

This chapter assesses the ability of the North American design standards (using the block shear equations) and the unified equation to predict the failure of tension members failing predominantly by bolt end tear-out through reliability analyses. A total of 184 specimens from this research project and the literature have been considered.

In general, an appropriate reliability index, β, which represents the probability of failure of a member or connection, can be achieved by selecting a suitable resistance factor, ϕ, for design. These two parameters are related by the bias coefficient for the resistance, ρ_R, and the coefficient of variation of resistance, V_R, which can be determined by the relevant material parameters, geometric parameters, professional parameters (in the form of test-to-predicted ratios), and discretization parameters. The basic equation for calculating the resistance factor, as proposed by Ravindra and Galambos (1978), is:

$$\phi = \rho_R \exp(-\beta \alpha_R V_R) \qquad [5\text{-}1]$$

where:

$$\rho_R = \rho_M \rho_G \rho_P \rho_d \qquad [5\text{-}2]$$

$$V_R = \sqrt{V_M^2 + V_G^2 + V_P^2 + V_d^2} \qquad [5\text{-}3]$$

where:

α_R is a separation variable;

ρ_M is the bias coefficient of the material factor;

ρ_G is the bias coefficient of the geometry factor;

ρ_P is the bias coefficient of the professional factor;

ρ_d is the bias coefficient of the discretization factor;

V_M is the coefficient of variation of material factor;

V_G is the coefficient of variation of geometry factor;

V_P is the coefficient of variation of the professional factor; and

V_d is the coefficient of variation of the discretization factor.

Ravindra and Galambos (1978) also proposed that the separation variable, α_R, be taken as 0.55.

For connections, the traditional target reliability index is from 4.0 to 4.5, so since Equation [5-1] was calibrated for a reliability index of 3.0 a modification factor, Φ_β, must be applied to the equation. Based on work by Fisher *et al*. (1978), Franchuk *et. al*. (2002) proposed the following equation for the modification factor that is suitable for mean (as opposed to nominal) live-to-dead load ratios ranging from 0.5 to 2.0, and reliability indices from 2.0 to 5.0:

$$\Phi_\beta = 0.0062\beta^2 - 0.131\beta + 1.338 \qquad [5\text{-}4]$$

The resistance factor equation therefore becomes:

$$\phi = (0.0062\beta^2 - 0.131\beta + 1.338)\rho_R \exp(-\beta\alpha_R V_R) \qquad [5\text{-}5]$$

5.2 Material Factor

Material property factors reflect the fact that the actual material strength is different from the nominal material strength used in design. Material factors used in this project were obtained from Schmidt and Bartlett (2002a). Since these authors presented values for plates and wide-flange shapes only, the values for wide-flange webs have been used for channels connected through the webs. All other specimens considered in this analysis are either plates, wide-flange shapes, or Tees cut from wide-flange shapes.

For bolt tear-out failure, both the yield and ultimate strength of the material are relevant to the connection strength, but it is conservative to use the values for the static yield stress since the mean bias coefficient is lower and the coefficient of variation higher than those for the ultimate strength. For plate thicknesses ranging from 10 mm to 20 mm the values are 1.07 and 0.054 for the bias coefficient and coefficient of variation, respectively. For wide-flange shapes, reliability parameters should consider the web

and/or flange according to their respective involvements in the mode of failure. The values of the bias coefficient and coefficient of variation for the flange static yield strength were given as 1.03 and 0.063, respectively, and these values were used for the cases where failure involves both the web and flange since the strength of the flange is typically slightly lower than the web. For cases where failure involves the web only, Schmidt and Bartlett (2002a) recommend that the web bias coefficient be taken as 1.02 times that of the flange, with the coefficient of variation remaining the same, to reflect that the higher web yield strength. The difference of the yield strength between the web and flanges is reduced from 5%—the value typically used—to 2% due to the modern rolling method of steel production; specifically W-shapes are rolled from dog-bone-shaped casts instead of rectangular blooms (Schmidt and Bartlett, 2002a). The values of the bias coefficient and coefficient of variation for the web static yield strength were obtained after applying the correction as 1.05 and 0.063, respectively.

5.3 Geometry Factor

Geometry factors represent the fact that the actual plate thickness and bolt hole layout usually differ from the nominal values. Franchuk *et. al*. (2002) found that the effect of the perimeter of the block at final failure was negligible compared to that of the material thickness. Therefore, the selection of geometry factors could be based on the thickness only for simplicity with reasonable accuracy.

For plates, the values for bias coefficient and coefficient of variation, which are based on web and flange thicknesses of WWF shapes, were reported by Schmidt and Bartlett (2002a) as 1.04 and 0.025, respectively. Since Schmidt and Bartlett (2002a) did not give thickness data for wide-flange shapes, geometric properties used for rolled shapes are based on the values given by Kennedy and Gad Aly (1980), who give the value of the bias coefficient and coefficient of variation for the flange thickness as 0.979 and 0.0417, and for web thickness as 1.017 and 0.0384, respectively. It is conservative to use the values for flange thickness instead of the web thickness for failure involving both the web and flanges because the flange has a lower bias coefficient and a higher coefficient of variation.

5.4 Discretization Factor

Discretization factors reflect the fact that certain design parameters can only be selected in discrete increments. For members, only discrete cross-section sizes are available for continuous ranges of demand. This generally results in a slightly larger section being selected than is actually needed. For bolted connections, the discretization arises due to the need to select an integer number of bolts and the use of standardized shop practices such as standard bolt pitches, *etc*. No specific data were found related to the discretization factor for bolted connections, but as a point of reference Schmidt and Bartlett (2002b) recommend a bias coefficient for wide-flange tension members of 1.04, with a coefficient of variation of 0.033. It is believed that the bias coefficient for the connections of tension members would be considerably greater than that for the members themselves, although the coefficient of variation could also be greater. As a conservative approach, the values for members are used in this reliability study, although if appropriate connection data become available the reliability indices could be re-evaluated and would be expected to increase slightly.

Table 5-1 lists all the values of the material, geometry, and discretization parameters used in the reliability analyses.

5.5 Professional Factor

The professional factor represents the accuracy of an equation in predicting the capacity of a connection, and it is the equivalent of the test-to-predicted ratio. Measured geometric and material properties (and no resistance factor) are used to calculate the predicted capacity, as was done in Chapter 4, and the actual capacity of a connection can be obtained through a laboratory test. The test-to-predicted ratios for bolt tear-out failure of the tests in this research project, namely for series A and series B, are listed in Table 4-2, and a summary of test-to-predicted ratios for previously published test results is listed in Appendix B.

In calculating the predicted capacity using the CSA-S16-01 and AISC 2005 design equations and the unified equation, the governing connection capacity was obtained by considering all possible failure modes such as gross section yielding, net section rupture,

block shear, bolt tear-out and bolt shear, and the governing failure mode should match the observed failure mode in the test. As strength equations are being evaluated, bearing failure was not included in the capacity calculations as they can be unrealistically conservative and the failure modes observed were consistently dominated by bolt tear-out.

For plates, most specimens in the database violated the minimum pitch and/or end distance requirements specified in the design standards in North America, although over a hundred tests had been conducted where the observed failure mode was bolt tear-out. As this research project is not intended to investigate the behaviour of high strength steels, the yield strengths of materials considered in the reliability analyses are limited to 550 MPa. Moreover, bolt tear-out failures in plates with more than three bolts in a single line were found to fail at lower loads than predicted; since in typical connections these long tear-out-out paths would be unlikely to form before another failure mode occurred, these were excluded from the reliability study. Only 30 out of 135 specimens that failed by bolt tear-out meet all the minimum end/edge distance and pitch requirements, have a yield strength that is not greater than 550 MPa, and had no more than three bolt rows. For rolled shapes, most specimens meet the minimum end/edge distance and pitch requirements, and only the five channels among 37 specimens slightly violated the minimum pitch requirement by $0.2d_b$. As a result, 62 specimens, which include 30 plates, 14 Tees, 12 series A W-shapes, and six series B W-shapes, meet all the limitations of the reliability study. The professional factors are listed in Table 5-2.

The data pool could be enlarged by including the plates that have no more than three bolt rows and their yield strength is not greater than 550 MPa, regardless of whether or not the specimens meet the minimum end/edge distance and pitch requirements, in order to assess the consequence of misplaced holes. This results in a total of 127 specimens, which include 91 plates, 14 Tees, four channels, 12 series A W-shapes, and six series B W-shapes. These professional factors are also listed in Table 5-2. It should be emphasized that the majority of the connections in the groups marked by an asterisk in the table would not be permitted by North American standards.

Figures 5-1a and 5-1b show test vs. predicted capacity plots of the 62 test results that meet all the minimum end/edge distance and pitch requirements using CSA-S16-01/AISC 2005 and the unified equation, while Figures 5-2a and 5-2b show test vs. predicted capacity plots of the 127 test results that include those that violate the minimum end/edge distance and pitch requirements. These figures show that CSA-S16-01 and AISC 2005 generally give highly conservative predictions of capacity for the bolt tear-out mode of failure, while the unified equation gives accurate predictions over the entire database. Also, the coefficients of variation of the test-to-predicted ratios given by the unified equation are less than the values given by CSA-S16-01/AISC 2005 in both cases. For the 62 tests, the coefficient of variation of the unified equation is 0.10, while it is 0.14 for CSA-S16-01/AISC 2005. For the 127 tests, the coefficient of variation of the unified equation is 0.10, while it is 0.16 for CSA-S16-01/AISC 2005. This means that the unified equation describes the bolt tear-out behaviour better than the block shear equations of CSA-S16-01/AISC 2005.

5.6 Reliability Indices

Table 5-3 shows reliability indices provided by the design equations based on the test data from the literature and this research project. The desirable reliability index for connections is a value from 4.0 to 4.5. The resistance factor specified in CSA-S16-01 for block shear failure is 0.9, resulting in reliability indices that vary from 3.2 to 5.3. In AISC 2005, the resistance factor is 0.75 for block shear failure, resulting in reliability indices from 4.3 to 6.6. The unified equation, with a resistance factor of 0.75, provides a desired level of safety, with reliability indices ranging from 4.2 to 4.7. The greatly improved consistency over the various connection types indicates that the unified equation provides a better representation of the bolt tear-out failure behaviour than the current block shear equations in the North American standards.

5.7 Summary

Using the test results from this research project in addition to test data from the literature, it has been shown that the current design standards do not predict connection capacities for bolt tear-out failure accurately and provide inconsistent levels of safety. On the other hand, the unified equation, which can predict connection capacities of block shear, bolt

tear-out, and net section rupture, shows a significant improvement in accuracy of predicting capacities for bolt tear-out failure, and also results in adequate and more consistent levels of safety.

Table 5-1: Parameters for Reliability Analyses

Reliability Parameter	Plates	Wide-Flange Shape	
		(For Web Failure)	(For Web and Flange Failure)
ρ_M	1.07	1.05	1.03
V_M	0.054	0.063	0.063
ρ_G	1.04	1.017	0.979
V_G	0.025	0.0384	0.0417
ρ_d	1.04	1.04	1.04
V_d	0.033	0.033	0.033

Table 5-2: Professional Factors Provided by Design Equations

Section	Number of Tests	S16-01		AISC 2005		Unified Equation	
		ρ_P	V_P	ρ_P	V_P	ρ_P	V_P
Plates	30	1.21	0.11	1.21	0.11	0.97	0.11
Plates	91*	1.33	0.16	1.33	0.16	0.94	0.09
Channels	4*	1.20	0.03	1.20	0.03	0.95	0.03
W-Shapes (Web Failure)	12	1.46	0.10	1.46	0.10	1.08	0.09
W-Shapes (Web and Flange Failure)	6	1.24	0.03	1.24	0.03	1.00	0.02
Tees (Web and Flange Failure)	14	1.08	0.09	1.08	0.09	1.05	0.09

* Specimens that have no more than three bolt rows and yield strengths no greater than 550 MPa, regardless of whether or not they meet the minimum end/edge distance and pitch requirements.

Table 5-3: Reliability Indices Provided by Design Equations

Section	Number of Tests	S16-01 ($\phi = 0.9$)			AISC 2005 ($\phi = 0.75$)			Unified Equation ($\phi = 0.75$)		
		ρ_R	V_R	β	ρ_R	V_R	β	ρ_R	V_R	β
Plates	30	1.39	0.13	**4.4**	1.39	0.13	**5.5**	1.13	0.13	**4.3**
Plates	91*	1.54	0.18	**4.3**	1.54	0.18	**5.3**	1.09	0.12	**4.2**
Channels	4*	1.33	0.09	**4.9**	1.33	0.09	**6.3**	1.02	0.08	**4.5**
W-Shapes (Web Failure)	12	1.62	0.13	**5.3**	1.62	0.13	**6.6**	1.20	0.12	**4.7**
W-Shapes (Web and Flange Failure)	6	1.30	0.09	**4.6**	1.30	0.09	**6.0**	1.05	0.08	**4.4**
Tees (Web and Flange Failure)	14	1.14	0.12	**3.2**	1.14	0.12	**4.3**	1.10	0.12	**4.2**

* Specimens that have no more than three bolt rows and yield strengths no greater than 550 MPa, regardless of whether or not they meet the minimum end/edge distance and pitch requirements.

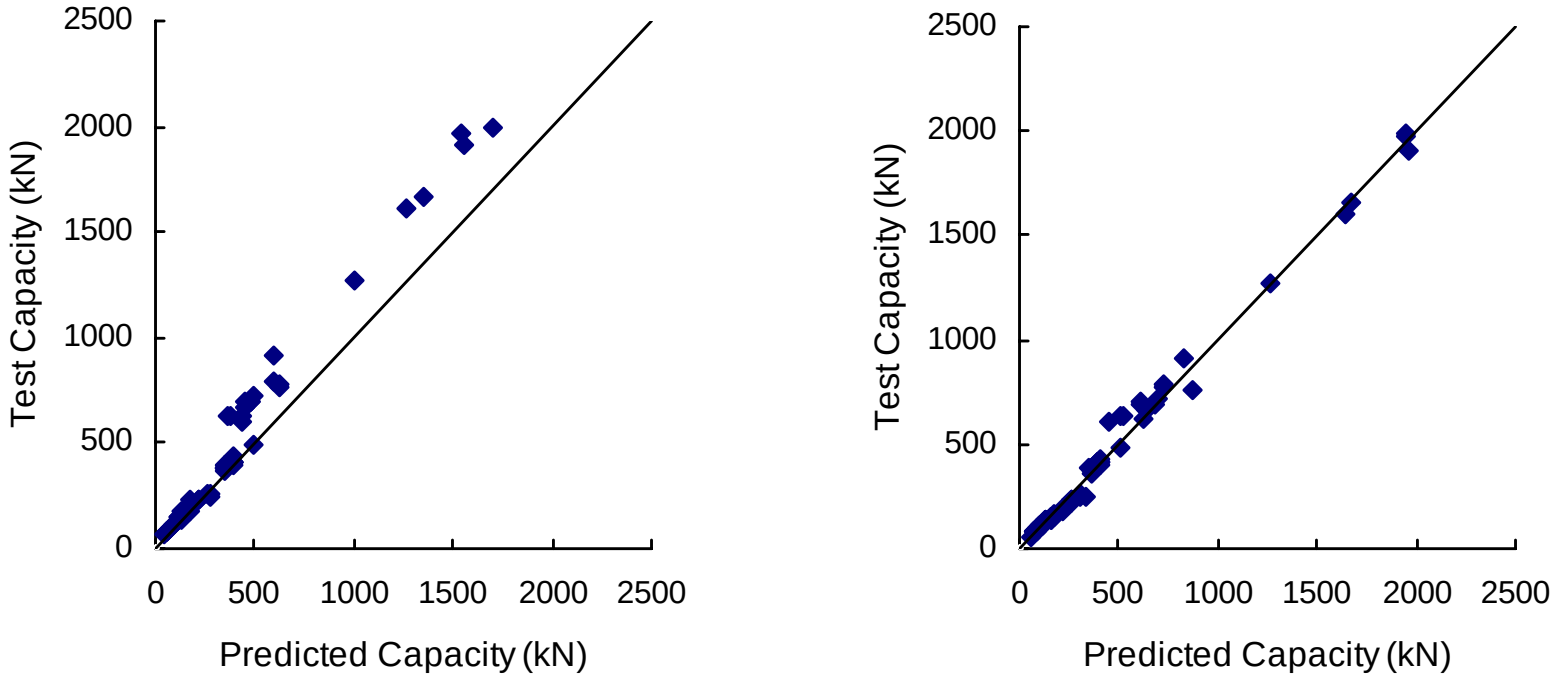

(a) CSA-S16-01/AISC 2005 **(b) Unified Equation**

Figure 5-1: Test vs. Predicted Capacities
(62 specimens that meet the minimum end distance and pitch requirements and $F_y \leq 550$ MPa)

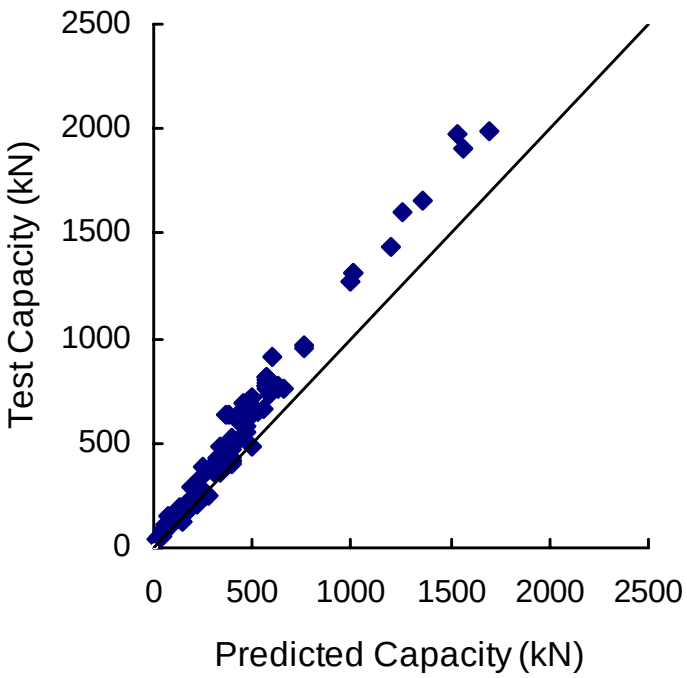

(a) CSA-S16-01/AISC 2005

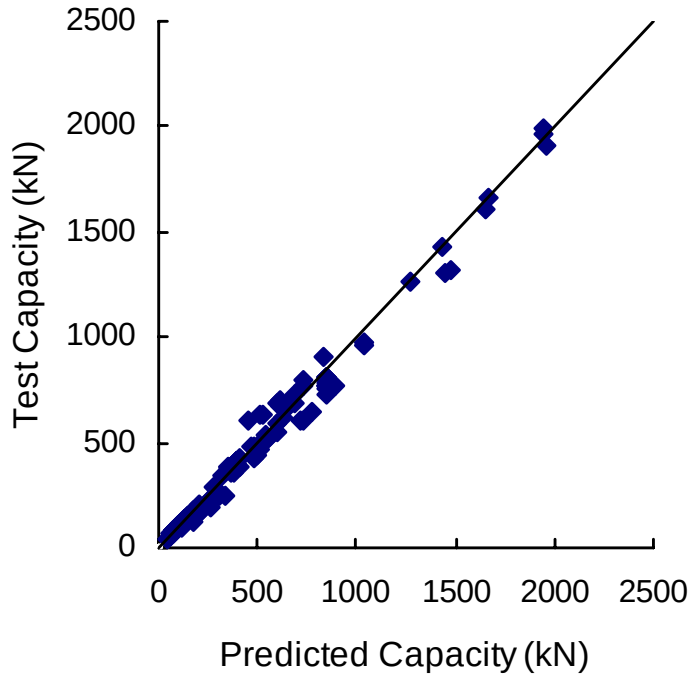

(b) Unified Equation

Figure 5-2: Test vs. Predicted Capacities
(127 specimens that have no more than three bolt rows and $F_y \leq 550$ MPa)

6. SUMMARY, CONCLUSIONS AND RECOMMENDATIONS

6.1 Summary

Bolt tear-out failure has not been clearly addressed in current design standards in North America, although the shear terms of block shear equations could be used. A unified block shear equation was proposed from a reliability-based study by Driver *et al*. (2006) using a large database of block shear tests from the literature collected by Kulak and Grondin (2001). As compared to other block shear equations from the literature and those in design standards CSA-S16-01 and AISC 2005, the unified equation has been proven to provide better predictions and more consistent levels of safety for block shear failure in a variety of connection types. Due to the similarities of net section rupture, block shear failure, and bolt tear-out failure, the application of the unified block shear equation can be extended to become a truly unified equation for these three closely related failure modes.

A total of 50 full-scale tests have been completed on wide-flange shapes, and 18 of them were designed specifically to investigate bolt tear-out failure. Twelve specimens connected by the web only and six by both the web and flanges were tested in tension. The main variables in the experiments were web bolt gauge, the number of bolt rows in the web, and end distance. The remaining 32 specimens were conducted to investigate the effect of end distance and material thickness on the overall behaviour larger bolt groups.

Along with the tests previously conducted by other researchers, a total of 127 test results of specimens failing by bolt tear-out were analyzed. Reliability analyses of the equations in current design standards in North America and the unified equation were conducted in order to evaluate their accuracy and the safety level provided. It was found that use of the block shear equations in CSA-S16-01/AISC 2005 for bolt tear-out provides highly conservative capacity predictions, while the unified equation gives accurate strength predictions and less scatter in the test-to-predicted ratios. With the resistance factor of 0.9, CSA-S16-01 provides reasonable reliability indices, although they are quite high in some cases. For Tees failing in the so-called alternate block shear mode, the low reliability index implies a probability of failure higher than what is typically considered

acceptable for connections, while the unified equation—with a resistance factor of 0.75—provides an adequate level of safety. With the resistance factor of 0.75, AISC 2005 generally provides high and inconsistent reliability indices. The unified equation achieves desired levels of reliability indices for bolt tear-out failure with a resistance factor of 0.75.

6.2 Conclusions

The following conclusions can be drawn from the test results of this research project along with the test results from the literature:

1. In spite of the occurrence of tensile splitting cracks at the end bolts of some specimens that failed by bolt tear-out, the laboratory tests and strength calculations proved that two shear planes adjacent to each bolt line carry the load until the peak is reached.

2. For the bolt tear-out failure mode, the average stress on the shear planes at failure exceeds the shear yield stress but may not reach the ultimate shear stress.

3. The unified equation gives good predictions for bolt tear-out failure for typical connection lengths up to three bolt rows, while CSA-S16-01 and AISC 2005 give very conservative results. Connection lengths longer than this are unlikely to fail in this mode.

4. All series B specimens except specimen B4R2 had a shorter connection length in the web than the flanges by one bolt row. The resulting failure mode in all cases was shear fracture in the web and tension fracture in the flanges, which occurred well before shear fracture in the flanges since the material ductility in tension is inadequate for those shear tears to take place. The unified equation gives excellent predictions of the capacities of these members simply by the summation of the block shear capacities of the four flanges and the bolt tear-out capacities of the web.

5. For connections with large pitch and relatively small end distance, inner bolts and end bolts may fail in different modes, but the ductility of the connection is sufficient for each of the bolt locations to develop their individual capacities.

6.3 Recommendations

Although many connection parameters have been investigated in this research project, more physical tests are recommended to broaden the database for the bolt tear-out failure mode. Connection configurations similar to the series B tests, but with very different connection lengths in the web and flanges and with large pitch, are recommended to be investigated to verify the criteria of additive capacities for combined failure modes, since the sequential failure may be an important factor that would affect the strength of connections. Connection tests with slotted holes are also recommended in order to determine whether they need to be treated differently from standard holes for bolt tear-out failure.

Based on the comparisons of predicted capacities and safety levels of design equations in North America and the unified equation using test results of this research project and the literature, the following unified equation, which is identical to the unified block shear equation, is recommended for the three closely related failure modes of net section rupture, block shear, and bolt tear-out.

$$P_r = \phi A_{nt} F_u + \phi A_{gv} \left(\frac{F_y + F_u}{2\sqrt{3}} \right) \qquad [6\text{-}1]$$

where the resistance factor ϕ is recommended to be taken as 0.75.

For net section rupture, the unified equation can be simplified by using the tension component only. It becomes:

$$P_r = \phi A_{nt} F_u \qquad [6\text{-}2]$$

For bolt tear-out failure, the unified equation can be simplified by using the shear component only. It becomes:

$$P_r = \phi A_{gv}\left(\frac{F_y + F_u}{2\sqrt{3}}\right) \qquad [6\text{-}3]$$

It has been proven that the unified equation gives much more accurate test-to-predicted ratios and more consistent reliability indices compared to the design equations in North American standards for bolt tear-out failure.

REFERENCES

Aalberg, A and Larsen, P.K. (2001). "Bearing Strength of Bolted Connections in High Strength Steel," Proceedings, 9th Nordic Steel Construction Conference, Helsinki, Finland. pp. 859-866

Aalberg, A and Larsen, P.K. (2002). "The Effect of Steel Strength and Ductility on Bearing Failure of Bolted Connections," Proceedings, 3rd European Conference Steel Structures, Coimbra, Portugal. pp. 869-878

AISC (2005). "Specification for Structural Steel Buildings," American Institute of Steel Construction, Chicago, IL, USA.

CSA. (2001). "Limit States Design of Steel Structures," CSA-S16-01, Canadian Standards Association, Toronto, ON, Canada.

ASTM (2007). "A370-97 Standard Test Methods and Definitions for Mechanical Testing of Steel Products," American Society for Testing and Materials, Philadelphia, PA, USA.

Driver, R.G., Grondin, G.Y., and Kulak, G.L. (2006). "Unified Block Shear Equation for Achieving Consistent Reliability," Journal of Constructional Steel Research, Vol. 62, pp. 210-222.

Epstein, H.I., and Stamberg, H. (2002). "Block Shear and Net Section Capacities of Structural Tees in Tension: Test Results and Code Implications," Engineering Journal, American Institute of Steel Construction, Vol. 39, Fourth quarter, pp. 228-239.

ESC (1992). "ENV 1993-1-1 Eurocode 3: Design of Steel Structures," European Committee for Standardization, Brussels, Belgium.

Fisher, J.W., Galambos, T.V., Kulak, G.L., and Ravindra, M.K. (1978). "Load and Resistance Factor Design Criteria for Connectors," Journal of the Structural Division, ASCE, Vol. 104, No. ST9, pp. 1427-1441.

Franchuk, C.R., Driver, R.G., and Grondin, G.Y. (2002). "Block Shear Behaviour of Coped Steel Beams," Structural Engineering Report No. 244, Department of Civil and Environmental Engineering, University of Alberta, Edmonton, AB, Canada.

Franchuk, C.R., Driver, R.G., and Grondin, G.Y. (2003). "Experimental Investigation of Block Shear Failure in Coped Steel Beams," Canadian Journal of Civil Engineering, Vol. 30, pp. 871-881.

Hardash, S.G. and Bjorhovde, R. (1985). "New Design Criteria for Gusset Plates in Tension," Engineering Journal, AISC, Vol. 22, No. 2, pp. 77-94

Huns, B.B.S., Grondin, G.Y., and Driver, R.G. (2002). "Block Shear Behaviour of Bolted Gusset Plates," Structural Engineering Report No. 248, Department of Civil and Environmental Engineering, University of Alberta, Edmonton, AB, Canada.

Kato, B. (2003a). "Unified Strength Evaluation of Bolted Joints," International Journal of Steel Structures, Vol. 3, pp. 137-144.

Kato, B. (2003b). "Unified Strength Evaluation of Bolted Joints of Shapes," International Journal of Steel Structures, Vol. 3, pp. 145-154.

Kennedy, D.J.L. and Gad Aly, M. (1980). "Limit States Design of Steel Structures—Performance Factors," Canadian Journal of Civil Engineering, Vol. 7 pp. 45-77

Kim, H.J. and Yura, J.A. (1999). "The Effect of Ultimate-to-Yield Ratio on the Bearing Strength of Bolted Connections," Journal of Constructional Steel Research, Vol. 49, pp. 255-269.

Kulak, G.L. and Grondin, G.Y. (2001). "Block Shear Failure in Steel Members—A Review of Design Practice," Engineering Journal, American Institute of Steel Construction, Vol. 38, Fourth quarter, pp. 199-203.

Puthli, R. and Fleischer, O. (2001). "Investigations on Bolted Connections for High Strength Steel Members," Journal of Constructional Steel Research, Vol. 57, pp. 313-326.

Ravindra, M.K. and Galambos, T.V. (1978). "Load and Resistance Factor Design for Steel," Journal of the Structural Division, ASCE, Vol. 104, No. ST9, pp. 1337-1353.

Rex, C.O. and Easterling, W.S. (2003). "Behavior and Modeling of a Bolt Bearing on a Single Plate." Journal of Structural Engineering, ASCE, 792-800.

Schmidt, B.J. and Bartlett, F.M. (2002a). "Review of Resistance Factor for Steel: Data Collection," Canadian Journal of Civil Engineering, Vol. 29, pp. 98-108.

Schmidt, B.J. and Bartlett, F.M. (2002b). "Review of Resistance Factor for Steel: Resistance Distributions and Resistance Factor Calibration," Canadian Journal of Civil Engineering, Vol. 29, pp. 109-118.

Udagawa, K. and Yamada, T. (1998). "Failure Modes and Ultimate Tensile Strength of Steel Plates Jointed with High Strength Bolts," Journal of Structural and Construction Engineering, Architectural Institute of Japan, No. 505, pp. 115-122. (in Japanese)

Udagawa, K. and Yamada, T. (2004). "Ultimate Strength and Failure Modes of Tension Channels Jointed with High-Strength Bolts," Proceedings, 13th World Conference on Earthquake Engineering, Vancouver, BC, Canada.

APPENDIX A

Published Test Results

Table A-1: Published Test Results of Bolt Tear-Out Failure

Specimen	Bolt Diameter (mm)	Plate Thickness (mm)	End Distance (mm)	Bolt Pitch (mm)	Number of Bolt Lines	Number of Bolt Rows	Yield Stress (MPa)	Ultimate Stress (MPa)	Test Capacity (kN)
Udagawa and Yamada (1998)									
121.4	16	12	15.7	40	1	2	277.6	443.4	288.4
122.4	16	12	23.4	40	1	2	277.6	443.4	337.5
123.4	16	12	31.2	40	1	2	277.6	443.4	375.7
124.4	16	12	39.7	40	1	2	277.6	443.4	413.0
131.4	16	12	16.0	40	1	3	277.6	443.4	421.8
132.4	16	12	20.0	40	1	3	279.6	444.4	438.5
133.4	16	12	24.0	40	1	3	265.9	452.2	468.9
134.4	16	12	31.7	40	1	3	277.6	443.4	517.0
135.4	16	12	40.5	40	1	3	265.9	452.2	547.4
141.4	16	12	16.2	40	1	4	277.6	443.4	557.2
142.4	16	12	23.4	40	1	4	277.6	443.4	600.4
143.4	16	12	31.4	40	1	4	277.6	443.4	657.3
144.4	16	12	39.0	40	1	4	277.6	443.4	724.0
23D.4	16	12	24.0	40	2	3	279.6	444.4	955.5
23N.4	16	12	24.0	40	2	3	279.6	444.4	972.2
121.6	16	12	15.7	40	1	2	476.8	601.4	391.4
122.6	16	12	25.0	40	1	2	472.8	604.3	483.6
123.6	16	12	32.0	40	1	2	493.4	615.1	522.9
124.6	16	12	40.6	40	1	2	477.8	600.4	584.7
131.6	16	12	16.0	40	1	3	474.8	618.0	600.4
132.6	16	12	20.3	40	1	3	447.3	589.6	602.3
133.6	16	12	24.0	40	1	3	459.1	616.1	652.4
134.6	16	12	32.3	40	1	3	480.7	607.2	730.8
135.6	16	12	39.5	40	1	3	459.1	616.1	765.2

Table A-1: Published Test Results of Bolt Tear-Out Failure (Cont'd)

Specimen	Bolt Diameter (mm)	Plate Thickness (mm)	End Distance (mm)	Bolt Pitch (mm)	Number of Bolt Lines	Number of Bolt Rows	Yield Stress (MPa)	Ultimate Stress (MPa)	Test Capacity (kN)
Udagawa and Yamada (1998) Cont'd									
141.6	16	12	17.0	40	1	4	480.7	603.3	799.5
142.6	16	12	24.0	40	1	4	478.7	601.4	875.1
143.6	16	12	32.6	40	1	4	491.5	615.1	951.6
144.6	16	12	39.7	40	1	4	478.7	602.3	1012.4
23D.6	16	12	24.0	40	2	3	447.3	589.6	1312.6
23N.6	16	12	24.0	40	2	3	447.3	589.6	1306.7
23P.6	16	12	35.2	40	2	3	447.3	589.6	1435.2
121.8	16	12	15.2	40	1	2	622.0	741.6	449.3
122.8	16	12	23.5	40	1	2	622.0	741.6	531.7
123.8	16	12	31.5	40	1	2	674.0	775.0	618.0
124.8	16	12	39.7	40	1	2	674.0	775.0	680.8
131.8	16	12	16.0	40	1	3	654.3	800.5	756.4
132.8	16	12	20.3	40	1	3	649.4	801.5	793.6
133.8	16	12	24.5	40	1	3	648.4	799.5	822.1
134.8	16	12	31.2	40	1	3	674.0	775.0	868.2
135.8	16	12	39.5	40	1	3	648.4	799.5	947.6
141.8	16	12	15.4	40	1	4	619.0	748.5	898.6
142.8	16	12	23.2	40	1	4	619.0	748.5	984.9
143.8	16	12	31.8	40	1	4	619.0	748.5	1049.7
144.8	16	12	39.7	40	1	4	627.8	747.5	1124.2
23D.8	16	12	24.0	40	2	3	649.4	801.5	1740.3
23N.8	16	12	19.2	40	2	3	649.4	801.5	1594.1
23P.8	16	12	40.0	40	2	3	649.4	801.5	1962.0

Table A-1 A: Published Test Results of Bolt Tear-Out Failure (Cont'd)

Specimen	Bolt Diameter (mm)	Plate Thickness (mm)	End Distance (mm)	Bolt Pitch (mm)	Number of Bolt Lines	Number of Bolt Rows	Yield Stress (MPa)	Ultimate Stress (MPa)	Test Capacity (kN)
Kim and Yura (1999)									
AO050,R	19	4.7	19.6	–	1	1	267	430	38
AO100*	19	4.7	29.3	–	1	1	267	430	62
AO150*	19	4.7	39.0	–	1	1	267	430	81
AT0510,R	19	4.7	19.8	40.4	1	2	267	430	102
AT0520,R	19	4.6	19.5	54.6	1	2	267	430	120
AT0530,R	19	4.6	19.6	76.9	1	2	267	430	122
AT1510,R	19	4.7	38.3	39.8	1	2	267	430	146
AT1520,R*	19	4.6	38.3	54.8	1	2	267	430	172
AT1530,R*	19	4.7	40.2	76.9	1	2	267	430	177
BO050,R	19	4.8	19.6	–	1	1	483	545	49
BO100,R*	19	4.8	29.3	–	1	1	483	545	80
BO150,R*	19	4.8	39.1	–	1	1	483	545	108
BO200,R*	19	4.8	48.9	–	1	1	483	545	133
BT0510,R	19	4.8	19.3	40.1	1	2	483	545	146
BT0520,R	19	4.8	19.6	54.2	1	2	483	545	171
BT0530,R	19	4.8	18.3	76.6	1	2	483	545	191
BT1510,R	19	4.8	38.3	40.0	1	2	483	545	199
BT1520*	19	4.8	38.3	54.2	1	2	483	545	226
BT1530,R*	19	4.8	40.2	76.9	1	2	483	545	254
Aalberg and Larsen (2001)									
S355--1a	20	5.0	20.2	–	1	1	388	539	53.8
S355--1b	20	5.0	20.3	–	1	1	388	539	53.8
S355--2a*	20	5.0	29.9	–	1	1	388	539	83.6
S355--2b*	20	5.0	29.8	–	1	1	388	539	83.7

Table A-1: Published Test Results of Bolt Tear-Out Failure (Cont'd)

Specimen	Bolt Diameter (mm)	Plate Thickness (mm)	End Distance (mm)	Bolt Pitch (mm)	Number of Bolt Lines	Number of Bolt Rows	Yield Stress (MPa)	Ultimate Stress (MPa)	Test Capacity (kN)
Aalberg and Larsen (2001) Cont'd									
S355--3a*	20	4.9	39.2	–	1	1	388	539	112.6
S355--3b*	20	4.9	39.3	–	1	1	388	539	112.8
S355--4a*	20	4.9	48.8	–	1	1	388	539	136.5
S355--4b*	20	4.9	48.7	–	1	1	388	539	138.4
W700--1	20	4.8	20.6	–	1	1	830	871	78.8
*W700--2***	20	4.8	30.1	–	1	1	830	871	122.3
*W700--3***	20	4.8	39.9	–	1	1	830	871	156.3
*W700--4***	20	4.8	48.5	–	1	1	830	871	188.3
W1100--1	20	5.2	20.8	–	1	1	1340	1440	137.8
W1100--2	20	5.2	29.4	–	1	1	1340	1440	210.5
*W1100--3***	20	5.2	39.4	–	1	1	1340	1440	279.0
*W1100--4***	20	5.2	48.7	–	1	1	1340	1440	337.4
Aalberg and Larsen (2002)									
S355--5a	20	5.0	20.4	40.4	1	2	388	539	145
S355--5b	20	5.0	20.5	40.5	1	2	388	539	150
S355--6a	20	5.0	20.0	59.1	1	2	388	539	181
S355--6b	20	5.0	20.2	58.9	1	2	388	539	181
S355--7a	20	5.0	20.6	77.7	1	2	388	539	217
S355--7b	20	5.0	20.5	77.7	1	2	388	539	214
S355--8a	20	5.0	39.3	40.0	1	2	388	539	198
S355--8b	20	5.0	39.3	40.1	1	2	388	539	201
S355--9a*	20	5.0	39.2	59.0	1	2	388	539	231
S355--9b*	20	5.0	39.2	59.1	1	2	388	539	235
S355--10a*	20	5.0	39.7	77.5	1	2	388	539	259
S355--10b*	20	5.0	39.6	77.7	1	2	388	539	246

Table A-1: Published Test Results of Bolt Tear-Out Failure (Cont'd)

Specimen	Bolt Diameter (mm)	Plate Thickness (mm)	End Distance (mm)	Bolt Pitch (mm)	Number of Bolt Lines	Number of Bolt Rows	Yield Stress (MPa)	Ultimate Stress (MPa)	Test Capacity (kN)
Aalberg and Larsen (2002) Cont'd									
W700-5	20	4.9	21.2	39.7	1	2	830	871	220
W700-6	20	4.9	20.7	58.9	1	2	830	871	272
W700-7	20	5.0	20.0	78.7	1	2	830	871	304
W700-8	20	4.9	39.0	39.6	1	2	830	871	281
*W700-9***	20	5.0	39.2	59.2	1	2	830	871	331
*W700-10***	20	5.0	39.6	78.1	1	2	830	871	375
W1100-5	20	5.2	21.2	39.5	1	2	1340	1440	353
W1100-6	20	5.2	21.5	58.1	1	2	1340	1440	444
W1100-7	20	5.2	20.4	77.6	1	2	1340	1440	498
W1100-8	20	5.2	39.7	39.7	1	2	1340	1440	478
*W1100-9***	20	5.2	39.7	58.9	1	2	1340	1440	567
*W1100-10***	20	5.2	39.7	77.8	1	2	1340	1440	613
Puthli and Fleischer (2001)									
144×400	27	17.5	36	–	2	1	524	645	817
153×400	27	17.5	36	–	2	1	524	645	774
162×400	27	17.5	36	–	2	1	524	645	785
153×400	27	17.5	36	–	2	1	524	645	755
162×400	27	17.5	36	–	2	1	524	645	772
171×450	27	17.5	36	–	2	1	524	645	771
162×550	27	17.5	36	–	2	1	524	645	811
171×550	27	17.5	36	–	2	1	524	645	801
180×550	27	17.5	36	–	2	1	524	645	813

Table A-1: Published Test Results of Bolt Tear-Out Failure (Cont'd)

Specimen	Bolt Diameter (mm)	Plate Thickness (mm)	End Distance (mm)	Bolt Pitch (mm)	Number of Bolt Lines	Number of Bolt Rows	Yield Stress (MPa)	Ultimate Stress (MPa)	Test Capacity (kN)
Rex and Easterling (2003)									
1	25	6.5	25	–	1	1	414	690	108.1
2	25	6.5	25	–	1	1	414	690	99.2
3	25	6.5	38	–	1	1	414	690	152.1
4	25	6.5	38	–	1	1	414	690	150.3
5	25	6.5	51	–	1	1	414	690	192.2
11	25	6.5	25	–	1	1	407	665	105.9
12	25	6.5	25	–	1	1	407	665	98.3
29	25	9.5	38	–	1	1	301	439	144.6
30	25	9.5	38	–	1	1	301	439	136.6
37	25	9.5	44	–	1	1	299	441	157.5
39	25	6.5	38	–	1	1	307	452	113.4
40	25	6.5	38	–	1	1	307	452	115.2
41	25	6.5	38	–	1	1	307	452	114.3
42	25	6.5	25	–	1	1	307	452	72.5
43	25	6.5	25	–	1	1	307	452	72.5
44	22	6.5	25	–	1	1	307	452	71.6
45	22	6.5	25	–	1	1	307	452	71.2
46	22	6.5	33	–	1	1	307	452	100.1
47	22	6.5	33	–	1	1	307	452	100.5
48	25	6.5	25	–	1	1	307	452	77.0

Table A-1: Published Test Results of Bolt Tear-Out Failure (Cont'd)

Specimen	Bolt Diameter (mm)	Plate Thickness (mm)	End Distance (mm)	Bolt Pitch (mm)	Number of Bolt Lines	Number of Bolt Rows	Yield Stress (MPa)	Ultimate Stress (MPa)	Test Capacity (kN)
Udagawa and Yamada (2004)									
A121	16	5.0	40.2	40.2	1	2	332.6	479.7	353.2
A123	20	5.0	50.2	50.0	1	2	338.5	482.7	475.9
A131	16	5.0	40.5	40.0	1	3	332.6	479.7	530.3
A133	20	5.0	50.2	50.0	1	3	338.5	482.7	668.9
A141	16	5.0	40.2	40.0	1	4	332.6	479.7	664.9

* Specimens that meet all the minimum end/edge distance and pitch requirements specified in CSA-S16-01 and AISC 2005 and have nominal yield strength not greater than 550 MPa;

** Specimens that meet all the minimum end/edge distance and pitch requirements specified in CSA- S16-01 and AISC 2005.

Italicized specimens have either more than three bolt rows or a nominal yield strength greater than 550 MPa and were excluded from the reliability analyses.

Table A-2: Published Test Results of Combined Failures

Specimen	Bolt Diameter (mm)	Number of Bolt Rows		Web Bolt Lines	Thickness (mm)		End Distance (mm)		Bolt Pitch (mm)	Yield Stress (MPa)	Ultimate Stress (MPa)	Test Capacity (kN)
		Web	Flange		Web	Flange	Web	Flange				
Kato (2003)												
21	16	1	2	3	7.0	10.0	24.0	23.7	40	277.6	443.4	1248
24	16	2	2	3	7.0	10.0	24.2	23.8	40	277.6	443.4	1526
29	16	1	2	4	7.0	10.0	24.2	23.8	40	277.6	443.4	1297
42	16	1	2	3	7.0	10.0	32.0	32.3	40	277.6	443.4	1399
45	16	2	2	3	7.0	10.0	31.8	31.8	40	277.6	443.4	1613
4A	16	1	2	4	7.0	10.0	32.2	31.8	40	277.6	443.4	1369
6B	16	1	2	4	7.0	10.0	40.0	39.8	40	277.6	443.4	1462
6E	16	2	2	4	7.0	10.0	40.0	40.0	40	277.6	443.4	1515
93	16	1	3	3	7.0	10.0	40.0	24.0	40	277.6	443.4	1651
B3	16	1	3	3	7.0	10.0	40.2	31.8	40	277.6	443.4	1675
BB	16	1	3	4	7.0	10.0	40.2	32.0	40	277.6	443.4	1670
C3	16	1	3	3	7.0	10.0	40.0	40.0	40	277.6	443.4	1693

Italicized specimens were excluded from the reliability analyses. (Nominal values of sectional and material properties are shown because measured values were not obtained.)

Table A-3: Published Test Results of Alternate Block Shear Failure in Tees

Specimen	Bolt Diameter (mm)	Section Depth (mm)	Flange Thickness (mm)	Web Thickness (mm)	End Distance (mm)	Bolt Pitch (mm)	Number of Bolt Rows	Yield Stress (MPa)	Ultimate Stress (MPa)	Test Capacity (kN)
Epstein and Stamberg (2002)										
E1	19.1	226.9	5.3	4.8	38.1	76.2	2	402	534	388.3
E1/C1	19.1	201.5	5.3	4.8	38.1	76.2	2	402	534	378.5
E1/C2	19.1	176.1	5.3	4.8	38.1	76.2	2	402	534	363.4
E1/C3	19.1	150.7	5.3	4.8	38.1	76.2	2	402	534	386.1
E2	19.1	226.9	5.3	4.8	38.1	114.3	2	402	534	431.5
E5/C8	19.1	152.3	6.7	5.6	38.1	76.2	2	399	477	398.1
E5/C8	19.1	152.3	6.7	5.6	38.1	76.2	2	399	477	415.0
E5/C8	19.1	152.3	6.7	5.6	38.1	76.2	2	399	477	416.4
E5	19.1	126.9	6.7	5.6	38.1	76.2	2	399	477	408.8
E5	19.1	126.9	6.7	5.6	38.1	76.2	2	399	477	407.9
E5	19.1	126.9	6.7	5.6	38.1	76.2	2	399	477	405.2
E5	19.1	101.5	6.7	5.6	38.1	76.2	2	399	477	389.7
C8	19.1	152.3	6.7	5.6	38.1	76.2	3	399	477	489.7
E6	19.1	154.4	8.9	6.0	38.1	76.2	2	343	457	601.0

APPENDIX B

Test-to-Predicted Ratios of Published Test Results

Table B-1: Test-to-Predicted Ratios of Published Test Results

Specimen	Capacity				Test-to-Predicted Ratio		
	Test Capacity (kN)	CSA S16-01 (kN)	AISC 2005 (kN)	Unified Equation (kN)	CSA S16-01	AISC 2005	Unified Equation
Udagawa and Yamada (1998)							
121.4	288.4	183.1	183.1	278.1	1.57	1.57	1.04
122.4	337.5	232.2	232.2	316.5	1.45	1.45	1.07
123.4	375.7	282.2	282.2	355.7	1.33	1.33	1.06
124.4	413.0	318.5	318.5	398.0	1.30	1.30	1.04
131.4	421.8	325.6	325.6	479.6	1.30	1.30	0.88
132.4	438.5	352.0	352.0	501.6	1.25	1.25	0.87
133.4	468.9	384.2	384.2	517.4	1.22	1.22	0.91
134.4	517.0	425.8	425.8	557.9	1.21	1.21	0.93
135.4	547.4	461.2	461.2	599.4	1.19	1.19	0.91
141.4	557.2	467.1	467.1	680.2	1.19	1.19	0.82
142.4	600.4	513.1	513.1	716.2	1.17	1.17	0.84
143.4	657.3	564.2	564.2	756.1	1.16	1.16	0.87
144.4	724.0	613.2	613.2	794.5	1.18	1.18	0.91
23D.4	955.5	755.1	755.1	1043.3	1.27	1.27	0.92
23N.4	972.2	755.1	755.1	1043.3	1.29	1.29	0.93
121.6	391.4	248.4	248.4	415.9	1.58	1.58	0.94
122.6	483.6	330.3	330.3	484.8	1.46	1.46	1.00
123.6	522.9	398.6	398.6	553.0	1.31	1.31	0.95
124.6	584.7	463.7	463.7	602.3	1.26	1.26	0.97
131.6	600.4	453.9	453.9	726.9	1.32	1.32	0.83
132.6	602.3	469.7	469.7	720.7	1.28	1.28	0.84
133.6	652.4	523.4	523.4	774.7	1.25	1.25	0.84
134.6	730.8	588.7	588.7	846.6	1.24	1.24	0.86
135.6	765.2	661.1	661.1	890.3	1.16	1.16	0.86
141.6	799.5	642.5	642.5	1028.6	1.24	1.24	0.78
142.6	875.1	701.4	701.4	1077.6	1.25	1.25	0.81
143.6	951.6	794.0	794.0	1170.2	1.20	1.20	0.81
144.6	1012.4	838.6	838.6	1196.0	1.21	1.21	0.85
23D.6	1312.6	1001.8	1001.8	1494.3	1.31	1.31	0.89
23N.6	1306.7	1001.8	1001.8	1494.3	1.30	1.30	0.90
23P.6	1435.2	1192.0	1192.0	1655.2	1.20	1.20	1.00
121.8	449.3	301.2	301.2	521.5	1.49	1.49	0.86
122.8	531.7	390.0	390.0	600.1	1.36	1.36	0.89
123.8	618.0	496.8	496.8	718.0	1.24	1.24	0.86
124.8	680.8	587.9	587.9	799.9	1.16	1.16	0.85
131.8	756.4	587.9	587.9	967.6	1.29	1.29	0.78
132.8	793.6	638.5	638.5	1008.4	1.24	1.24	0.79
133.8	822.1	684.8	684.8	1048.1	1.20	1.20	0.78
134.8	868.2	738.8	738.8	1116.3	1.18	1.18	0.78
135.8	947.6	857.9	857.9	1199.0	1.10	1.10	0.79
141.8	898.6	779.9	779.9	1282.5	1.15	1.15	0.70
142.8	984.9	864.4	864.4	1356.7	1.14	1.14	0.73
143.8	1049.7	957.6	957.6	1438.6	1.10	1.10	0.73

Table B-1: Test-to-Predicted Ratios of Published Test Results (Cont'd)

Specimen	Capacity				Test-to-Predicted Ratio		
	Test Capacity (kN)	CSA S16-01 (kN)	AISC 2005 (kN)	Unified Equation (kN)	CSA S16-01	AISC 2005	Unified Equation
Udagawa and Yamada (1998) Cont'd							
144.8	1124.2	1040.7	1040.7	1521.6	1.08	1.08	0.74
23D.8	1740.3	1361.9	1361.9	2090.8	1.28	1.28	0.86
23N.8	1594.1	1251.1	1251.1	1994.3	1.27	1.27	0.81
23P.8	1962.0	1731.2	1716.8	2412.5	1.13	1.13	0.99
Kim and Yura (1999)							
AO050,R	38	19.4	19.4	36.7	1.96	1.96	1.04
AO100*	62	42.9	42.9	55.1	1.45	1.45	1.13
AO150*	81	58.1	58.1	73.0	1.39	1.39	1.11
AT0510,R	102	61.7	61.7	112.6	1.65	1.65	0.91
AT0520,R	120	94.4	94.4	137.8	1.27	1.27	0.87
AT0530,R	122	142.8	142.8	179.4	0.85	0.85	0.68
AT1510,R	146	104.6	104.6	146.1	1.40	1.40	1.00
AT1520,R*	172	137.8	137.8	173.1	1.25	1.25	0.99
AT1530,R*	177	174.5	174.5	219.1	1.01	1.01	0.81
BO050,R	49	25.2	25.2	55.3	1.95	1.95	0.89
BO100,R*	80	55.9	55.9	83.5	1.43	1.43	0.96
BO150,R*	108	86.3	86.3	110.9	1.25	1.25	0.97
BO200,R*	133	116.2	116.2	137.9	1.14	1.14	0.96
BT0510,R	146	77.4	77.4	167.5	1.89	1.89	0.87
BT0520,R	171	122.9	122.9	209.4	1.39	1.39	0.82
BT0530,R	191	187.6	187.6	267.5	1.02	1.02	0.71
BT1510,R	199	136.9	136.9	222.1	1.45	1.45	0.90
BT1520*	226	181.3	181.3	262.4	1.25	1.25	0.86
BT1530,R*	254	256.6	256.6	330.1	0.99	0.99	0.77
Aalberg and Larsen (2001)							
S355--1a	53.8	31.1	31.1	53.5	1.73	1.73	1.01
S355--1b	53.8	31.3	31.3	53.7	1.72	1.72	1.00
S355--2a*	83.6	62.2	62.2	79.1	1.35	1.35	1.06
S355--2b*	83.7	61.8	61.8	78.9	1.35	1.35	1.06
S355--3a*	112.6	89.9	89.9	103.3	1.25	1.25	1.09
S355--3b*	112.8	90.1	90.1	103.6	1.25	1.25	1.09
S355--4a*	136.5	112.1	112.1	128.9	1.22	1.22	1.06
S355--4b*	138.4	111.9	111.9	128.6	1.24	1.24	1.08
W700—1	78.8	51.2	51.2	97.9	1.54	1.54	0.81
*W700—2***	122.3	98.9	98.9	143.0	1.24	1.24	0.86
*W700--3***	156.3	145.5	145.5	189.6	1.07	1.07	0.82
*W700--4***	188.3	192.1	192.1	230.5	0.98	0.98	0.82
W1100--1	137.8	92.4	92.4	173.9	1.49	1.49	0.79
W1100--2	210.5	169.8	169.8	245.8	1.24	1.24	0.86
*W1100--3***	279.0	261.1	261.1	330.7	1.07	1.07	0.84
*W1100--4***	337.4	344.8	344.8	408.0	0.98	0.98	0.83

Table B-1: Test-to-Predicted Ratios of Published Test Results (Cont'd)

Specimen	Capacity				Test-to-Predicted Ratio		
	Test Capacity (kN)	CSA S16-01 (kN)	AISC 2005 (kN)	Unified Equation (kN)	CSA S16-01	AISC 2005	Unified Equation
Aalberg and Larsen (2002)							
S355--5a	145	94.3	94.3	161.2	1.54	1.54	0.90
S355--5b	150	95.0	95.0	161.7	1.58	1.58	0.93
S355--6a	181	153.0	153.0	209.7	1.18	1.18	0.86
S355--6b	181	152.8	152.8	209.7	1.18	1.18	0.86
S355--7a	217	214.1	214.1	260.6	1.01	1.01	0.83
S355--7b	214	214.0	214.0	260.3	1.00	1.00	0.82
S355--8a	198	153.0	153.0	209.8	1.29	1.29	0.94
S355--8b	201	153.8	153.8	210.4	1.31	1.31	0.96
S355--9a*	231	214.0	214.0	260.5	1.08	1.08	0.89
S355--9b*	235	214.2	214.2	260.5	1.10	1.10	0.90
S355--10a*	259	270.2	270.2	310.6	0.96	0.96	0.83
S355--10b*	246	271.1	271.1	311.7	0.91	0.91	0.79
W700-5	220	151.8	151.8	294.2	1.45	1.45	0.75
W700-6	272	248.1	248.1	385.3	1.10	1.10	0.71
W700-7	304	348.4	348.4	480.7	0.87	0.87	0.63
W700-8	281	242.5	242.5	379.7	1.16	1.16	0.74
*W700-9***	331	346.0	346.0	478.1	0.96	0.96	0.69
*W700-10***	375	447.5	447.5	575.4	0.84	0.84	0.65
W1100-5	353	256.5	256.5	507.1	1.38	1.38	0.70
W1100-6	444	430.6	430.6	661.5	1.03	1.03	0.67
W1100-7	498	593.8	593.8	812.0	0.84	0.84	0.61
W1100-8	478	430.3	430.3	662.5	1.11	1.11	0.72
*W1100-9***	567	602.4	602.4	821.3	0.94	0.94	0.69
*W1100-10***	613	767.9	767.9	974.9	0.80	0.80	0.63
Puthli and Fleischer (2001)							
144×400	817	568.9	568.9	850.4	1.44	1.44	0.96
153×400	774	568.9	568.9	850.4	1.36	1.36	0.91
162×400	785	568.9	568.9	850.4	1.38	1.38	0.92
153×400	755	568.9	568.9	850.4	1.33	1.33	0.89
162×400	772	568.9	568.9	850.4	1.36	1.36	0.91
171×450	771	568.9	568.9	850.4	1.36	1.36	0.91
162×550	811	568.9	568.9	850.4	1.43	1.43	0.95
171×550	801	568.9	568.9	850.4	1.41	1.41	0.94
180×550	813	568.9	568.9	850.4	1.43	1.43	0.96
Rex and Easterling (2003)							
1	108.1	67.28	67.28	103.58	1.61	1.61	1.04
2	99.2	67.28	67.28	103.58	1.47	1.47	0.96
3	152.1	122.71	122.71	157.44	1.24	1.24	0.97
4	150.3	122.71	122.71	157.44	1.22	1.22	0.95
5	192.2	164.69	164.69	211.30	1.17	1.17	0.91
11	105.9	64.84	64.84	100.57	1.63	1.63	1.05
12	98.3	64.84	64.84	100.57	1.52	1.52	0.98

Table B-1: Test-to-Predicted Ratios of Published Test Results (Cont'd)

Specimen	Capacity				Test-to-Predicted Ratio		
	Test Capacity (kN)	CSA S16-01 (kN)	AISC 2005 (kN)	Unified Equation (kN)	CSA S16-01	AISC 2005	Unified Equation
Rex and Easterling (2003) Cont'd							
29	144.6	127.62	127.62	154.23	1.13	1.13	0.94
30	136.6	127.62	127.62	154.23	1.07	1.07	0.89
37	157.5	149.98	149.98	178.59	1.05	1.05	0.88
39	113.4	89.90	89.90	108.24	1.26	1.26	1.05
40	115.2	89.90	89.90	108.24	1.28	1.28	1.06
41	114.3	89.90	89.90	108.24	1.27	1.27	1.06
42	72.5	44.07	44.07	71.21	1.65	1.65	1.02
43	72.5	44.07	44.07	71.21	1.65	1.65	1.02
44	71.6	49.36	49.36	71.21	1.45	1.45	1.01
45	71.2	49.36	49.36	71.21	1.44	1.44	1.00
46	100.1	77.56	77.56	94.00	1.29	1.29	1.06
47	100.5	77.56	77.56	94.00	1.30	1.30	1.07
48	77.0	44.07	44.07	71.21	1.75	1.75	1.08
Udagawa and Yamada (2004)							
A121	353.2	306.9	306.9	376.7	1.15	1.15	0.94
A123	475.9	389.2	389.2	475.0	1.22	1.22	1.00
A131	530.3	434.5	434.5	565.0	1.22	1.22	0.94
A133	668.9	551.4	551.4	712.0	1.21	1.21	0.94
A141	664.9	559.3	559.3	751.1	1.19	1.19	0.89
Kato (2003)							
21	1248	932.4	932.4	1114.4	1.34	1.34	1.12
24	1526	1161.6	1161.6	1349.7	1.31	1.31	1.13
29	1297	988.8	988.8	1177.2	1.31	1.31	1.10
42	1399	1079.8	1079.8	1255.9	1.30	1.30	1.11
45	1613	1275.0	1275.0	1438.4	1.27	1.27	1.12
4A	1369	1129.0	1129.0	1267.2	1.21	1.21	1.08
6B	1462	1204.1	1204.1	1360.0	1.21	1.21	1.07
6E	1515	1295.1	1295.1	1474.7	1.17	1.17	1.03
93	1651	1343.5	1343.5	1586.2	1.23	1.23	1.04
B3	1675	1400.4	1400.4	1656.5	1.20	1.20	1.01
BB	1670	1406.6	1406.6	1577.1	1.19	1.19	1.06
C3	1693	1453.6	1453.6	1723.0	1.16	1.16	0.98
Epstein and Stamberg (2002)							
E1	388.3	343.3	343.3	359.3	1.13	1.13	1.08
E1/C1	378.5	343.3	343.3	359.3	1.10	1.10	1.05
E1/C2	363.4	343.3	343.3	359.3	1.06	1.06	1.01
E1/C3	386.1	343.3	343.3	359.3	1.12	1.12	1.07
E2	431.5	387.6	387.6	409.0	1.11	1.11	1.05
E5/C8	398.1	391.4	391.4	400.2	1.02	1.02	0.99
E5/C8	415.0	391.4	391.4	400.2	1.06	1.06	1.04
E5/C8	416.4	391.4	391.4	400.2	1.06	1.06	1.04

Table B-1: Test-to-Predicted Ratios of Published Test Results (Cont'd)

Specimen	Capacity				Test-to-Predicted Ratio		
	Test Capacity (kN)	CSA S16-01 (kN)	AISC 2005 (kN)	Unified Equation (kN)	CSA S16-01	AISC 2005	Unified Equation
Epstein and Stamberg (2002) Cont'd							
E5	408.8	391.4	391.4	394.6	1.04	1.04	1.04
E5	407.9	391.4	391.4	394.6	1.04	1.04	1.03
E5	405.2	391.4	391.4	394.6	1.04	1.04	1.03
E5	389.7	343.8	343.8	343.8	1.13	1.13	1.13
C8	489.7	493.2	493.2	504.8	0.99	0.99	0.97
E6	601.0	430.1	430.1	447.1	1.40	1.40	1.34

* Specimens that meet all the minimum end/edge distance and pitch requirements specified in CSA-S16-01 and AISC 2005 and have nominal yield strength not greater than 550 MPa;

** Specimens that meet all the minimum end/edge distance and pitch requirements specified in CSA-S16-01 and AISC 2005.

Italicized specimens have either more than three bolt rows or a nominal yield strength greater than 550 MPa and were excluded from the reliability analyses. (For Kato (2003), nominal values of sectional and material properties were used because measured values were not obtained.)

APPENDIX C

Load vs. Deformation Curves for Specimens in Series C

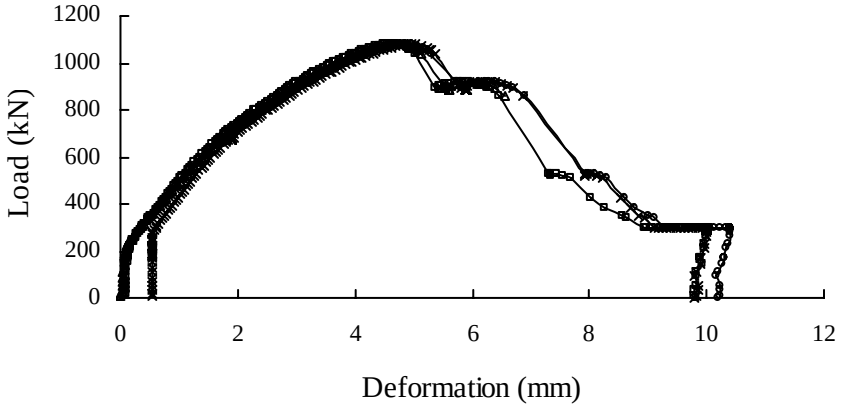

Figure C-1: Load vs. Deformation Curves for C1E1a

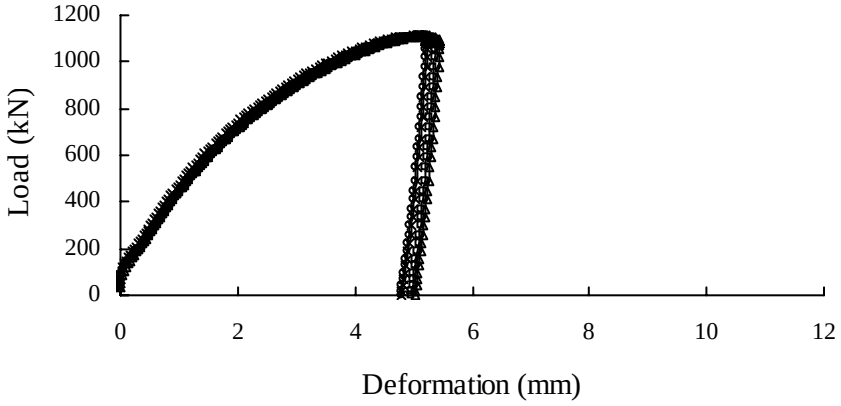

Figure C-2: Load vs. Deformation Curves for C2E1b

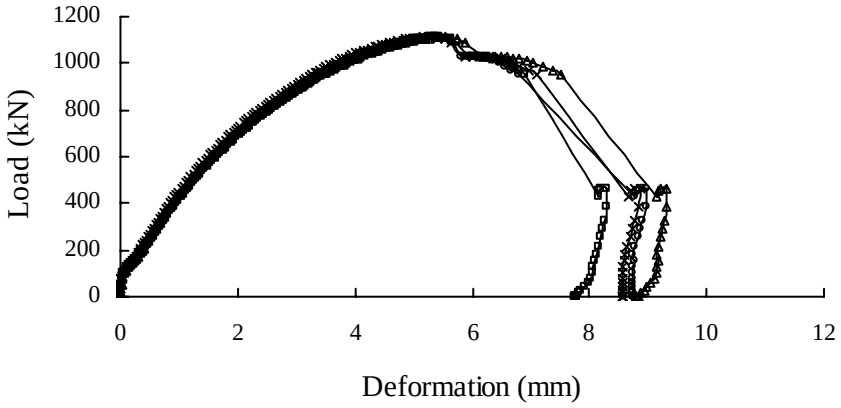

Figure C-3: Load vs. Deformation Curves for C3E1c

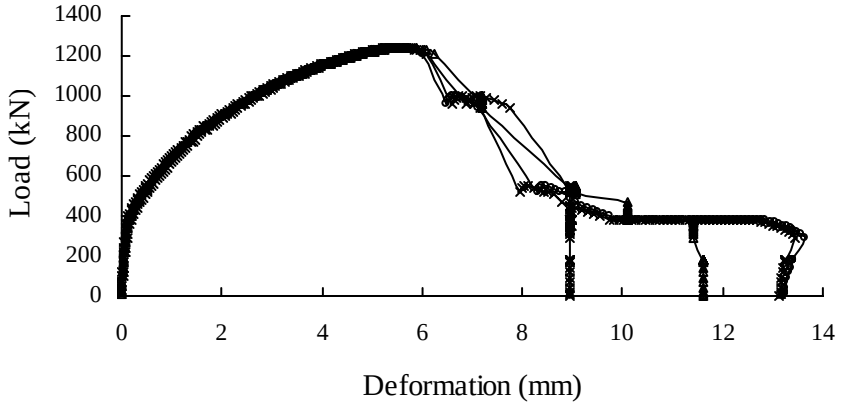

Figure C-4: Load vs. Deformation Curves for C4E2a

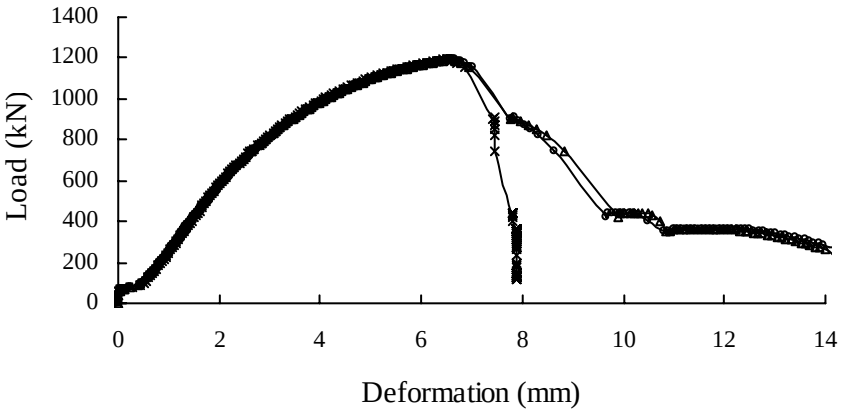

Figure C-5: Load vs. Deformation Curves for C5E2b

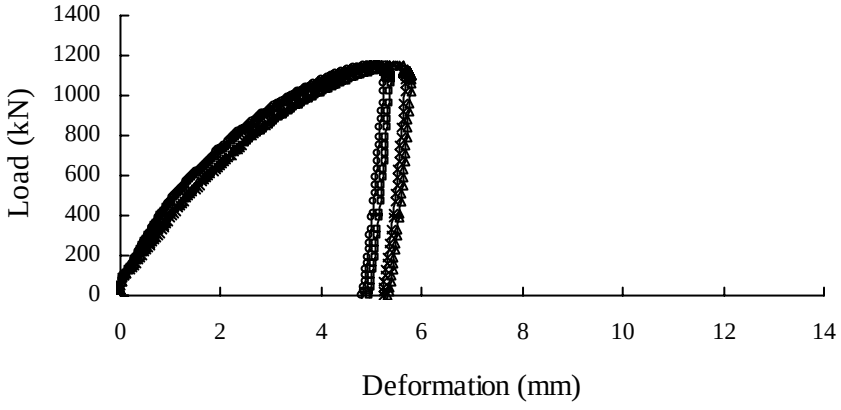

Figure C-6: Load vs. Deformation Curves for C6E2c

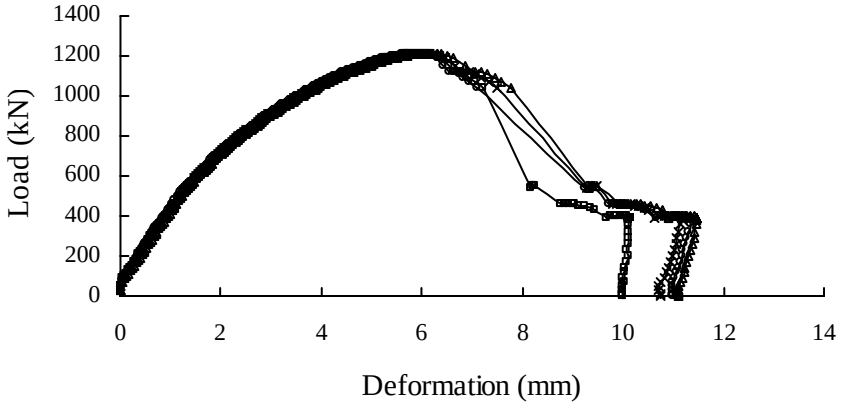

Figure C-7: Load vs. Deformation Curves for C7E3a

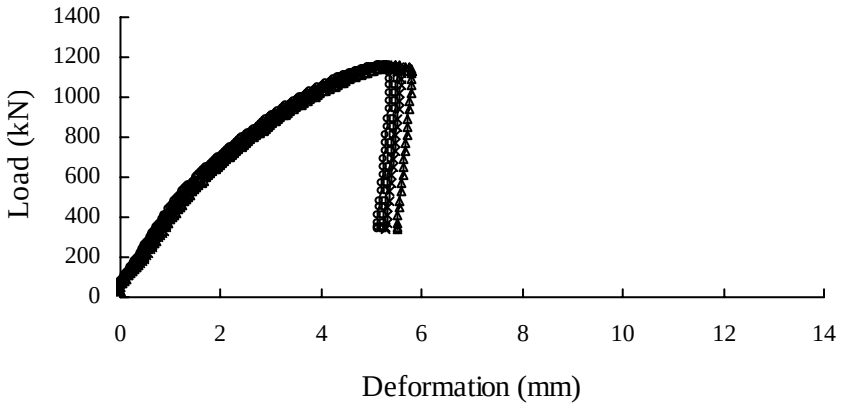

Figure C-8: Load vs. Deformation Curves for C8E3b

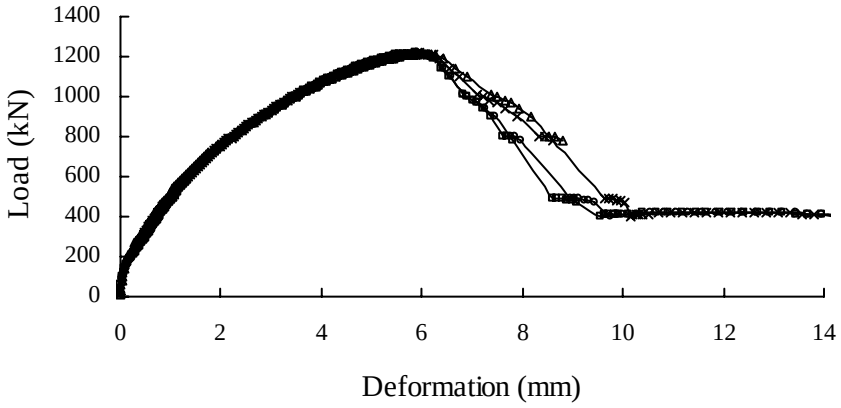

Figure C-9: Load vs. Deformation Curves for C9E3c

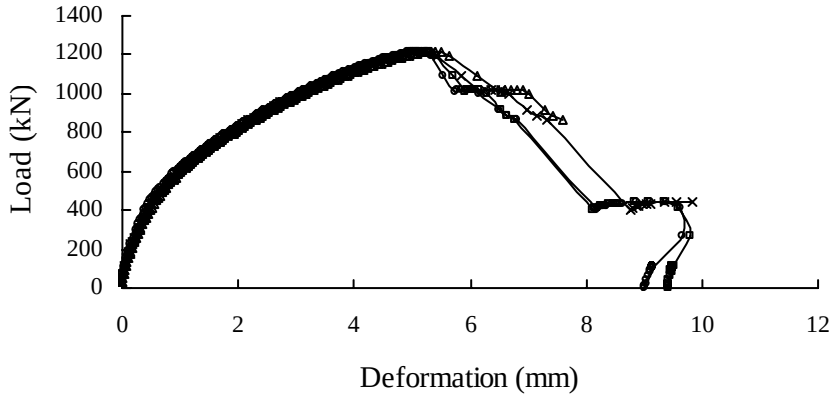

Figure C-10: Load vs. Deformation Curves for C10E4a

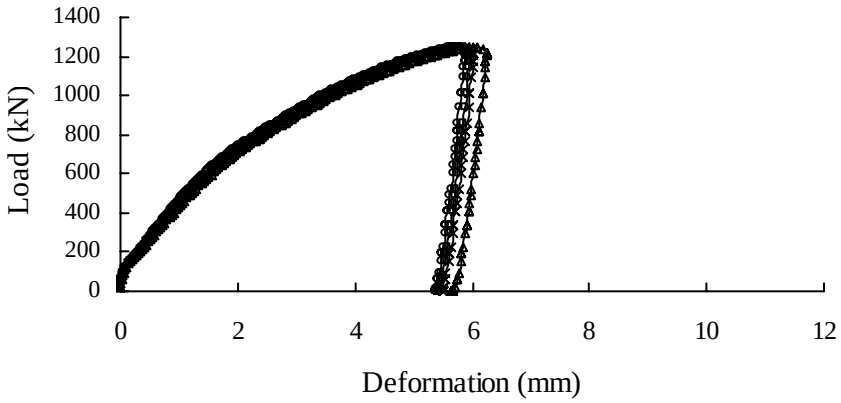

Figure C-11: Load vs. Deformation Curves for C11E4b

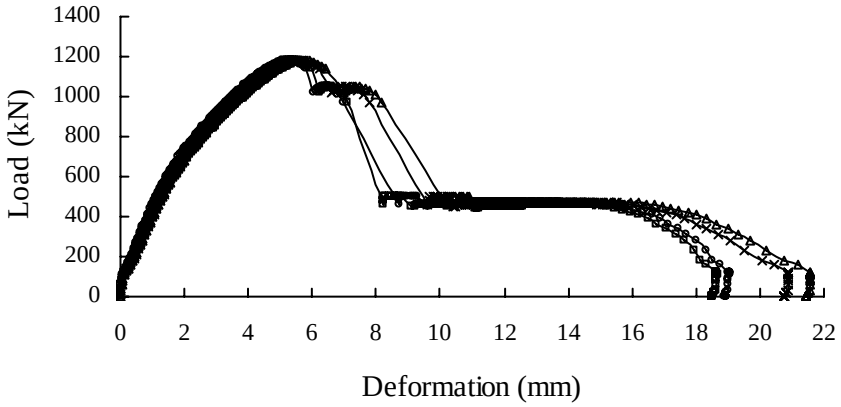

Figure C-12: Load vs. Deformation Curves for C12E4c

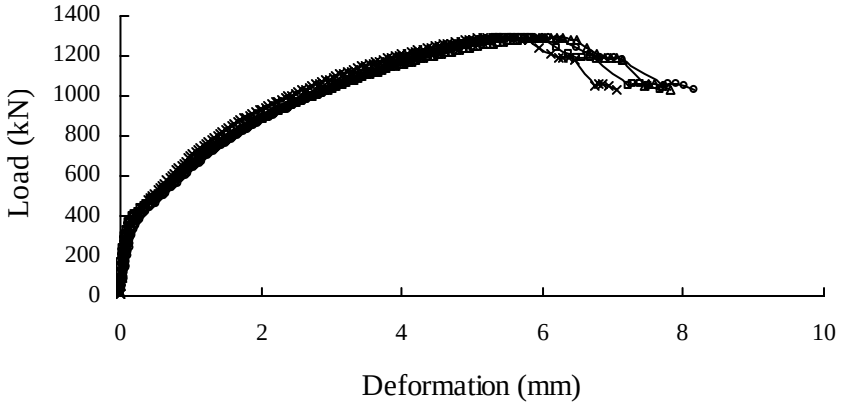

Figure C-13: Load vs. Deformation Curves for C13E5a

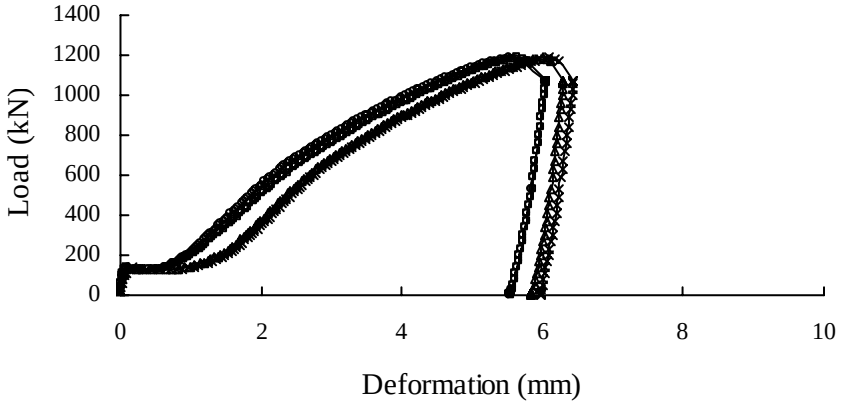

Figure C-14: Load vs. Deformation Curves for C14E5b

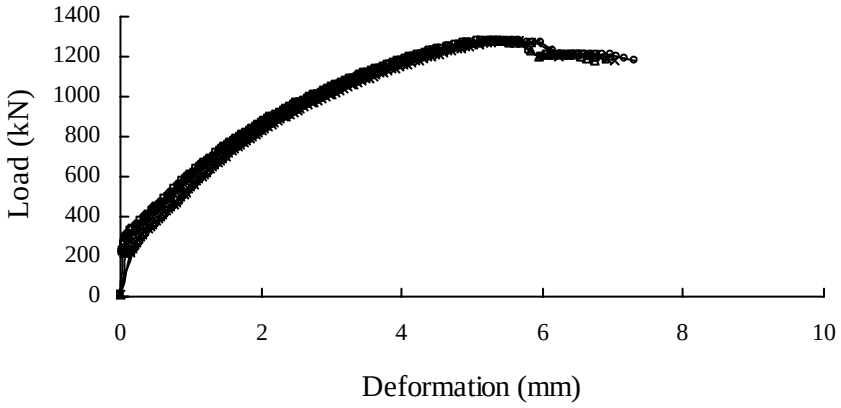

Figure C-15: Load vs. Deformation Curves for C15E5c

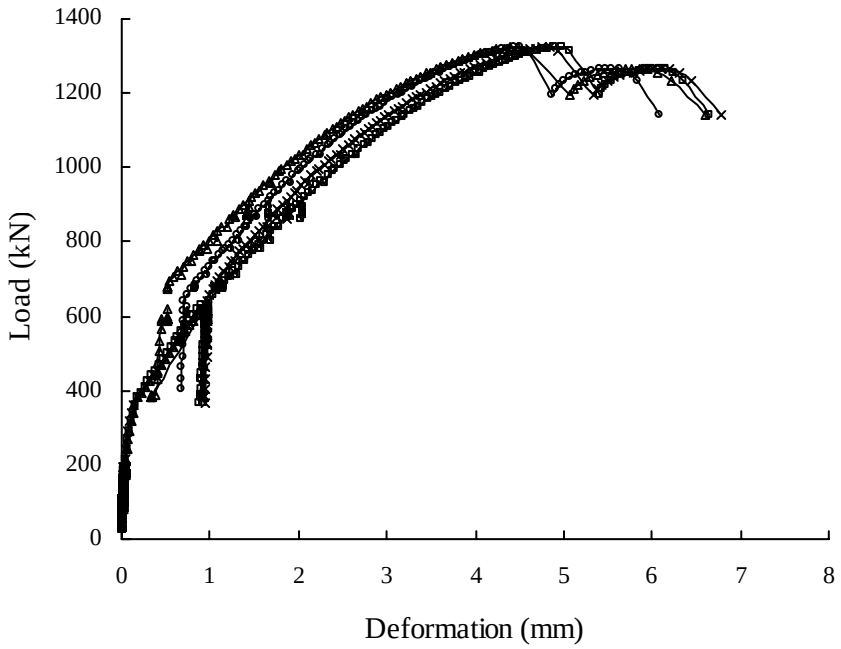

Figure C-16: Load vs. Deformation Curves for C16E6

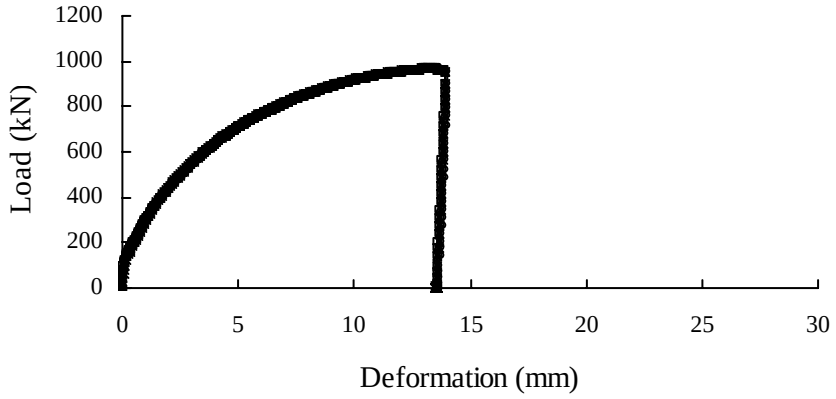

Figure C-17: Load vs. Deformation Curves for C17E1a

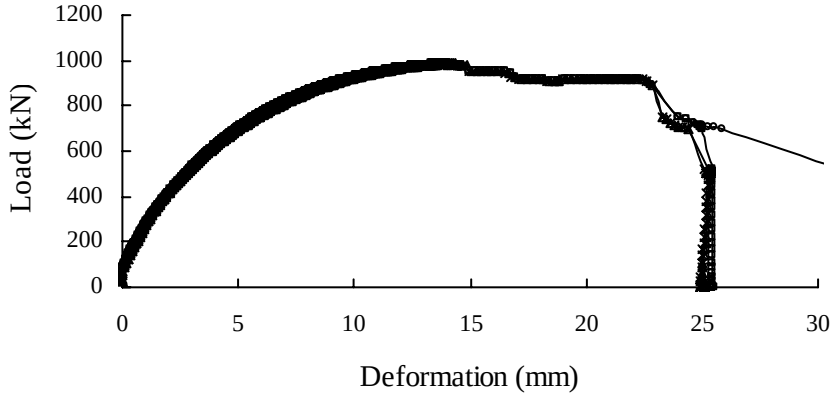

Figure C-18: Load vs. Deformation Curves for C18E1b

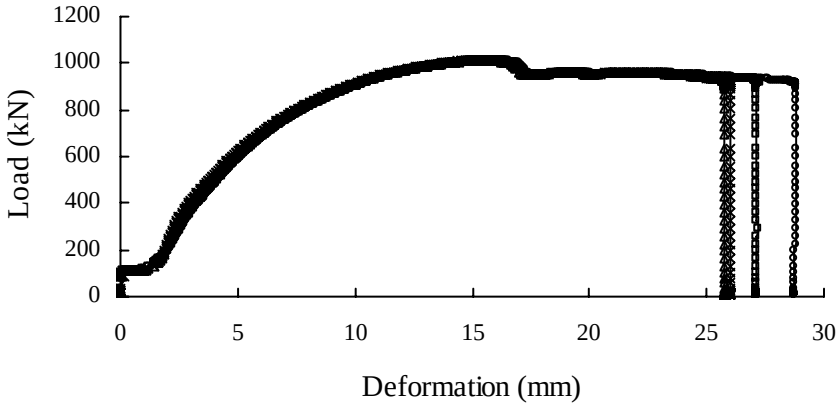

Figure C-19: Load vs. Deformation Curves for C19E1c

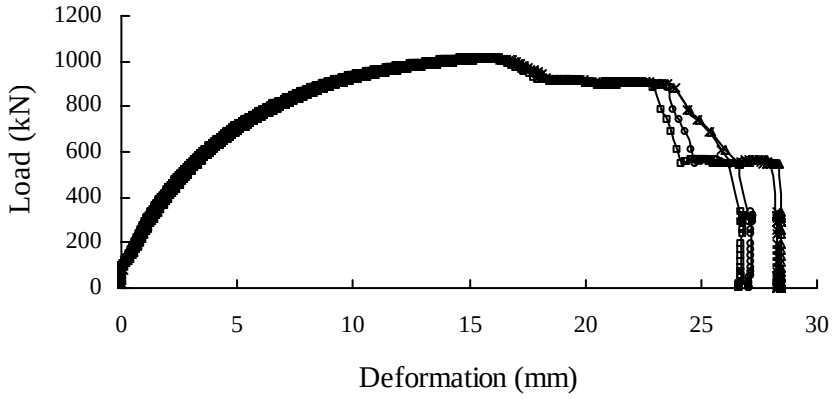

Figure C-20: Load vs. Deformation Curves for C20E2a

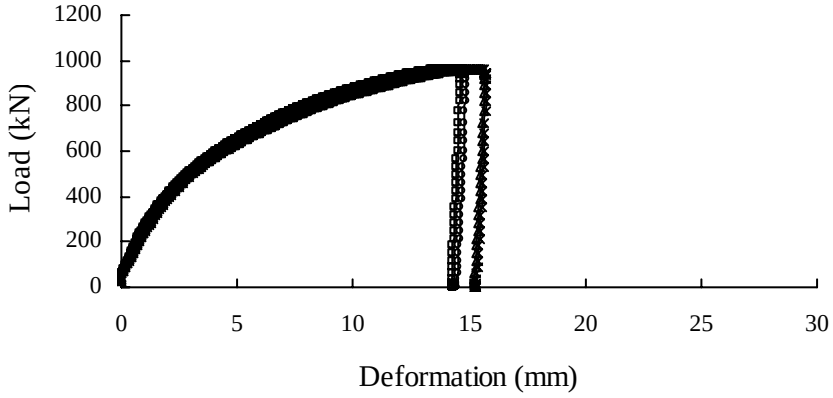

Figure C-21: Load vs. Deformation Curves for C21E2b

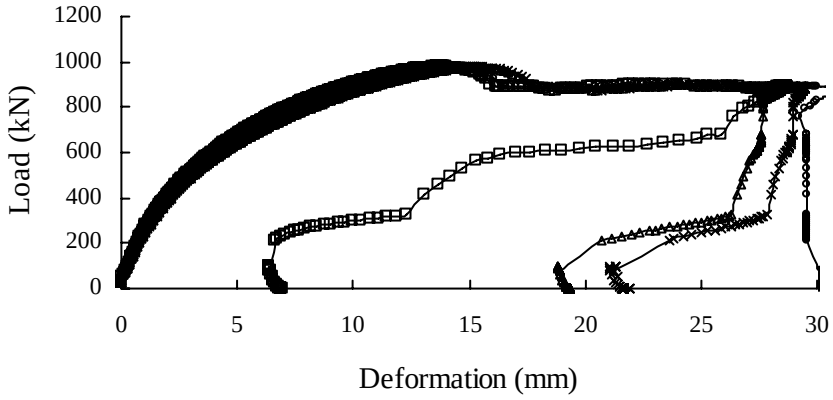

Figure C-22: Load vs. Deformation Curves for C22E2c

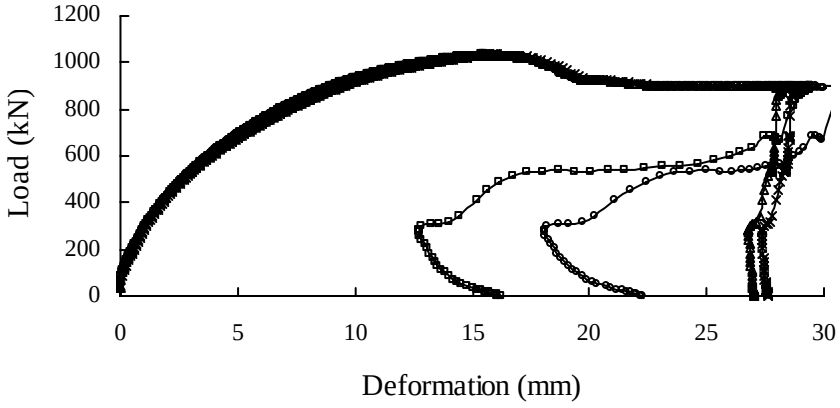

Figure C-23: Load vs. Deformation Curves for C23E3a

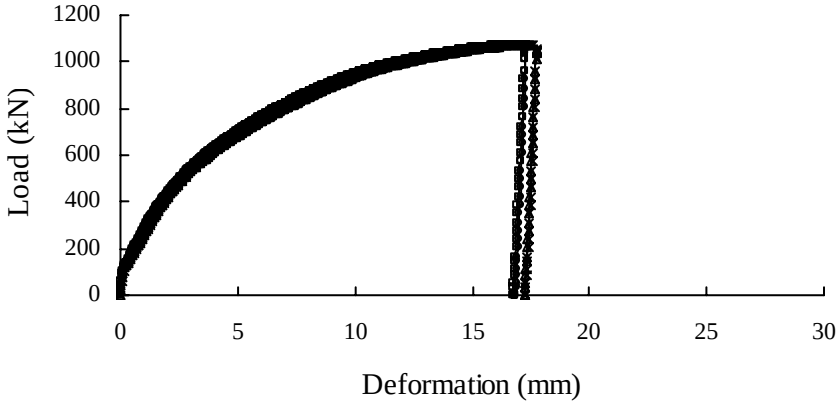

Figure C-24: Load vs. Deformation Curves for C24E3b

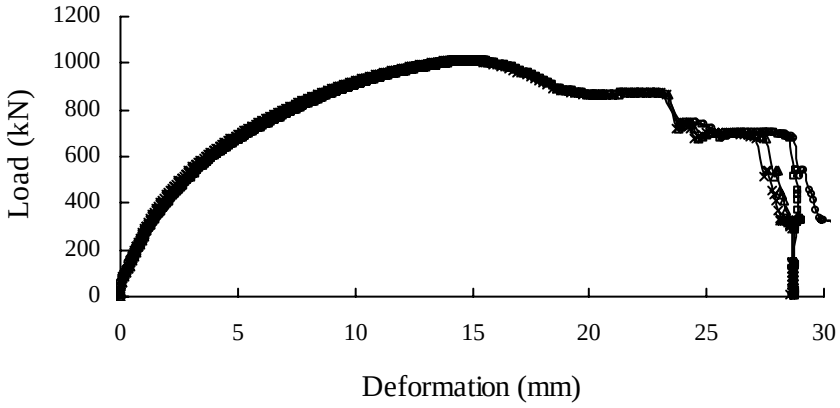

Figure C-25: Load vs. Deformation Curves for C25E3c

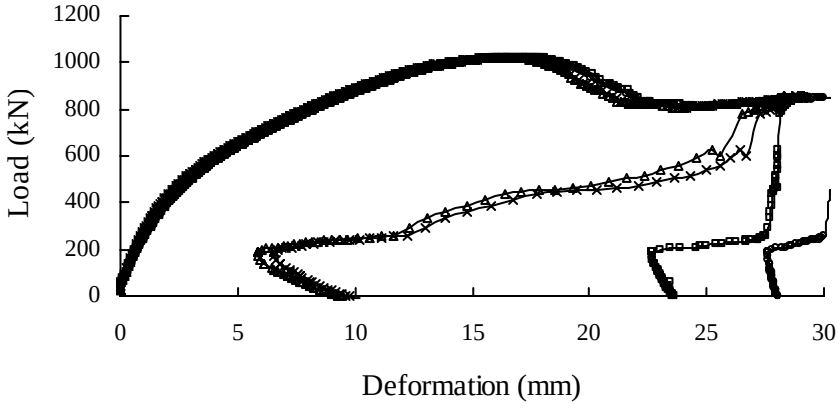

Figure C-26: Load vs. Deformation Curves for C26E4a

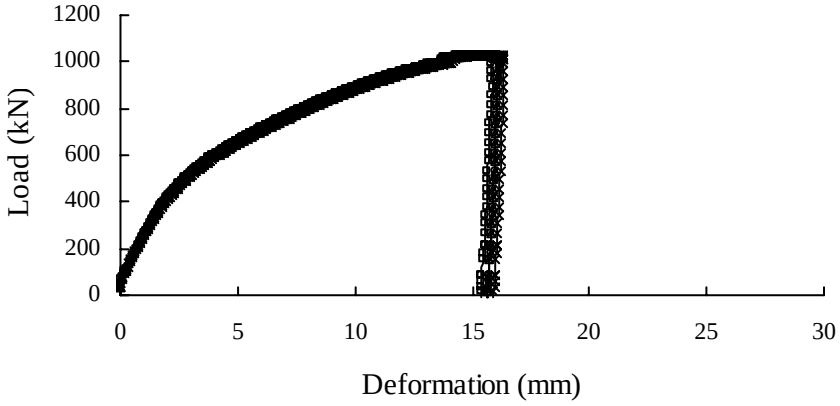

Figure C-27: Load vs. Deformation Curves for C27E4b

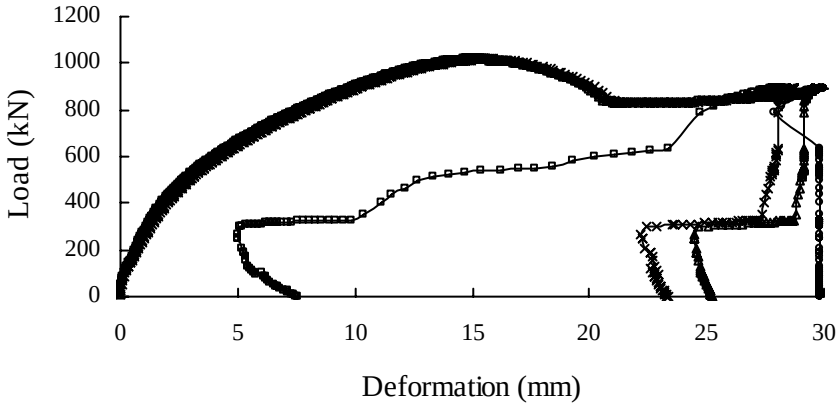

Figure C-28: Load vs. Deformation Curves for C28E4c

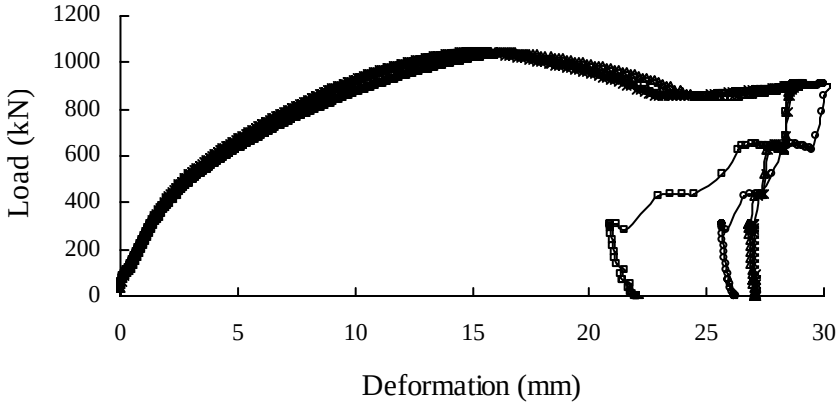

Figure C-29: Load vs. Deformation Curves for C29E5a

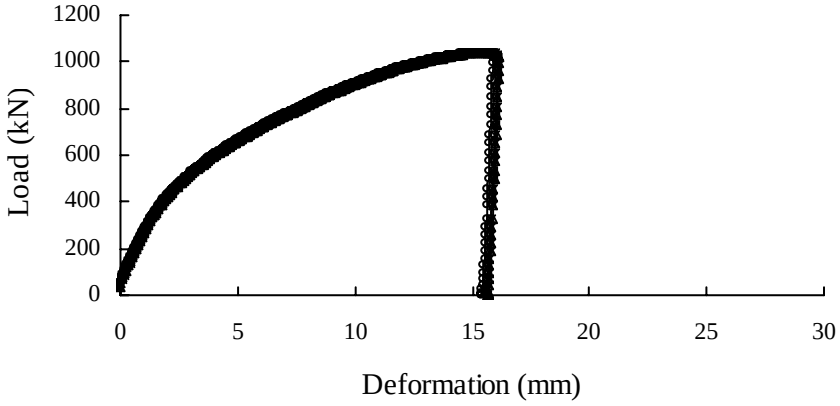

Figure C-30: Load vs. Deformation Curves for C30E5b

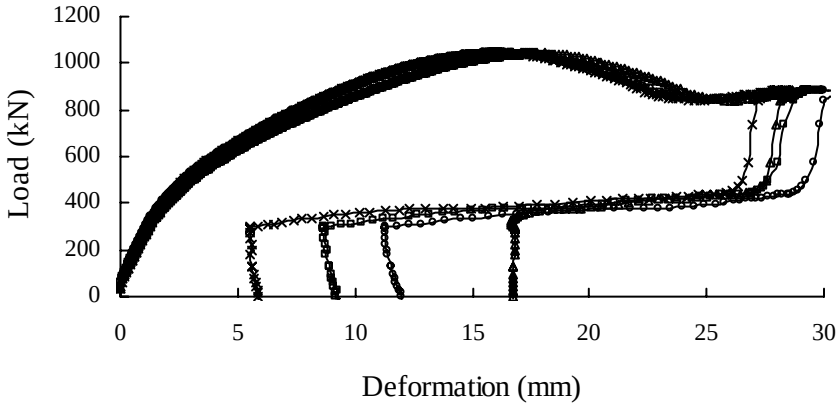

Figure C-31: Load vs. Deformation Curves for C31E5c

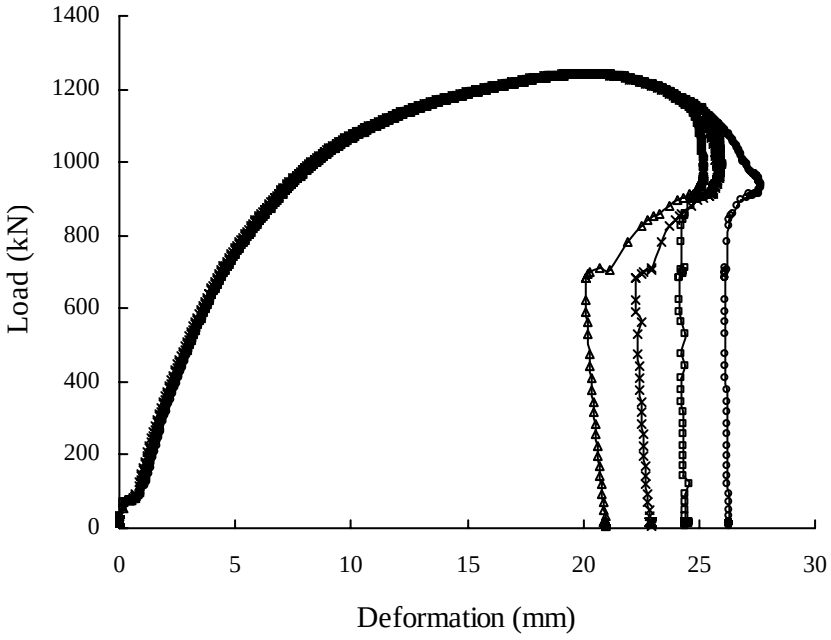

Figure C-32: Load vs. Deformation Curves for C32E6

APPENDIX D

Photos of Series C Failed Connections

Figure D-1: E1 Group Failed Connections with Thicker Webs

Figure D -2: E2 Group Failed Connections with Thicker Webs

Figure D -3: E3 Group Failed Connections with Thicker Webs

Figure D -4: E4 Group Failed Connections with Thicker Webs

Figure D -5: E5 Group Failed Connections with Thicker Webs

Figure D -6: E6 Failed Connection with Thicker Web

Figure D -7: E1 Group Failed Connections with Thinner Webs

Figure D -8: E2 Group Failed Connections with Thinner Webs

Figure D -9: E3 Group Failed Connections with Thinner Webs

Figure D -10: E4 Group Failed Connections with Thinner Webs

Figure D -11: E5 Group Failed Connections with Thinner Webs

Figure D -12: E6 Failed Connection with Thinner Web